Inelastic Behavior Of Solid Square Bar Under Combined Bending And Torsion

by

Sanjib Chandra Chowdhury

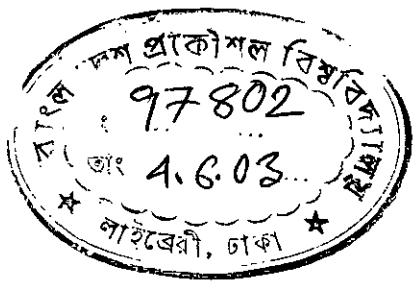

MASTER OF SCIENCE IN MECHANICAL ENGINEERING

Department of Mechanical Engineering

BANGLADESH UNIVERSITY OF ENGINEERING AND TECHNOLOGY

Dhaka-1000, Bangladesh

May 2003

The thesis titled "**Inelastic Behavior Of Solid Square Bar Under Combined Bending And Torsion**", Submitted by **Sanjib Chandra Chowdhury,** Roll No: 100010061P, Session: October 2000 has been accepted as satisfactory in partial fulfillment of the requirement for the degree of MASTER OF SCIENCE IN MECHANICAL ENGINEERING on May 07, 2003.

BOARD OF EXAMINERS

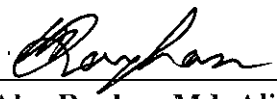

Dr. Abu Rayhan Md. Ali 07/05/03
Professor
Department of Mechanical Engineering
BUET, Dhaka, Bangladesh

Chairman

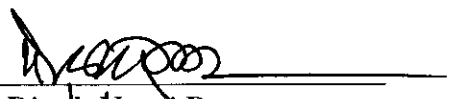

Dr. Dipak Kanti Das
Professor
Department of Mechanical Engineering
BUET, Dhaka, Bangladesh

Member

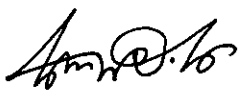

Dr. Muhammad Mahbubul Alam
Professor
Department of Mechanical Engineering
BUET, Dhaka, Bangladesh

Member

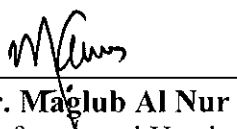

Dr. Maglub Al Nur
Professor and Head
Department of Mechanical Engineering
BUET, Dhaka, Bangladesh

Member
(Ex- officio)

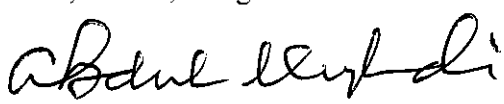

Dr. Abdul Muqtadir
Professor
Department of Civil Engineering
BUET, Dhaka, Bangladesh.

Member
(External)

CANDIDATE'S DECLARATION

It is hereby declared that this thesis or any part of it has not been submitted elsewhere for the award of any degree or diploma.

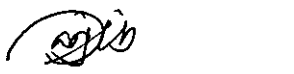

Author
Sanjib Chandra Chowdhury

To my late paternal grandfather and grandmother

Contents

List of Tables

List of Figures

Nomenclature

E	Modulus of elasticity
G	Modulus of rigidity
F, P	Axial or transverse load
I	Moment of inertia
J	Polar moment of inertia
J_2	Second invariant of deviatoric stress
L, l	Length or deflection
T	Torque
M	Moment
Y	Yield strength
U	Energy
S	Stress deviator tensor
A	Cross sectional area
a	Dimension of the side of the bar
r	Radius
d	Diameter
c	Elastic core distance
BL	Bending load
TL	Torque load
YBL	Yield bending load
YTL	Yield torsional load

Greek

σ	Axial or flexural stress
τ	Shear stress
ε	Axial strain
υ	Displacement
θ	Angle of twist
δ	Midpoint deflection

Subscript/Superscript

0	Initial value
e	Elastic region
o, p	Plastic region
oct	Octahedral
Y, y	Yield value
ut	Ultimate value
b	Bending value
t	Torsional value
d	Distorsion
by	Yield bending value
ty	Yield torsional value
max	Maximum value

Acknowledgement

The author would like to take this opportunity of expressing his heartfelt gratitude and indebtedness to his supervisor Dr. Abu Rayhan Md. Ali, Professor, Department of Mechanical Engineering, Bangladesh University of Engineering and Technology (BUET), Dhaka, Bangladesh for his valuable and continuous guidance, suggestions while the present work is being carried out.

The author feels grateful to Dr. Maglub Al Nur, Professor & Head, Department of Mechanical Engineering, Bangladesh University of Engineering and Technology (BUET), Dhaka, Bangladesh for his valuable co-operation from time to time.

The author feels grateful to Dr. Abdur Rashid Sarkar, Professor & Ex- Head, and Mr. Nazmul Huda Al Mamun, Assistant Professor, Department of Mechanical Engineering, Bangladesh University of Engineering and Technology (BUET), Dhaka, Bangladesh for their valuable suggestion and co-operation from time to time.

The author is also grateful to all of the technical staff of Applied Mechanics and Solid Mechanics Laboratories for their assistance to carry out the experiment.

Finally the author thanks his colleagues, family members, friends and other relatives who shared the troubles with him.

Abstract

In this work inelastic behavior of solid square bar under combined bending and torsion is studied. A test rig is designed and constructed to apply bending moment and torque both separately and simultaneously. Specimens of square cross section (8mm × 8mm) and constant length (0.71m) are subjected to the above-mentioned types of loading. For the present work two types of loading - proportional loading and non-proportional loading are investigated.

In proportional loading, the ratio of bending moment to torque (i.e., M/T) is kept constant. Six ratios, 0 (pure torsion), 0.56, 1.12, 2.24, 3.36 and ∞ (pure bending) are studied. Among these, ratios 0 and ∞ are studied merely to justify the accuracy of the test rig.

In non-proportional loading, the ratio of bending moment to torque is not kept constant. Two types of non-proportional loading arrangements are studied. In the first type of non-proportional loading, different levels of initial torques are applied and maintaining each of these initial torques constant, bending moments are gradually applied. Three considered different levels of initial torque are 25 %, 50 % and 75 % of yield torque of pure torsion. In the second type of non-proportional loading, different levels of initial bending moments are applied and maintaining each of these initial bending moments constant, torques are gradually applied. Three considered different levels of initial bending moments are 25 %, 50 % and 75% of yield bending moment of pure bending.

For each loading arrangement, behaviour of the material of the bar in the elastic and in the plastic regions is investigated. Yield point of the material of the bar is also investigated for each type of loading condition and results obtained from this investigation are compared with the available results.

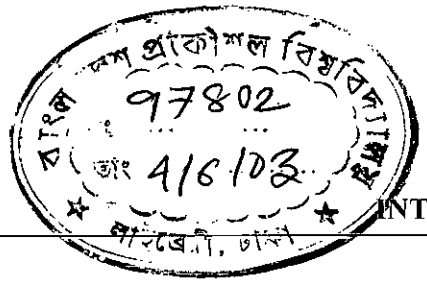

CHAPTER - 1
INTRODUCTION

1.1 GENERAL

There are many situations in design of mechanical elements where plastic behaviour is tolerated. In fact, for structures that are highly statically indeterminate, some standard analyses actually allow the maximum stresses to exceed the elastic limit. During recent years, there has been considerable interest in the application of the macroscopic theory of plasticity to engineering problems associated with structural designs and forming of metals. It is sometimes permissible and economical to tolerate plastic behaviour in small-localised areas undergoing high stresses.

The theory of plasticity as a science began in 1864 when Tresca published his results on punching and extrusion experiments and formulated his famous yield criterion. A few years later, using Tresca's results, Saint-Venant and Levy laid some of the foundations of the modern theory of plasticity. For the next 75 years, progress was slow and spotty, although important contributions were made by von Mises, Hencky, Prandtl and others. It is only since approximately 1945 that a unified theory began to emerge. Since that time, concentrated efforts by many researchers have produced a voluminous literature that is growing at a rapid rate. Brief but excellent historical sketches are furnished by Hill [1] and Westergaard [2].

The theory of plasticity fall into two categories: physical theories and mathematical theories. The physical theories seek to explain metals flow plastically. Looking at materials from a microscopic viewpoint, an attempt is made to determine what happens to the atoms, crystals, and grains of a material when plastic flow occurs. The mathematical theories, on the other hand, are phenomenological in nature and attempt to formalise and put into useful form the results of macroscopic experiments, without probing very deeply into their physical basis. The eventual hope, of course, is for a merger of these two approaches into one unified theory of plasticity that will explain both the material behaviour and provide the engineer and scientist with the necessary tools for practical applications.

In short, plasticity is the behaviour of solid bodies in which they deform permanently under the action of external loads, whereas elasticity is the behaviour of solid bodies in which they return to their original shape when the external forces are removed. Actually, however, the elastic body is an idealisation, because all bodies exhibit more or less plastic behaviour even at the smallest loads. For the so-called elastic body, however, this permanent deformation is so small as to be practically not measurable, if the loads are sufficiently small. Plasticity theory thus concerns itself with situations in which the loads are sufficiently large so that measurable amount of permanent deformation occur.

The theory of plasticity can conveniently be divided into two ranges. At one end are metal-forming processes such as forging, extrusion, drawing, rolling, etc., which involve very large plastic strains and deformations. For these types of problems the elastic strains can usually be neglected and the material can be assumed to be perfectly plastic. At the other end of the scale there are a host of problems involving small plastic strains on the order of the elastic strains. These types of problems are of prime importance to the structural and machine designer. With the great premium currently placed on the saving of weight in aircraft, missile, and space applications, the designer can no longer use large factors of safety and "beef up" his design. He must design for maximum load to weight ratio, and this inevitably means designing into the plastic range.

1.2 JUSTIFICATION

Structural elements and machine components are so designed that the materials may never reach the yield point under the expected loading conditions. The magnitude of the stress, which causes the material to yield under uniaxial or combined loading, can be well predicted from the knowledge of various yield criteria. Once yielding starts, the material is said to be either in plastic or elastic-plastic condition depending on the type of loading and material used. If a bar is subjected to combined bending and torsion, yielding does not occur until the combined stress state reaches a critical value, i.e., the yield locus of that particular material. Upon reaching the yield locus,

if the material is subjected to further torsional or bending load beyond the combined yield stress, holding either the initial bending moment or torque constant or increasing both of them in a manner in which the subsequently applied parameter affects the magnitude of the initial applied parameters and behaviour of the material of the specimen requires careful study.

There are numerous examples where solid shafts are subjected to the combined bending and torsion actions. But examples of solid square bars subjected to combined bending and torsion are very few. In case of some machine tools, robots and machineries, solid square bars are subjected to the combined bending and torsion actions. In practice nearly all the shafts which transmit power have been subjected to an axial couple producing torsional shear stress and to bending actions due to their own weight or that of pulleys, or to the thrust or pull of cranks and belts producing flexural stress. The component stresses in the shaft will therefore be (1) shear stress due to torsion, on planes perpendicular to and planes through the axis; (2) tensile and compressive bending stresses parallel to the axis; (3) shear stresses resulting from bending forces, on planes parallel to and perpendicular to the axis. In shafts which are not very short, the maximum principal stresses will generally occur at the circumference of the shaft, where the tensile and compressive stresses on opposite sides reach equal and opposite maximum values; in this case, the shear stress resulting from the bending forces need not be taken into account, being zero at the circumference. Maximum stress occurs at the circumference of the shaft and the entire outermost surface first goes to inelastic state from the elastic state. With the increase of combined loading this inelastic region increases approaching towards the centre.

But in case of the solid square bar, maximum stress concentrates at some localised points at the outermost surface and these points first go to inelastic state from elastic state and with the increase of combined loading these inelastic regions increase in volume approaching towards the centre. So variation of the deformation as well as stiffness of the square bar in case of combined loading will be a little bit different than that of the circular bar. So what happen in the elastic as well as in the plastic

regions when solid square bar is subjected to combined bending and torsion needs careful study.

1.3 OBJECTIVES

The main objectives of this work are as follows:

a. To design and construct an experimental set-up in order to conduct the present investigation.
b. To examine combined loading required for plastic yielding of horizontal square solid bars at different ratios of bending moment to torque.
c. To examine different torques required for plastic yielding of horizontal square solid bars for different constant initial bending moments.
d. To examine different moments required for plastic yielding of horizontal square solid bars for different constant initial torques.
e. To study the elastic-plastic load-deformation relationship of the bars under combined bending and torsion taking into account the effects of initial loading conditions.
f. To study the inelastic behaviour of the bars under combined bending and torsion.

1.4 LAYOUT OF THE THESIS

For the convenience of presentation, the contents of this thesis are divided into five chapters. Chapter-1 contains introduction, justification and objectives of this work. Chapter-2 contains a brief discussion on the available literature related to the present investigation. Chapter-3 contains a brief discussion on the design of the experimental set-up, specimen selection, data acquisition equipment, auxiliary equipment and experimental procedure. Chapter-4 consists of results the present investigation. Conclusions and recommendations are presented in Chapter-5.

CHAPTER - 2
THEORY AND LITERATURE SURVEY

2.1 GENERAL

If it is desired to limit working stress to values, which leave a known margin within the elastic limit, for a material under simple tension, it is easy to limit this tension accordingly. But if there are other stresses as well, these may play a part in causing elastic breakdown. Thus while a simple tension of, say, 15 N per square meter may be the elastic limit in a particular material, breakdown may occur at a much lower tensile stress if the tension is accompanied by a compressive stress of, say, 10 N per square meter at right angles to the tension. So for combined loading the failure criteria may be different.

2.2 PREVIOUS WORK

Many structures are subjected to both bending and torsion actions. Appreciable research works have not been performed in regard to nonlinear elastic-plastic behaviour of solid member under combined bending and torsion. Very few experimental works are available till now regarding the biaxial combined bending and torsion of solid square bar, particularly within the plastic region of the material. For simplicity, in most cases, thin walled specimens have been used to investigate these types of loading [3-7]. Bathe and Wieser [8] have conducted theoretical investigations regarding the biaxial bending and torsion of channel section whereas Pi and Trahair [9] have conducted theoretical investigations regarding the biaxial bending and torsion of I-beam. Pi and Trahair have conducted their research to develop a theory considering material inelasticity based on incremental theory of plasticity using the von-Mises yield criteria. They have also investigated the effect of bracing on the plastic moment and torque. Zhao and Hancock [10] have researched with square and rectangular hollow section bar to investigate the effect of the bearing length on the failure loads in case of combined loading.

2.3 DEFINITION OF YIELD

Determination of yield point is dependent on the definition of yielding used. From a theoretical point of view, the yield point can be defined as the point where permanent deformation begins to start. However, experimentally it is difficult to determine this point. For this reason, researchers have drawn several conclusions from numerous investigations. The major discrepancies are caused by different materials used in the experiments and most importantly by the different definitions of yielding used in the investigation. The commonly used definitions are - (i) the yield point is the point for which the relation between the stress and the strain is linear – proportional limit method. This method is sensitive to the very earliest positive indication of yielding. (ii) The yield point is defined as the point for which a pre-determined amount of plastic strain is developed – proof strain method. Typically, a value of 0.2 % strain offset is accepted. This method is widely used in most engineering applications. (iii) The yield point is determined by backward extrapolation of stress-strain curve to intersect the elastic line, or to the line of zero plastic strain - Load extrapolation method. This method requires an excessive amount of overstrain to define a yield point.

In the present experimental investigations, the proportional limit method has been used to define the yield stresses of the materials, as the differences between the yield and the ultimate stresses of the materials investigated are not large enough because of over hardening.

2.4 YIELD CRITERIA FOR COMBINED LOADING

Much of the design of parts in mechanical and civil engineering is complicated due to biaxial or triaxial stresses for which some failure state has to be determined. Some examples are in the components of high-pressure cylinders containing liquids or gases, and concrete hinges for large bridge bearings. For more than a century, physicists, mathematicians, and engineers have been proposing various theories of failure. Some theories have been attempts to describe observed failure while a few have tried to base a mechanism on fundamental properties of materials. It is evident

that there is a considerable difference between the behaviour of ductile and brittle materials. That apart, it is quite difficult to determine failure with sufficient accuracy in experiments designed to show which failure theory is most applicable. Hence, it is frequently found that codes of practice play a vital role in determining the failure criteria.

Numerous criteria have been proposed for the yielding of solids. Many of these were originally suggested as criteria for failure of brittle materials and were later adopted as yield criteria for ductile materials. For combined loading the designers show interest to Maximum Shear Theory and Distortion Energy Theory.

Maximum Shear Theory or Tresca Criterion

This theory (sometimes called the Coulomb theory) assumes that yielding will occur when the maximum shear stress reaches the value of the maximum shear stress occurring under simple tension. The maximum shear stress is equal to half the difference between the maximum and minimum principal stresses. For simple tension, therefore, since $\sigma_2 = \sigma_3 = 0$, the maximum shear stress at yield is $1/2\ \sigma_Y$. The Tresca criterion then asserts that yielding will occur when any one of the following six conditions is reached:

$$\begin{aligned} \sigma_1 - \sigma_2 &= \pm \sigma_Y \\ \sigma_2 - \sigma_3 &= \pm \sigma_Y \\ \sigma_3 - \sigma_1 &= \pm \sigma_Y \end{aligned} \qquad (2.1)$$

For the bi-axial case with $\sigma_3 = 0$, we have

$$\begin{aligned} \sigma_1 - \sigma_2 &= \sigma_Y && \text{if } \sigma_1 > 0,\ \sigma_2 < 0 \\ \sigma_1 - \sigma_2 &= -\sigma_Y && \text{if } \sigma_1 < 0,\ \sigma_2 > 0 \\ \sigma_2 &= \sigma_Y && \text{if } \sigma_2 > \sigma_1 > 0 \\ \sigma_1 &= \sigma_Y && \text{if } \sigma_1 > \sigma_2 > 0 \\ \sigma_1 &= -\sigma_Y && \text{if } \sigma_1 < \sigma_2 < 0 \\ \sigma_2 &= -\sigma_Y && \text{if } \sigma_2 < \sigma_1 < 0 \end{aligned} \qquad (2.2)$$

A plot in the $\sigma_1\sigma_2$ plane for this yield criterion is shown in Figure 2.1.

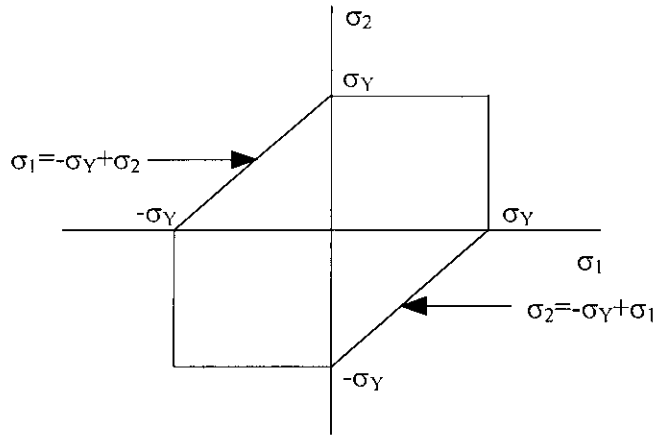

Figure 2.1: Maximum shear stress theory (From Meldenson [16].)

It is to be noted that one limitation of this theory is the requirement that the yield stresses in tension and compression be equal. The Tresca criterion is in fair agreement with experiment and is used to a considerable extent by designers. It suffers, however, from one major difficulty – it is necessary to know in advance which are the maximum and minimum principal stresses.

For the case of pure shear

$$\sigma_1 = -\sigma_2 = k \qquad \sigma_3 = 0$$

the Tresca criterion predicts yielding to occur when

$$\sigma_1 - \sigma_2 = 2k = \sigma_Y$$

or $$k = \frac{1}{2}\sigma_Y$$

That is, the yield stress in pure shear is ½ the yield stress in simple tension.

Distortion Energy Theory, or the von Mises Yield Criterion

The distortion energy theory (also associated with Hencky) assumes that yielding begins when the distortion energy equals the distortion energy at yield in simple tension. Thus

$$U_d = \frac{1}{2G} J_a = \frac{3}{4G} \tau^2_{oct}$$

at the yield point in simple tension

$$J_2 = \frac{1}{3} \sigma_Y^2$$

Therefore the yield condition becomes

$$\frac{1}{2}\left[(\sigma_1 - \sigma_2)^2 + (\sigma_2 - \sigma_3)^2 + (\sigma_3 - \sigma_1)^2\right] = \sigma_Y^2 \tag{2.3}$$

and, for the biaxial case,

$$\sigma_1^2 - \sigma_1\sigma_2 + \sigma_2^2 = \sigma_Y^2 \tag{2.4}$$

This plots as an ellipse, called the von Mises ellipse, in the $\sigma_1\sigma_2$ plane as shown in Figure 2.2.

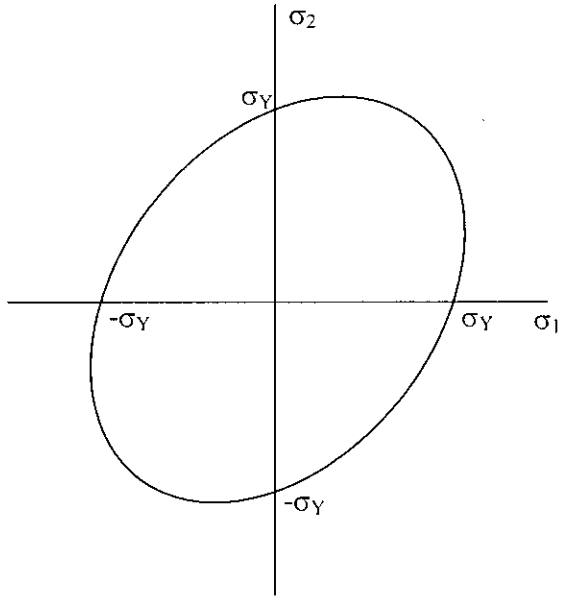

Figure 2.2: Distorsion energy theory (From Meldelson [16].)

For the case of pure shear

$$\sigma_1 = -\sigma_2 = k \qquad \sigma_3 = 0$$

$$J_2 = \frac{1}{6}\left[(\sigma_1 - \sigma_2)^2 + (\sigma_2 - \sigma_3)^2 + (\sigma_3 - \sigma_1)^2\right]$$

$$= \sigma_1^{\,2} = k^2$$

and the von Mises criterion would predict yielding to occur when

$$k^2 = \frac{1}{3}\sigma_Y^{\,2}$$

or $$k = \frac{1}{\sqrt{3}}\sigma_Y$$

That is, the yield stress in pure shear is $1/\sqrt{3}$ times the yield stress in simple tension. Thus the von Mises criterion predicts a pure shear yield stress that is about 15 percent higher than predicted by the Tresca criterion. The von Mises yield criterion usually fits (but not always) the experimental data better than the other theories, and it is usually easier to apply than the Tresca criterion because no knowledge is needed regarding the relative magnitude of the principal stresses. For these reasons, this criterion is widely used at the present time. If, however, the relative magnitudes of the principal stresses are known, as in the case of thick-walled tubes, the Tresca criterion is easier to apply.

von Mises originally proposed his criterion because of mathematical convenience. Hencky later showed that it was equivalent to assuming that yielding will take place when the distortion or shear strain energy reaches a critical value, as shown above. Also, since the octahedral shear stress is equal to

$$\tau_{oct} = \frac{1}{3}\sqrt{(\sigma_1 - \sigma_2)^2 + (\sigma_2 - \sigma_3)^2 + (\sigma_3 - \sigma_1)^2}$$

which for simple tension at yield becomes

$$\tau_{oct,Y} = \frac{\sqrt{2}}{3}\sigma_Y$$

then equation (2.3) can be written as

$$\tau_{oct} = \tau_{oct,Y}$$

That is, yielding will occur when the octahedral shear stress reaches the octahedral shear stress at yield in simple tension.

Alternatively, the criterion (2.3) can be looked upon as stating that yielding will occur when the second invariant J_2 of the stress deviator tensor reaches a critical value, i.e., the value of J_2 at yield in simple tension.

2.5 STRESS STRAIN RELATION

Elastic Stress-Strain Relation

The nominal stress, defined as the load divided by the original cross-sectional area, is plotted against the conventional or engineering strain, defined as the increase in length per unit original length. Nominal stress is represented by

$$\sigma_n = \frac{P}{A_o}$$

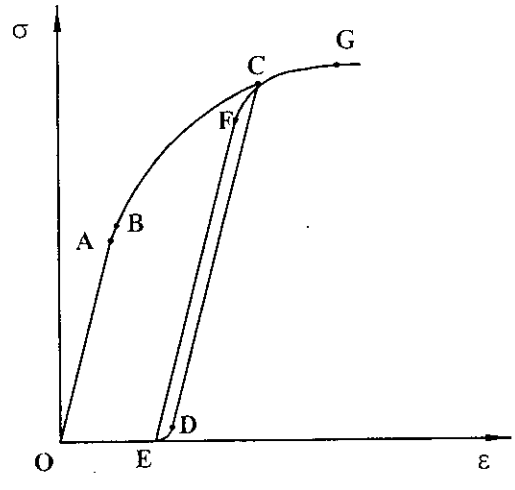

Figure 2.3: Stress-strain curve of metal with effects of unloading and reloading (From Chakrabarty [15].)

and conventional strain by

$$\varepsilon = \frac{l - l_o}{l_o}$$

Initially the relation between stress and strain is essentially linear. This linear part of the curve extends up to the point A as shown in Figure 2.3, which is called the proportional limit. It is in this range that the linear theory of elasticity, using Hooke's law is valid. Upon further increase of the load, the strain no longer increases linearly with stress, although the material still remains elastic; i.e., upon removal of the load the specimen returns to its original length. This condition prevails until some point B, called the elastic limit, or yield point, is reached. In most materials there is very little difference between the proportional limit and the elastic limit. Furthermore, the values of these points depend on the sensitivity of the measuring instruments. For some materials, the yield point is so poorly defined that it is arbitrarily taken to be at some fixed value of permanent strain, such as 0.2 percent. Beyond the elastic limit, permanent deformation, called plastic deformation, takes place.

Beyond the yield point, the stress continually increases with further plastic strain, while the slope of the stress-strain curve, representing the rate of strain-hardening, steadily decreases with increasing stress. If the specimen is stressed to some point C in the plastic range and the load is subsequently released, there is an elastic recovery following the path CD which is very nearly a straight line of slope E called Young's modulus of elasticity. The permanent strain that remains on complete unloading is equal to OE. On reapplication of the load, the specimen deforms elastically until a new yield point F is reached. Neglecting the hysteresis loop of narrow width formed during loading and unloading, F may be taken as coincident with C. On further loading, the stress-strain curve proceeds along FG, virtually as a continuation of the curve BC. The curve EFG may be regarded as the stress-strain curve of the metal when prestrained by the amount OE. The greater the degree of prestrain, the higher the new yield point and the flatter the strain-hardening curve. For a heavily prestrained metal, the rate of strain-hardening is so small that the material may be regarded as approximately nonhardening or ideally plastic.

Plastic Stress- Strain Relation

Whereas the strains are linearly related to the stresses by Hooke's law in the elastic range, the relation will generally be nonlinear in the plastic range, as is evident from the uniaxial stress-strain curve. A more complicated distinction between elastic and plastic stress-strain relations arises from the fact that whereas in the elastic range the strains are uniquely determined by the stresses, i.e., for a given set of stresses we can compute the strains directly using Hooke's law without any regard as to how this stress state was attained, in the plastic range the strains are in general not uniquely determined by the stresses but depend on the whole history of loading or how the stress state was reached.

Consider the initial yield curve to be as shown in Figure 2.4. Let the specimen be strained in uniaxial tension beyond the initial yield to some point C, where CDE defines the subsequent yield curve.

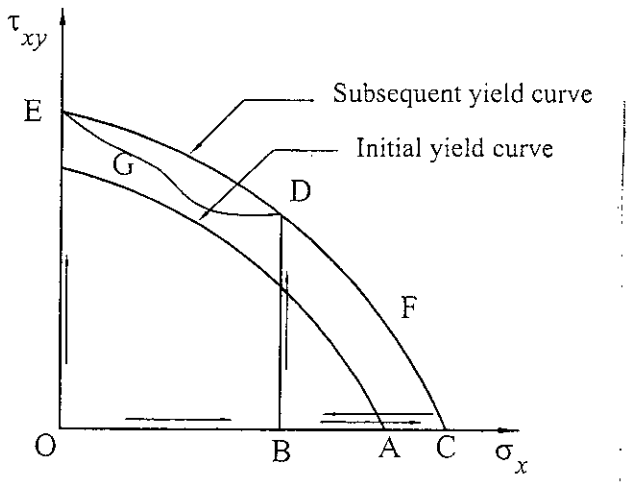

Figure 2.4: Effect of loading path on plastic strains (From Meldelson [16].)

The plastic strains will then be

$$\varepsilon_x^{\,p} = \varepsilon_p$$

$$\varepsilon_y{}^p = \varepsilon_z{}^p = -\frac{1}{2}\varepsilon_p$$

$$\varepsilon_{xy}{}^p = \varepsilon_{yz}{}^p = \varepsilon_{zx}{}^p = 0$$

Let the specimen now be unloaded to the point B and let us apply a shear stress increasing from B to D on the new yield locus. The plastic strains will still be as given above. Any other path could have been used in arriving at D from C such as OCFD, as long as we do not move outside the yield locus. Now suppose that the specimen were first stressed in shear to the point E on the new yield locus and then, by any other path inside EDC, such as EGD, were stressed to the point D. The plastic strains would be

$$\varepsilon^p{}_{xy} = \gamma_p$$

$$\varepsilon^p{}_x = \varepsilon^p{}_y = \varepsilon^p{}_z = \varepsilon^p{}_{xz} = \varepsilon^p{}_{yz} = 0$$

which is completely unrelated to the previous strain state. Thus even though the same stress state at D exists for both loading paths, and therefore the elastic strain states are the same, the plastic strain states are different.

Because of the above-illustrated dependence of the plastic strains on the loading path, it becomes necessary, in general, to compute the differentials or increments of plastic strain throughout the loading history and then obtain the total strains by integration or summation.

The first approach to plastic stress-strain relations was suggested by Saint-Venant in 1870, which proposed that the principal axes of strain increment coincided with the principal stress axes. The general three-dimensional equations relating the increments of total strain to the stress deviations were given by Levy in 1871 and independently by von Mises in 1913. These are known as the Levy-Mises equations. These equations are

$$\frac{d\varepsilon_x}{S_x} = \frac{d\varepsilon_y}{S_y} = \frac{d\varepsilon_z}{S_z} = \frac{d\varepsilon_{xy}}{\tau_{xy}} = \frac{d\varepsilon_{yz}}{\tau_{yz}} = \frac{d\varepsilon_{zx}}{\tau_{zx}} = d\lambda \qquad (2.5)$$

or $d\varepsilon_{ij} = S_{ij}\, d\lambda$

where S_{ij} is the stress deviator tensor and $d\lambda$ is a nonnegative constant which may vary throughout the loading history. In these equations the total strain increments are assumed to be equal to the plastic strain increments, the elastic strains being ignored. Thus these equations can only be applied to problems of large plastic flow and cannot be used in the elastoplastic range. The generalisation of equations (2.5) to include both elastic and plastic components of strain is due to Prandtl and Reuss and is known as the Prandtl-Reuss equations.

Reuss assumed that the plastic strain increment at any instant of loading is proportional to the instantaneous stress deviation; i.e.,

$$\frac{d\varepsilon^{p}_{x}}{S_x} = \frac{d\varepsilon^{p}_{y}}{S_y} = \frac{d\varepsilon^{p}_{z}}{S_z} = \frac{d\varepsilon^{p}_{xy}}{\tau_{xy}} = \frac{d\varepsilon^{p}_{yz}}{\tau_{yz}} = \frac{d\varepsilon^{p}_{zx}}{\tau_{zx}} = d\lambda \qquad (2.6)$$

Or $d\varepsilon^{p}_{ij} = S_{ij} d\lambda$

Equations (2.5) can then be considered as a special case of (2.6) where the elastic strain components are neglected.

Equations (2.6) state that the increments of plastic strain depend on the current values of the deviatoric stress state, and not on the stress increment required to reach this state.

2.6 THE PLANE STRESS YIELD LOCUS

Tresca Criterion:

$$\sigma_1 - \sigma_2 = \pm \sigma_Y$$

$$\sigma_1 = \pm\sigma_Y$$

$$\sigma_2 = \pm\sigma_Y$$

and Von Mises Criterion:

$$\sigma_1^{\,2} - \sigma_1\sigma_2 + \sigma_2^{\,2} = \sigma_Y^{\,2}$$

For Tresca Criterion when $\sigma_x\sigma_y \le \tau_{xy}^{\,2}$, is

$$(\sigma_1 - \sigma_2) = \pm\sigma_Y$$

or $$(\sigma_1 - \sigma_2)^2 = \sigma_Y^{\,2}$$

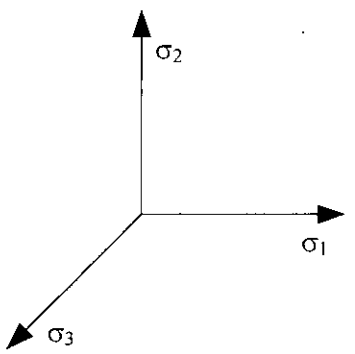

Figure 2.5: Direction of the principal stresses

or $$(\sigma_x - \sigma_y)^2 + 4\tau_{xy} = \sigma_Y^2 \tag{2.7}$$

When $\sigma_x \sigma_y \geq \tau_{xy}^2$ then

$$(\sigma_1 \mp \sigma_Y)(\sigma_2 \mp \sigma_Y) = 0$$

or $$\sigma_1\sigma_2 \pm \sigma_1\sigma_Y \pm \sigma_2\sigma_Y = \sigma_Y^2$$

or $$\sigma_1\sigma_2 \pm \sigma_Y(\sigma_1 + \sigma_2) = \sigma_Y^2$$

or $$(\sigma_x\sigma_y - \tau_{xy}^2) \pm \sigma_Y(\sigma_x + \sigma_y) = \sigma_Y^2$$

The Mises criterion:

$$\sigma_1^2 - \sigma_1\sigma_2 + \sigma_2^2 = \sigma_Y^2$$

or $$(\sigma_1 + \sigma_2)^2 - 3\sigma_1\sigma_2 = \sigma_Y^2$$

or $$(\sigma_x + \sigma_y)^2 - 3\sigma_x\sigma_y + 3\tau_{xy}^2 = \sigma_Y^2$$

or $$\sigma_x^2 - \sigma_x\sigma_y + \sigma_y^2 + 3\tau_{xy}^2 = \sigma_Y^2 \tag{2.8}$$

For combined loading (i.e. bending and torsion) where longitudinal stress σ and shear stress τ present then $\sigma_x = \sigma, \sigma_y = 0, \tau_{xy} = \tau$

So equation (2.7) and (2.8) become

$$\sigma^2 + \alpha\tau^2 = \sigma_Y^2 \tag{2.9}$$

where $\alpha = 4$ for Tresca criterion and $\alpha = 3$ for von Mises criterion.

2.7 LOWER BOUND APPROXIMATIONS

The rate of work of the external forces is given by

$$W = \iint \left[\tau_{xz} v_x + \tau_{yz} v_y + \sigma_z v_z\right] dxdy \tag{2.10}$$

The rate of work of the external forces given by equation (2.10) is either less or equal to the rate of work performed by the actual external forces. This enables us to find lower bounds for bending moment M and torque T, i.e., we can select an admissible stress system and be assured that the M and T computed from these stresses is always

a combination which is less than or equal to the actual initial combination causing yield.

Let T_0 denote the fully plastic torque under pure torsion, and M_0 the fully plastic moment under pure bending about the considered axes of symmetry. The former is associated with a shear stress of magnitude k throughout the cross section, while the latter involves normal stresses $\pm\sqrt{3}\,k$ on opposite sides of the neutral plane. To obtain a lower bound on the yield point couples under combined loading, we assume a distribution of constant shear stress $\tau < k$ similar to that in pure torsion, and combine this with a distribution of normal stress of constant magnitude $\sigma < \sqrt{3}\,k$ similar to that in pure bending. Then

$$\frac{T}{T_0} = \frac{\tau}{k} \quad \text{and} \quad \frac{M}{M_0} = \frac{\sigma}{\sqrt{3k}}$$

Since the fictitious stress state must not violate the yield criterion, the best approximation corresponds to $\sigma^2 + 3\tau^2 = 3k^2$, which gives

$$\left(\frac{T}{T_0}\right)^2 + \left(\frac{M}{M_0}\right)^2 = 1 \qquad (2.11)$$

2.8 TORSION IN THE SOLID CIRCULAR AND SQUARE BARS

When circular bars are subjected to torsional loading it is assumed that

(a) Plane sections remain plane

(b) The shearing strain γ varies linearly from the centerline of the bar.

(c) Shearing stress τ is related to γ through the shear modulus, G and hence varies linearly from zero at the center to a maximum at the surface as shown in Figure 2.6 (a).

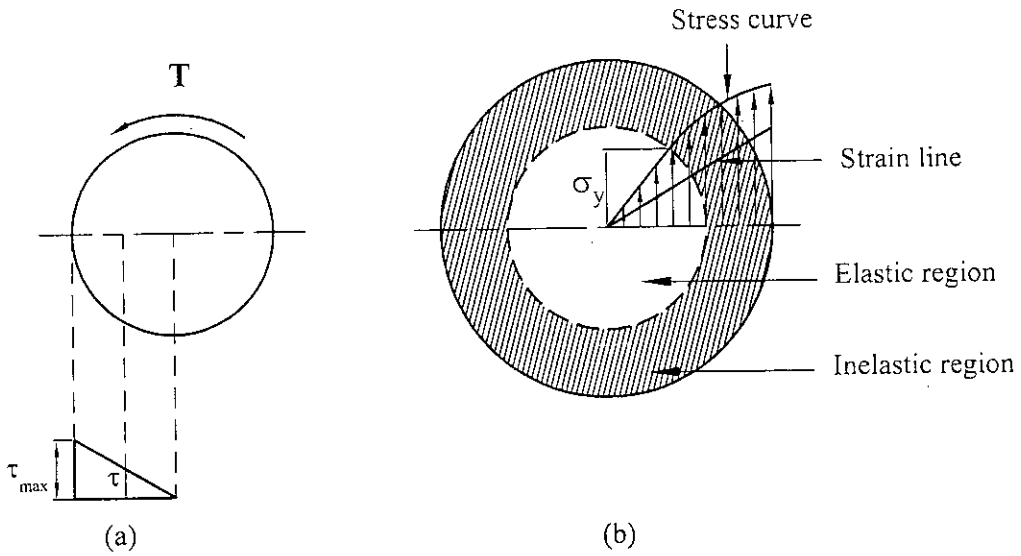

Figure 2.6: Circular bar in torsion. (a) Stress distribution (b) Elastic plastic regions (From Bowes et al. [19].)

Conditions (b) and (c) are applicable up to the elastic limit. Since maximum shear stress occurs at the circumference of the bars so when torsional loads are gradually increased beyond the elastic limit the outer most section of the bar first goes to plastic range and as the loads continue to increase the plastic region increases reducing the elastic region. In the plastic region, stress is not proportional to strain and thus stress does not vary linearly with distance from the centre. The variation in stress and strain then takes a path as shown in Figure 2.6 (b). The shape of the portion of the stress curve in the plastic region will depend on the plastic stress-strain relationship. In the elastic limit of the circular bar, angle of twist and developed stress are express as follows:

$$\text{Angle of twist, } \theta = \frac{TL}{GJ} \tag{2.12}$$

$$\text{Stress, } \tau_{max} = \frac{Tr}{J} \tag{2.13}$$

But in case of square bar the situation is vastly different from the case of a circular bar. The greatest torsional stress occurs at the midpoints of the sides and at the

corners there is zero stress, which has been shown schematically in Figure 2.7 (a). Besides plane section does not remain plane in case of square bar. So application of the circular-shaft formulas to square sections will give meaningless results.

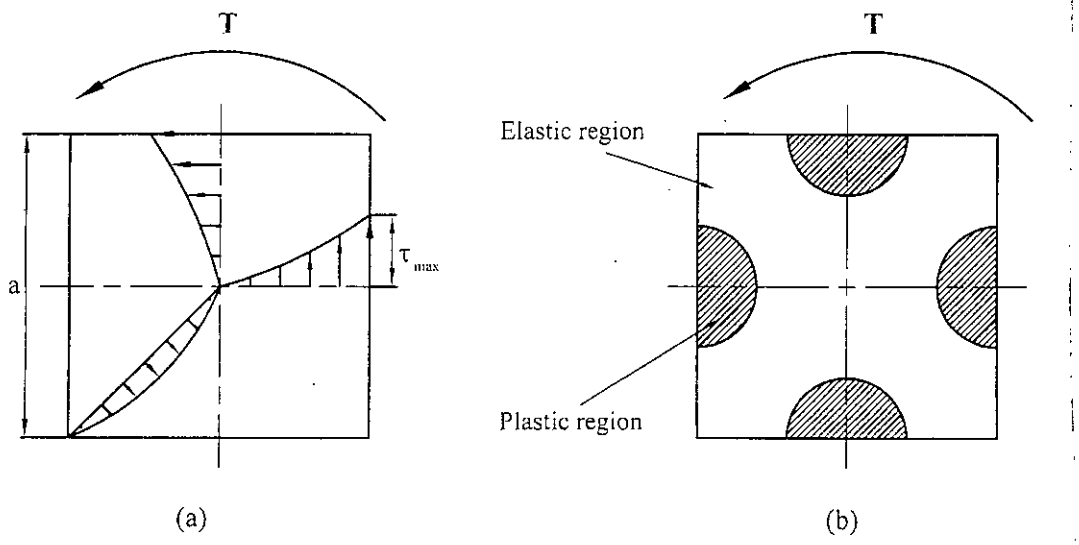

Figure 2.7: Square bar in torsion. (a) Stress distribution (b) Elastic plastic regions (From Bowes et al. [19].)

The correct solution to the square cross section in torsion can be found either by the membrane analogy or by using the theory of elasticity. By either method the following formulas can be derived:

$$\theta = \frac{TL}{k_1 G a^4} \tag{2.14}$$

$$\tau_{max} = \frac{T}{k_2 a^3} \tag{2.15}$$

where $k_1 = 0.141$ and $k_2 = 0.208$ (From Boresi et al. [20].)

Since in case of a solid square bar for a given torque maximum shear stress occur at the midpoints of the sides of the bar so if the torque is increased then at first the midpoints go to the plastic range. With further increase of the torque this plastic region increases towards the centre of the bar as shown in Figure 2.7 (b).

2.9 BEAM FIXED AT BOTH ENDS

When a concentrated load is applied at the midspan of a beam whose both ends are fixed, two restraint moments and two reactions are developed at the ends of the beam as shown in Figure 2.8. Because of the symmetrical loading condition imposed upon the beam, maximum deflection and maximum moment occur at the midspan of the beam. As a result, maximum flexural stress occurs at the midspan of the beam, obviously at the outer most fibre. For both ends fixed beam

$$\text{Maximum moment, } M_{\max} = -\frac{FL}{8} + \frac{FL}{4} = \frac{FL}{8} \tag{2.16}$$

$$\text{Maximum deflection, } \delta_{\max} = \frac{FL^3}{192EI} \tag{2.17}$$

$$\text{Flexural stress, } \sigma = \frac{Mc}{I} \tag{2.18}$$

But in case of a partially restrained beam, whose ends are not perfectly fixed, the magnitude of the restraint moments decrease and consequently magnitude of the maximum moment (i.e. midpoint moment of the beam) and maximum deflection (i.e., midpoint deflection of the beam) increase for a particular load.

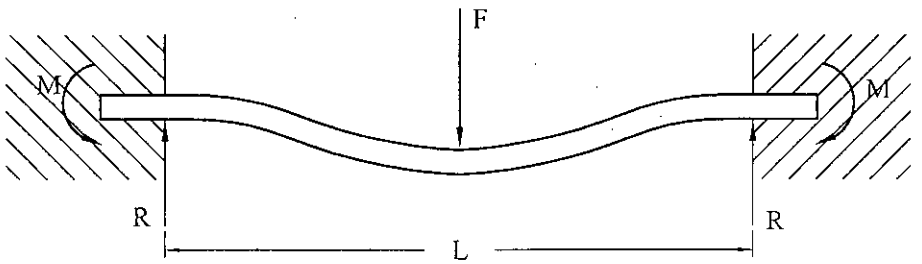

Figure 2.8: Both ends fixed beam with concentrated load (From Olsen [21].)

So in case of partially restrained beam, a correction factor for end conditions is introduced in equations (2.16) and (2.17) whose value depends on the level of fixing of the ends of the -beam. So the corrected equations for partially restraint beam are as follows:

$$\text{Maximum moment, } M_{max} = -\frac{FL}{8x} + \frac{FL}{4} \tag{2.19}$$

$$\text{Maximum deflection, } \delta_{max} = \frac{FL^3 x}{192EI} \tag{2.20}$$

Where x is the correction factor for the end condition of the beam.

CHAPTER – 3
DESIGN OF TEST RIG, SPECIMEN SELECTION AND EXPERIMENTAL PROCEDURE

3.1 GENERAL

An experimental test rig along with the auxiliary components/parts was designed and fabricated to perform this work. This apparatus with its different features extends the range of experiments to cover virtually all requirements relating to pure bending, pure torsion and combined bending and torsion loadings. Its basic unit provides facilities for supporting horizontal bars on fixed supports, applying concentrated loads, and measuring beam deflections and twist angles. The details of the test rig and experimental procedures are discussed in this chapter.

3.2 DESCRIPTION OF THE TEST RIG

The experimental test rig, which was designed and fabricated for this research work, is shown in Figures 3.1 to 3.3 and Photographs 1 to 6 of Appendix C. The main frame of the apparatus consisted of two I-section columns with welded cross-angle bars, two separators, and four loading shafts with bush and sprocket. The hydraulic jack with its base plates was placed on the separators. Base plates of the specimen were screwed in the I-section columns at a height of 1030 mm. The specimen was placed on these base plates and clamped with clamping plates. A loading wheel was placed in the mid point of the specimen in such a manner that no slipping would occur. Two magnetic dial gauges were placed under the flat plates of the loading wheel in such a way that their floating shafts could touch the flat plates. From the readings of the two dial gauges, deflections and angles of twist of the specimens were determined. Other devices of the apparatus were loading chains, clamps, hexagonal nuts, dead weights etc.

3.3 DETAILS OF THE COMPONENTS

I-Section Column

Figure 3.4 represents the schematic diagram of I-section columns with cross bars, loading shafts and separators. They act as the main supports for other devices of the setup. The columns stood on flat plates of dimensions 300 mm × 300 mm × 10 mm. On one side of the flat plates an angle bar of 300 mm length was welded so that the test rig did not tilt in case of differential loadings. The length of the column was 1220 mm and the dimensions of its flange were 120 mm × 60 mm × 8 mm. The material of the columns was mild steel.

Separators

Schematic diagram of the separators is shown in Figure 3.4. Separators were 50 mm angle bars. The thickness and length of the bars were 5 mm and 915 mm respectively. The functions of the separators were to hold the I-section columns at a certain distance, to support the base plate of the hydraulic jack and table of the magnetic dial gauge. The separators were screwed to the I-section columns. At one end of the separators, there was one hole but at the other end, there were three holes at different distance in order to keep options to change the distance between the I-section columns. The distance between the columns depends on the strength of the materials of the specimen. If a strong material was used, then the distance should be large and if a weak material was used, then the distance should be small. In this research work the distance between the columns was 768 mm, which was kept constant throughout all the experiments. The material of the separators was mild steel.

Crossbar

Figure 3.4 represents the schematic diagram of the cross bars. The function of the crossbars was to support the loading shaft. The lengths of the upper and lower crossbars were 750 mm and 600 mm respectively. At each end of the bar there were 10 mm slots for proper positioning and clamping of the loading shafts with the cross bars. Material of the cross bars was mild steel.

Loading Shaft

The schematic diagram of the loading shaft is shown in Figure-3.4. Four loading shafts were used in the test rig. Length and diameter of the shaft were 915 mm and 25 mm respectively. In the middle of the shaft there were bush and sprocket. The pitch circle diameter and the number of teeth of the sprocket were 85 mm and 22 respectively. The functions of the loading shafts were to apply load to the loading wheel with the help of dead weights and restrain the lateral movement of the I-section columns.

Lever–arm Plate

Figure-3.5 represents the schematic diagram of the lever-arm plate. Its dimensions were 610 mm × 120 mm × 7 mm. It was used to get mechanical advantages in producing downward load. One end of the plate was placed on the shaft of the hydraulic jack and the other end transferred load to the loading wheel through chain. A 120 mm × 50 mm × 7 mm plate was welded at 45^0 at the end that was placed on the shaft of the hydraulic jack. Due to this inclined plate, slip between the shaft of the hydraulic jack and the lever-arm plate was restrained, and as a result, the hydraulic jack could give more loads to the loading wheel. Material of the lever-arm plate was mild steel.

Stand Plate

The schematic diagram of the stand plates is shown the Figure 3.5. They were placed on the base plate with the hydraulic jack. There was a 30 mm hole in each plate at a height of 170 mm from the base plate to hold the fulcrum of the lever arm plate. Material of the stand plate was mild steel.

Hydraulic Jack

One hydraulic jack made by a Chinese company named Corp Ltd., was used to power the lever-arm plate.

The specification of the hydraulic jack was as follows:

Capacity: 5 ton

Body: Diameter- 70 mm

Height- 180 mm

Shaft: Length- 115 mm

Diameter- 34 mm

Trade Mark: Golden Gear.

Loading Wheel

Figure-3.6 represents the schematic diagram of the loading wheel. It consisted of three components; inner ring, intermediate ring and outer ring. In the inner ring, an 8 mm by 8 mm slot was cut so that the specimen could firmly pass through it. Diameter and thickness of this ring were 25 mm and 6.5 mm respectively and its material was high carbon steel so that it could resist wear due to abrasion or friction. The thickness was kept small so that the applied load could concentrate on the specimen. The inner ring was placed inside the intermediate ring and these two rings were placed inside the outer ring. A total of 44 teeth were cut in the outer ring with a pitch circle diameter of 180 mm. In the interface of the inner and intermediate rings, two screws were placed so that there could not be any slip between them and due to this interfacing system the inner ring could be replaced easily when its slot became large. The construction of the intermediate ring was slightly different than that of the other two rings. The thickness of the intermediate ring was kept 6.5 mm up to the radius of 25 mm, and then it was increased to 9 mm. This increased thickness continued up to the radius of 30 mm and then it was reduced to 3 mm removing metal from one side of the ring. This reduced thickness continued up to the outer diameter (120 mm) of the ring and it was done for proper placement of the intermediate ring with the outer ring. The inner radius of the outer ring was 30 mm and it was tightened with the intermediate ring with the help of 4 screws. In the outer ring, there were 8 holes of 3 mm diameter and these were equally placed at a radial distance of 82 mm so that chains and wire rope could be attached to the loading wheel easily. Material of the intermediate and the outer ring was mild steel and weight of the wheel was 8.83 N.

Flat Plate

The schematic diagram of the flat plate is shown in the Figure 3.7. The dimensions of these plates were 135 mm × 32 mm × 4.5 mm. There were 5 holes of 3 mm diameter in each plate for proper positioning of the tip of the needle of the magnetic dial gauge so that slip could not occur between the plate and the needle. The plates were axially welded at the loading wheel at a radius of 73 mm keeping them just diametrically opposite to each other. With the increase of the twisting angle of the specimen i. e., when it became approximately 12-14 degrees it was observed that slipping occured between the plate and the needle of the dial gauge. To overcome this problem a thin metal strip was welded at one side of the plate as shown in the figure. In that case the magnetic dial gauge was so placed that its tip of the needle could touch at the interface of the plate and strip. The dimensions of the strip were 110 mm × 25 mm × 1.5 mm.

Base and Clamping Plate of Specimen

Figure 3.8 shows the schematic diagram of the base and clamping plate of the specimen. The base plates were firmly screwed to the I-section columns at a height of 1030 mm. To increase the strength of the base plate its cross section was gradually increased from the free end to the fixed end. The dimensions of the clamping plate were 75 mm × 50 mm × 8 mm. In the clamping plate a slot of 8 mm by 3 mm was cut along the width of the plate, as shown in the figure, for proper clamping of the end of the specimen. The clamping plates were clamped with the base plates with the help of bolts.

Clamp

Clamps were used to clamp the loading shafts with the cross bars. At the end of each clamp there was a hole of 10 mm diameter for the bolt. The material of the clamp was mild steel.

Wooden Platform

Two wooden platforms were used in the test rig to put the dead weights on them. Weight of each wooden platform was 11.77 N.

Chain

In this experiment two chains were used to transfer the load from the lever-arm plate and the wooden platform to the loading wheel. These were made by a Taiwan company of grade *k m c* 420. The lengths of the chain were 2500 mm and 2200 mm respectively. The weight per unit length of the chain was 5.54 N/m.

Other Accessories

Other mentionable accessories used in this experimental set-up are as follows:

- Dead weights (made by S. B. M. Co. Ltd., Bangladesh)
- Wire rope of 3 mm diameter
- Wire rope clamps
- Nuts
- Bolts
- Hacksaw
- Adjustable wrench
- Pliers etc.

3.4 SPECIMEN

Schematic diagram of the specimen is shown in Figure 3.9. The cross section of the specimen was 8 mm by 8 mm and its length was 710 mm. Such cross section was chosen depending on the availability in the local market and load required to fail it. If the length of the specimen was made too large, then the weight of the loading wheel could considerably affect the yielding of the specimen. On the other hand, if the length of the specimen was made too short then more loads would be required to yield it and the space would also be congested to place dial gauges and others accessories. Considering these factors the length of the specimen was chosen as

mentioned above. The entire specimen came from the same long bar. The chemical compositions of the specimen are shown in Appendix-A.

3.5 DATA ACQUISITION EQUIPEMENT

Dial Gauge

Two dial gauges were used in the experiment to measure the vertical displacement of the flat plate of the loading wheel, from which midpoint deflection and twisting angle of the specimen were calculated.

The specifications of the dial gauges were as follows:

Dial Gauge – 1: Range 0.1-30 mm
No. – 2416
Company – Mitutoyo Co. Ltd., Japan.

Dial Gauge – 2: Range 0.001-3.0 inches
No. – 4887
Company – Mitutoyo Co. Ltd., Japan.

Spring Balance

Spring balance was used to indicate the amount of applied load to the loading wheel with the help of hydraulic jack. The specifications of the spring balance were as follows:

Motorcar Brand
Range 0.5 - 100 kg
Code No. 880127
Made in China.

3.6 AUXILIARY EQUIPMENT

Universal Testing Machine

A 100-ton capacity universal testing machine, situated at the SM Laboratory of Mechanical Engineering Department of BUET, was used to conduct the uniaxial tensile test of the virgin specimen to find out the tensile yield point, modulus of elasticity and percentage of elongation. It was hydraulically operated. An extensometer of range 0.1-30 mm was used to measure the deformed strain of the specimen.

Torsion Testing Machine

A torsion testing machine (SM1 mkII), situated at the Applied Mechanics Laboratory of Mechanical Engineering Department of BUET, was used to carry out the torsion test of the specimen to find out the shear yield point, modulus of rigidity of the material of the specimen. Its maximum torque applying capacity was 30 N.m and was capable of applying torque in both forward and reverse directions. It had a digital torque meter to record the applied torque and could be used for wide range of standard test specimens. It was electro-mechanically operated and could be used to measure the angle of twist with respect to applied torque.

3.7 EXPERIMENTAL PROCEDURE

3.7.1 Preliminary Test

Two preliminary tests were performed to know the mechanical properties of the material of the virgin specimen. These two tests were uniaxial tension test and torsion test.

Uniaxial Tension Test

The monotonic tension test is the most common testing methodology for determining the mechanical properties of metals. It is a very common testing procedure for quality control and specification validation. The objective of this test is to determine

yield strength, ultimate strength, proportional limit, % elongation at fracture and % reduction of area. But in this research work last two properties were not determined. The uniaxial tension test was carried out according to ASTM A 370-98 standard. The test was performed using universal testing machine, which is situated at the SM Laboratory of Mechanical Engineering Department of BUET. First of all, the specimen was held in the testing machine crossheads using wedge type grippers. Then extensometer was attached to the specimen so that its two extended arms indicated the specified gauge length. Initially the load readings and extensometer readings were made zero. Then uniaxial tensile load was gradually applied to the specimen and the corresponding extensometer reading was recorded. Stress and strain were calculated from the applied load and the extensometer reading respectively.

Torsion Test

The objective of this test is to determine the relationship between the angle of twist and the applied torque. In this research work, torsion yield strength and modulus of rigidity were determined from this test. The test was carried out according to ASTM E 143-99 standard. The test was performed using the torsion machine (SM1 mkII), situated at the Applied Mechanics Laboratory of Mechanical Engineering Department of BUET. The torque applied to the specimen was reacted by a torsion shaft at each end by self-aligning bearings. Test specimens were held at each end by hexagonal drive sockets, which were fitted on the gearbox output and torsion shafts. An arm was fitted to each end of the torsion shaft, the one at the far end being located by a turnbuckle and hand wheel for adjusting the angular position of the torsion shaft.

The arm at the inner end supported a dial gauge and could be adjusted using the turnbuckle to maintain one end of the specimen in a fixed position during the test. A linear potentiometer was fitted between the two arms and provided an output proportional to the angle of twist of the torsion shaft. The potentiometer was connected to a digital meter, which read directly in N. m and lb. in. A calibration

arm, weight hanger and weights were available for checking or re-calibrating the meter if required.

3.7.2 COMBINED LOADING ON TEST RIG

Two types of combined loading were studied in this research work. One was proportional loading and the other non-proportional loading.

3.7.2.1 Proportional Loading

In proportional loading, the ratio of bending moment to torque (i.e., M/T) was kept constant. In this work six ratios were studied. These were 0 (pure torsion), 0.56, 1.12, 2.24, 3.36 and ∞ (pure bending). Among these ratios, ratios 0 and ∞ were studied merely to justify the accuracy of the test rig and these two tests were treated as calibration tests.

Combined Loading of M/T = 0 (Pure Torsion)

At first the specimen was inserted in the loading wheel so that the wheel was firmly placed at the midspan of the specimen. Since this fit was interference type, the insertion of the specimen was done with the help of a hydraulic press. The test specimen with the loading wheel was then placed on steel base plates which were bolted in I section column at a height of 1030 mm. The two ends of the specimen were firmly clamped with the help of clamping plates and bolts. The setting of the specimen in the test rig was done by the above-mentioned procedure for all experiments. Then, one end of each chain was attached in the loading wheel, as shown in Figure 3.10 and Photograph 2. The chain, by which the upward load was applied, was passed over one of the upper sprockets situated in one of the upper loading shafts. In the other end of this chain, wooden platform was attached so that dead weights could be placed on it.

Other chain that produced downward load was attached to the upper hook of the spring balance. The lower hook of the spring balance was linked with the lever arm

plate. When the lever arm plate was powered by the hydraulic jack, a downward load was resulted which was eventually transferred to the loading wheel. It was also possible to produce the downward load using wooden platform and dead weights instead of using hydraulic jack and spring balance. One dial gauge was placed under the flat plate of the loading wheel so that its floating shaft could touch the flat plate. The reading of the dial gauge was set to zero when the spring balance's load was such that the summation of the load and its self-weight was equal to the summation of the weight of the suspended chain and the wooden platform. Then equal and opposite loads were gradually applied to the loading wheel by the dead weights and the hydraulic jack, and corresponding dial gauge readings were recorded. Initially, load was applied at a higher rate and when it was observed that the specimen had been reached at the yield point, then load was applied at a slower rate. Torques and angles of twist were determined from the torsional loads and dial gauge readings respectively.

Combined Loading of M/T = $\propto$(Pure Bending)

In case of pure bending, no chain was attached to the loading wheel. Here the upper hook of the spring balance was attached to the loading wheel with the help of wire rope as shown in Figure 3.11 and Photograph 3. The lower hook of the spring balance was linked with the lever arm plate. The wire rope was attached to the loading wheel in such a way that the downward load was always directed toward the centre of the wheel, though there was rotation of the loading wheel (when present in case of combined loading).

One dial gauge was placed under the flat plate of the loading wheel so that its floating shaft could touch the flat plate. At the start of the experiment, readings of the dial gauge and spring balance were set to zero. Then downward bending load was gradually applied to the loading wheel with the help of hydraulic jack and at the same time dial gauge and spring balance readings were recorded. Bending moments and midpoint deflections were calculated from the spring balance readings and the dial gauge readings respectively.

Combined Loading of M/T = 0.56

The experimental arrangement of combined loading with M/T ratio of 0.56, 1.12, 2.24 and 3.36 was similar to that of pure torsion. The difference was that in case of pure torsion the upward and downward loads were equal but in case of above-mentioned combined loadings these were not equal. Even in some cases both the loads were downward or only one downward load was present. Other difference was that in case of pure torsion only one dial gauge under one flat plate of loading wheel was sufficient to measure the twisting angle of the loading wheel, but in case of those types of combined loadings two dial gauges under two flat plates were needed to measure the twisting angle and vertical deflection of the loading wheel.

The arrangement of the combined loading of M/T = 0.56 is shown in Figure 3.10 and Photograph 2. Here the magnitude of the downward load was three times of that of the upward load as shown in Figure 3.16, i.e., when the upward load was 1 N then the downward load was 3 N and when the upward load was increased to 2 N then the downward load was increased to 6 N. The downward load was produced by the hydraulic jack and the upward load was produced by dead weights placed on the wooden platform. Initially the load produced by the hydraulic jack was such that the summation of the load and its self-weight was equal to three times of the summation of the weight of the chain and wooden platform. Then two dial gauges were placed under two flat plates and their readings were made equal to zero. After that opposite loads were produced by the dead weights and the hydraulic jack and the corresponding dial gauge readings were recorded. From the dial gauges' readings, midpoint deflections and angles of twist of the specimen were calculated while from the differential loads as shown in Figure 3.16, bending moment and torque were calculated.

Combined Loading of M/T = 1.12

The arrangement of this type of loading is shown in Figure 3.12 and Photograph 4. In this loading condition only one downward load was present as shown in Figure 3.17. Here the downward load was produced with the help of hydraulic jack. Two dial gauges were placed under two flat plates and their readings were made equal to zero

when the hydraulic jack produced no load. Then downward load was gradually applied to the loading wheel with the help of the hydraulic jack and the corresponding dial gauge readings were recorded. From the dial gauges' readings, midpoint deflections and angles of twist of the specimen were calculated whereas from the downward load, bending moment and torque were calculated.

Combined Loading of M/T = 2.24

The arrangement of this type of loading is shown in Figure 3.13 and Photograph 5. In this loading condition both the loads were downward. But the magnitude of one downward load was three times of that of other load, as shown in Figure 3.18, i.e., when one downward load was 1 N then the other was 3 N and when one downward load was increased to 2 N then the other was increased to 6 N. Hydraulic jack produced the higher downward load while dead weights on the wooden platform produced the lower downward load. Initially the load produced by the hydraulic jack was such that the summation of the load and its self-weight was equal to three times of the summation of the weight of the chain and wooden platform. Then two dial gauges were placed under two flat plates and their readings were made equal to zero. After that, differential downward loads were gradually applied to the loading wheel and the corresponding dial gauge readings were recorded. From the dial gauges' readings, midpoint deflections and angles of twist of the specimen were calculated while from the differential loads as shown in Figure 3.18, bending moment and torque were calculated.

Combined Loading of M/T = 3.36

The loading arrangement of M/T = 3.36 was similar to that of M/T = 2.24. In this loading condition both the loads were also downward. But the magnitude of one downward load was twice of that of other as shown in Figure 3.19, i.e., when one downward load was 1 N then the other was 2 N and when one downward load was increased to 2 N then the other was increased to 4 N. Hydraulic jack produced the higher downward load while the dead weights on the wooden platform produced the lower downward load. Initially the load produced by the hydraulic jack was such that

the summation of the load and its self-weight was equal to twice of the summation of the weight of the chain and wooden platform. Then two dial gauges were placed under two flat plates and their readings were made equal to zero. After that, differential downward loads were gradually applied to the loading wheel and the corresponding dial gauge readings were recorded. From the dial gauges' readings, midpoint deflections and angles of twist of the specimen while from differential loads, bending moment and torque were calculated.

3.7.2.2 Non-Proportional Loading

In non-proportional loading the ratio of bending moment to torque was not kept constant. Two types of non-proportional loading arrangements were studied in this research work.

1) In the first type of non-proportional combined loading, different levels of torque were initially applied and keeping each of these torques constant, bending load was gradually applied.
2) In the second type of non-proportional combined loading, different levels of bending moment were initially applied and keeping each of these moments constant, torsional load was gradually applied.

Combined Loading Maintaining Constant Initial Torque

In this type of loading arrangement three loading conditions were studied. In each condition certain amount of torque was initially applied to the specimen and keeping each of these initial torques constant, bending load was gradually applied to it. Initial torque was applied with the help of dead weights using wooden platform and chains, while bending loads were applied using hydraulic jack as shown in Figure 3.20 and Photograph 6. Three initial torques were 25 %, 50 % and 75 % of yield torque of pure torsion. One dial gauge was placed under one flat plate to measure the midpoint deflections of the specimen. The loading pattern for this type of non-proportional combined loading is shown in Figure 3.21.

Combined Loading Maintaining Constant Initial Bending Moment

Three loading conditions were also studied in this type of loading arrangement. In each condition certain amount of bending moment was initially applied to the specimen and keeping each of these bending moments constant, torsional load was gradually applied to it. Initial bending load was applied with the help of hydraulic jack while torsional loads were applied by dead weights using wooden platform and chains as shown in Figure 3.20 and Photograph 6. Three initial bending moments were 25 %, 50 % and 75% of yield bending moment of pure bending. One dial gauge was placed under one flat plate to measure the angles of twist of the specimen. The loading pattern of this type of non-proportional combined loading is shown in Figure 3.22.

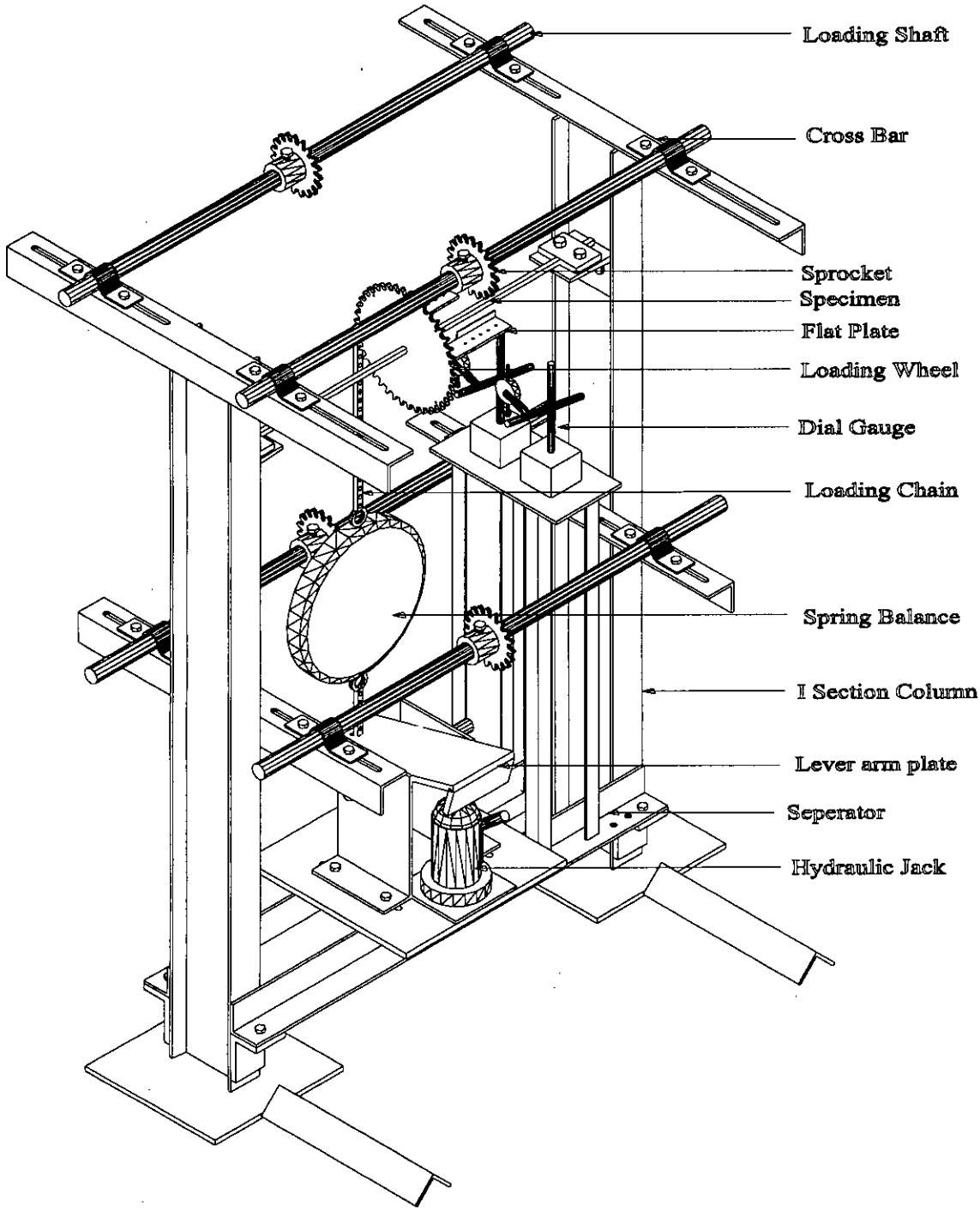

Figure 3.1: Isometric view of the test rig

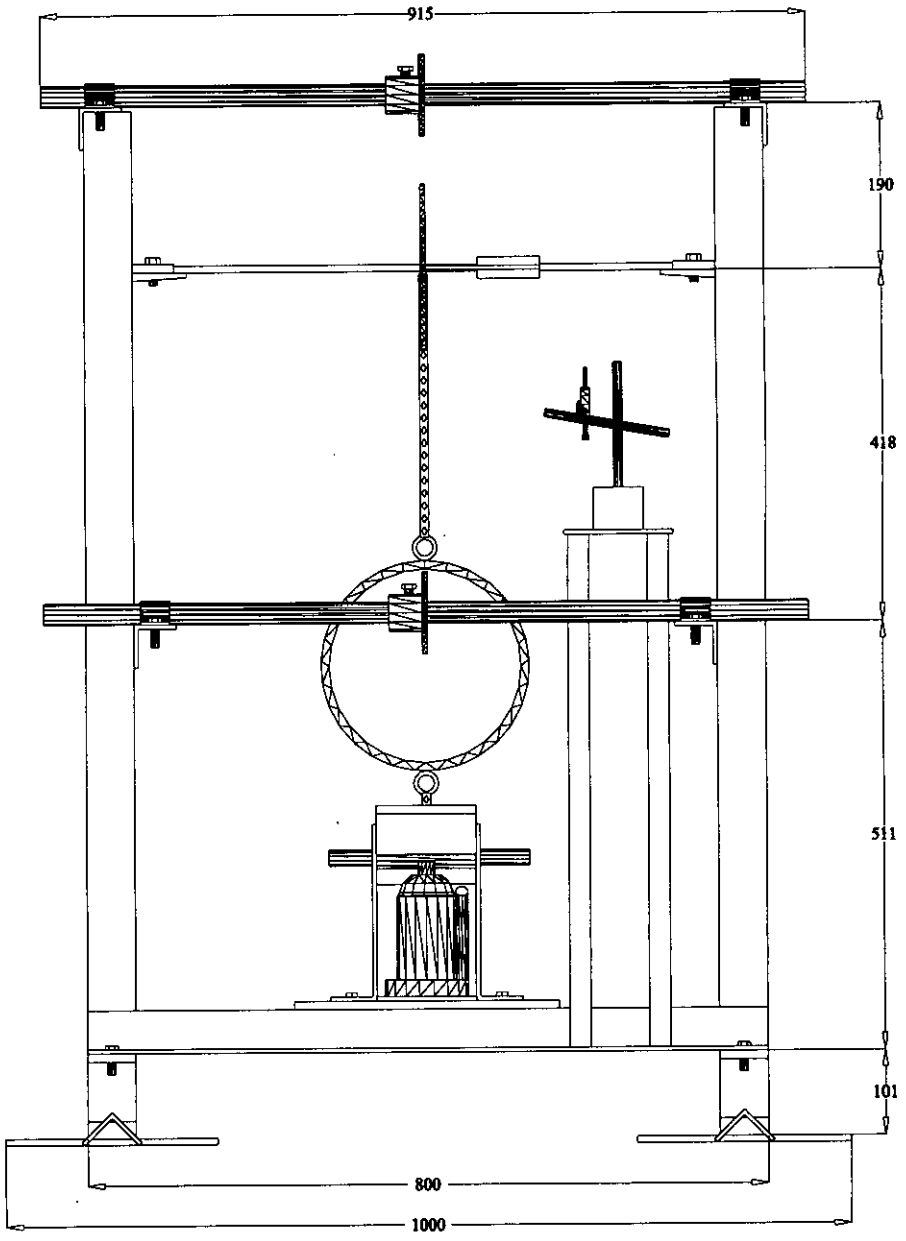

Figure 3.2: Front view of the test rig

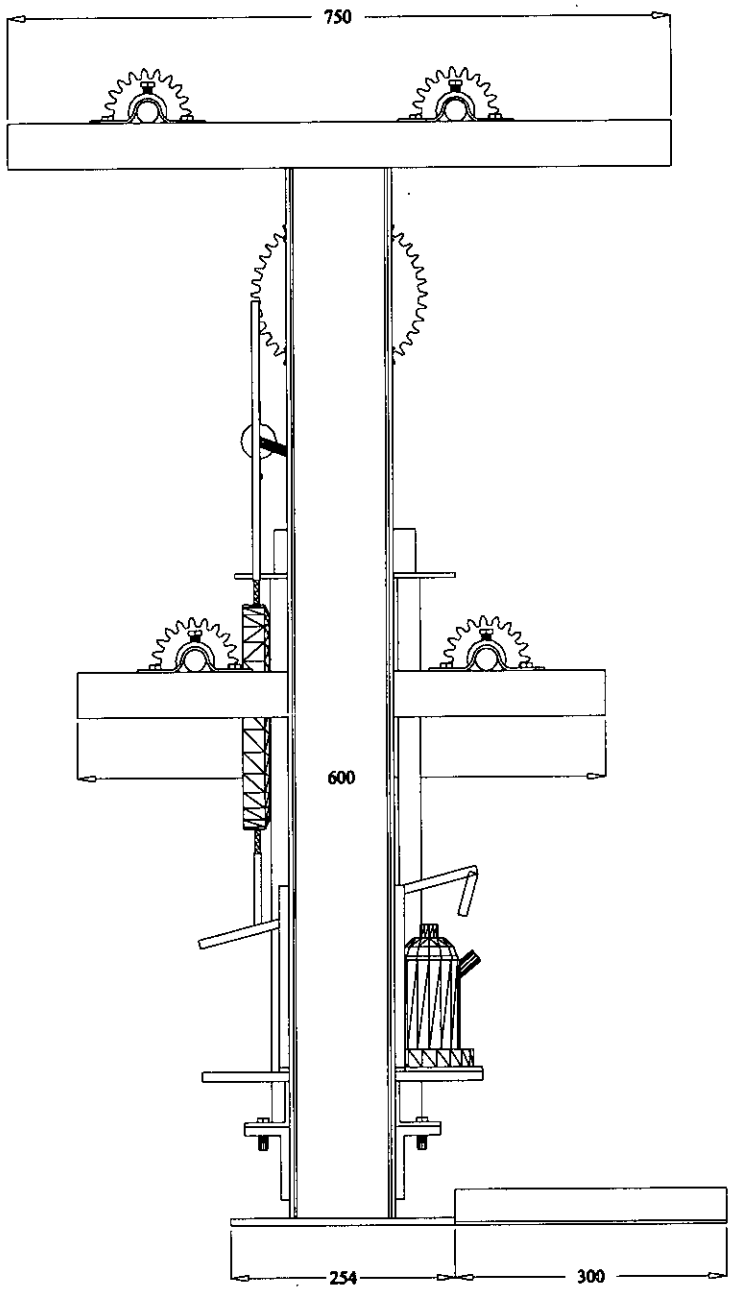

Figure 3.3: Side view of the test rig

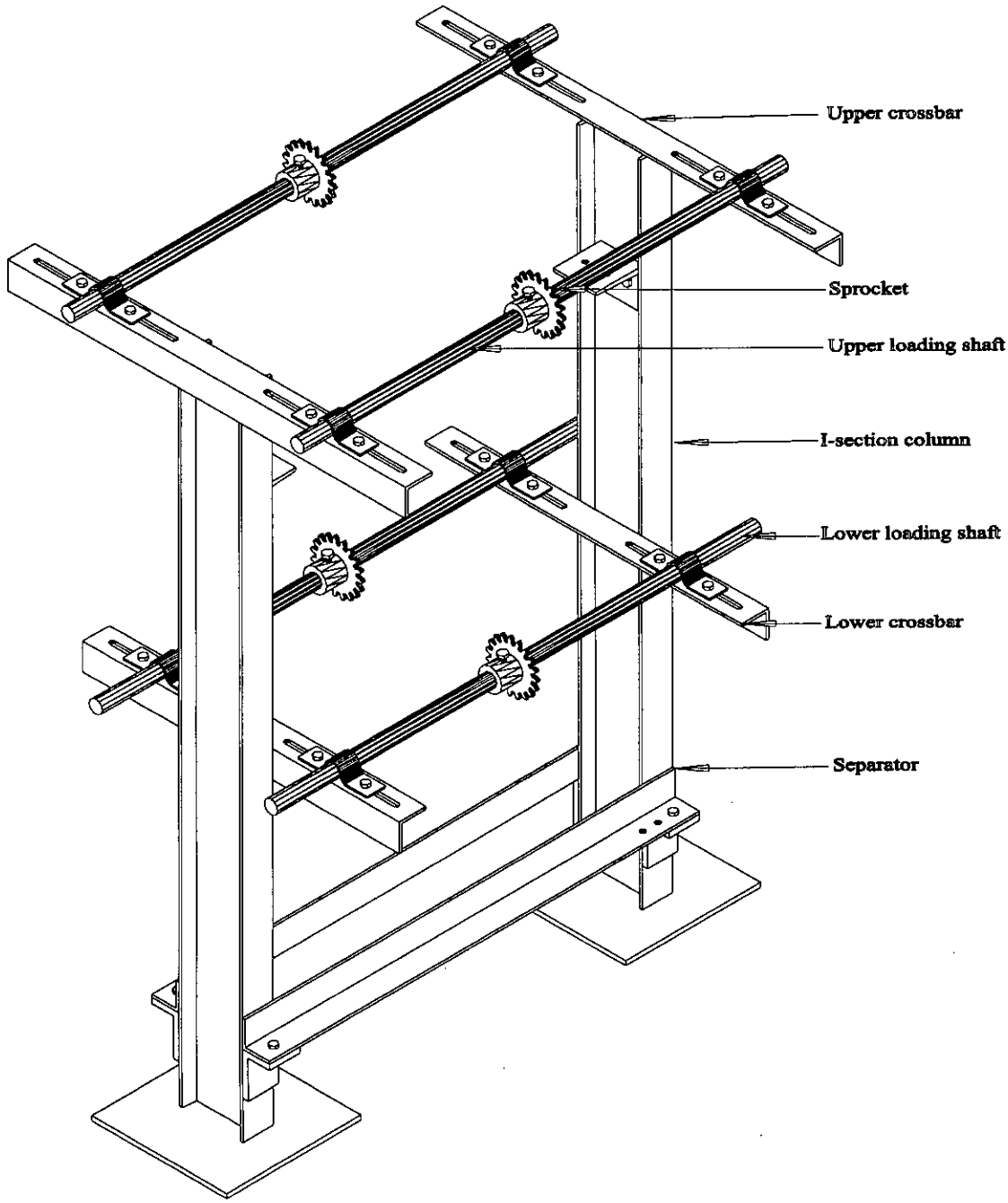

Figure 3.4: Main structure of the test rig

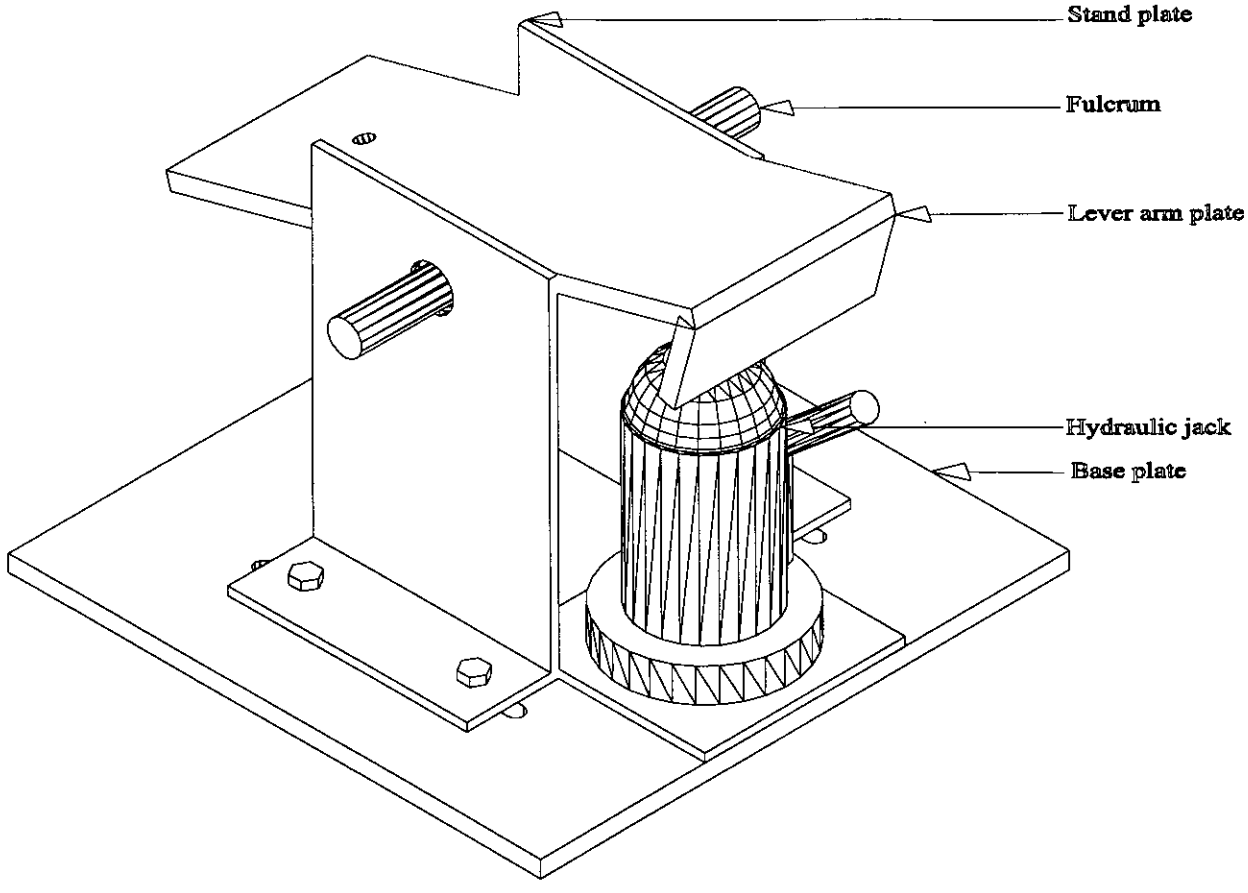

Figure 3.5: Hydraulic jack with its base plate, lever arm plate and stand plates

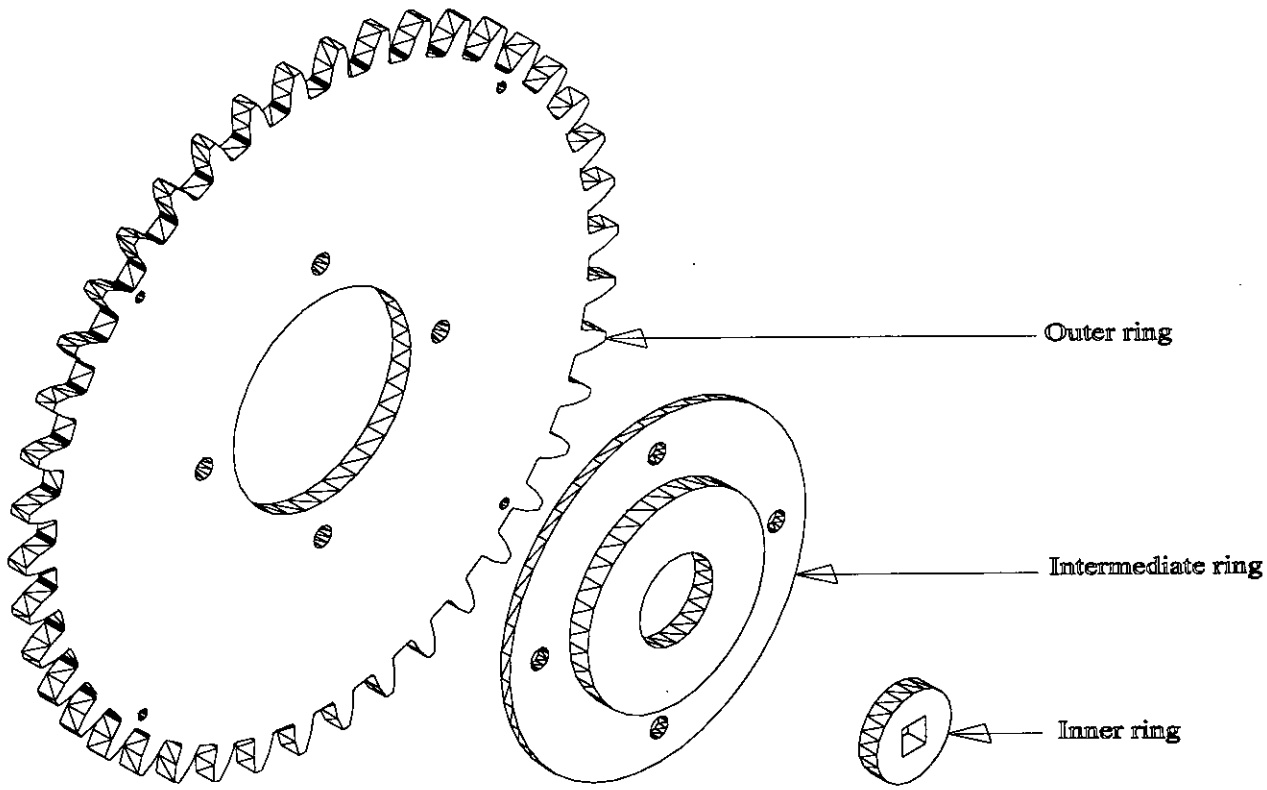

Figure 3.6: Schametic diagram of the loading wheel

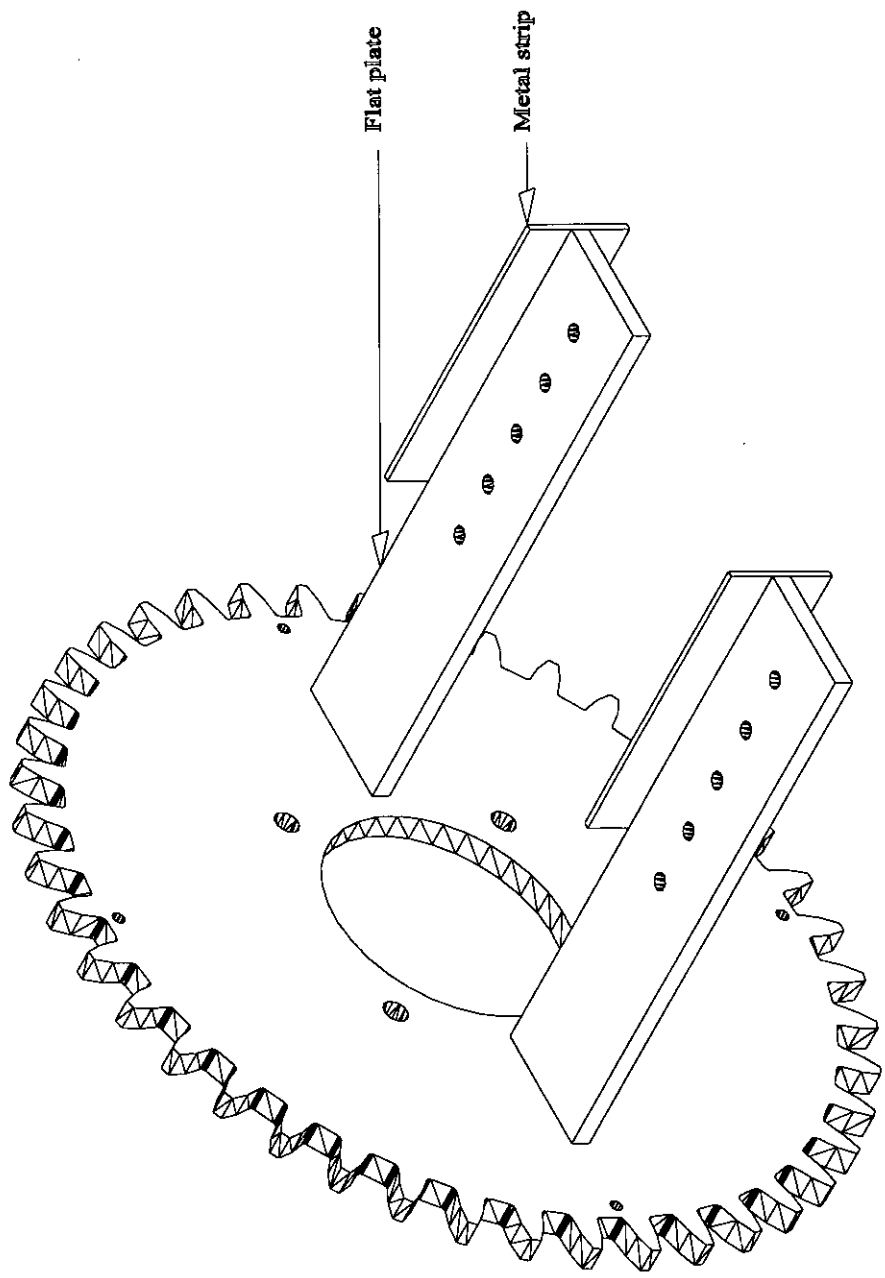

Figure 3.7: Schematic of the flat plate with its metal strip

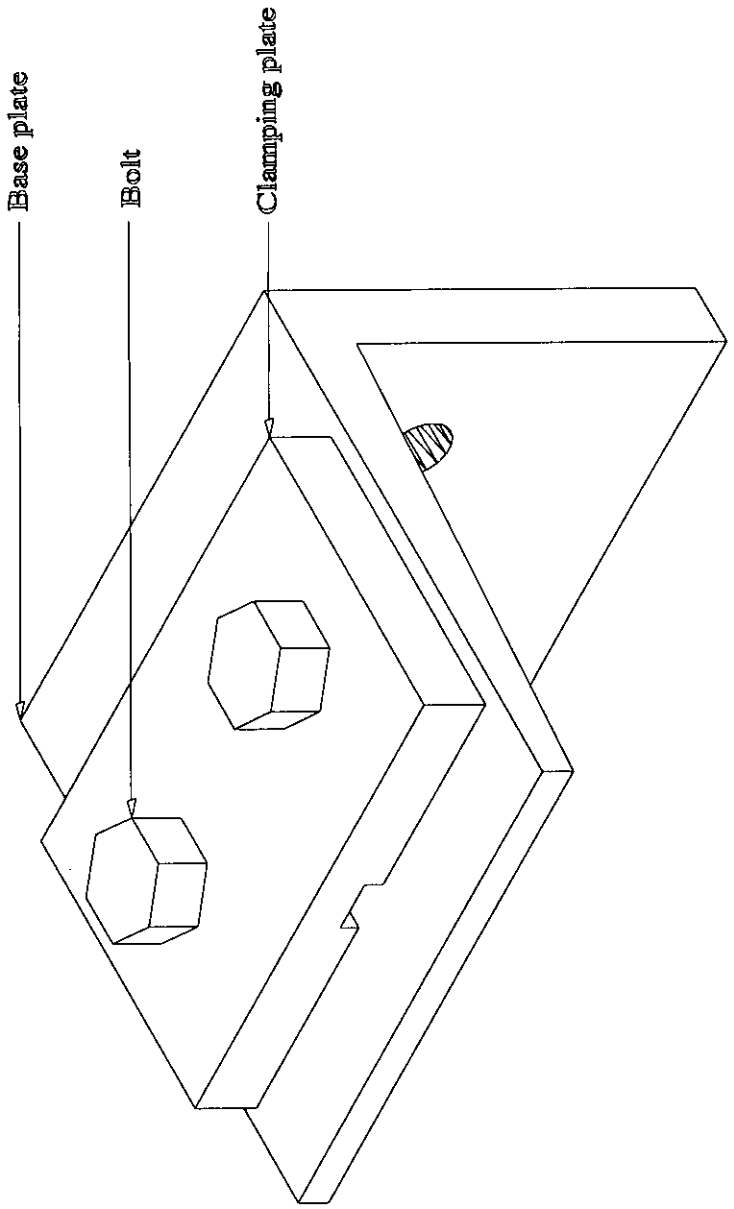

Figure 3.8: Base and Clamping plate for the specimen

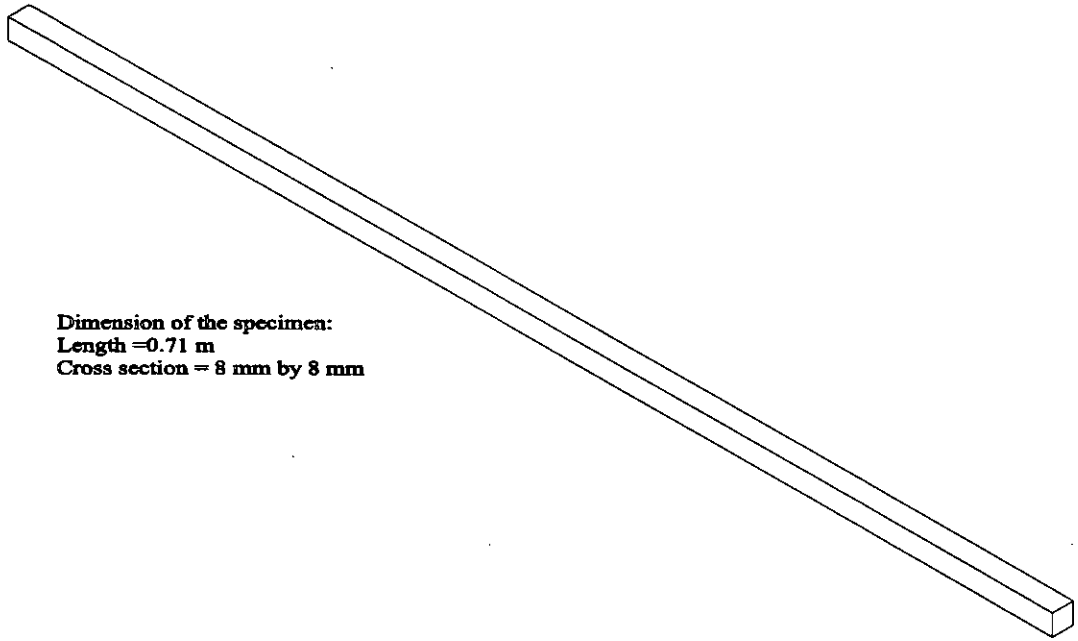

Figure 3.9: Schematic of the specimen

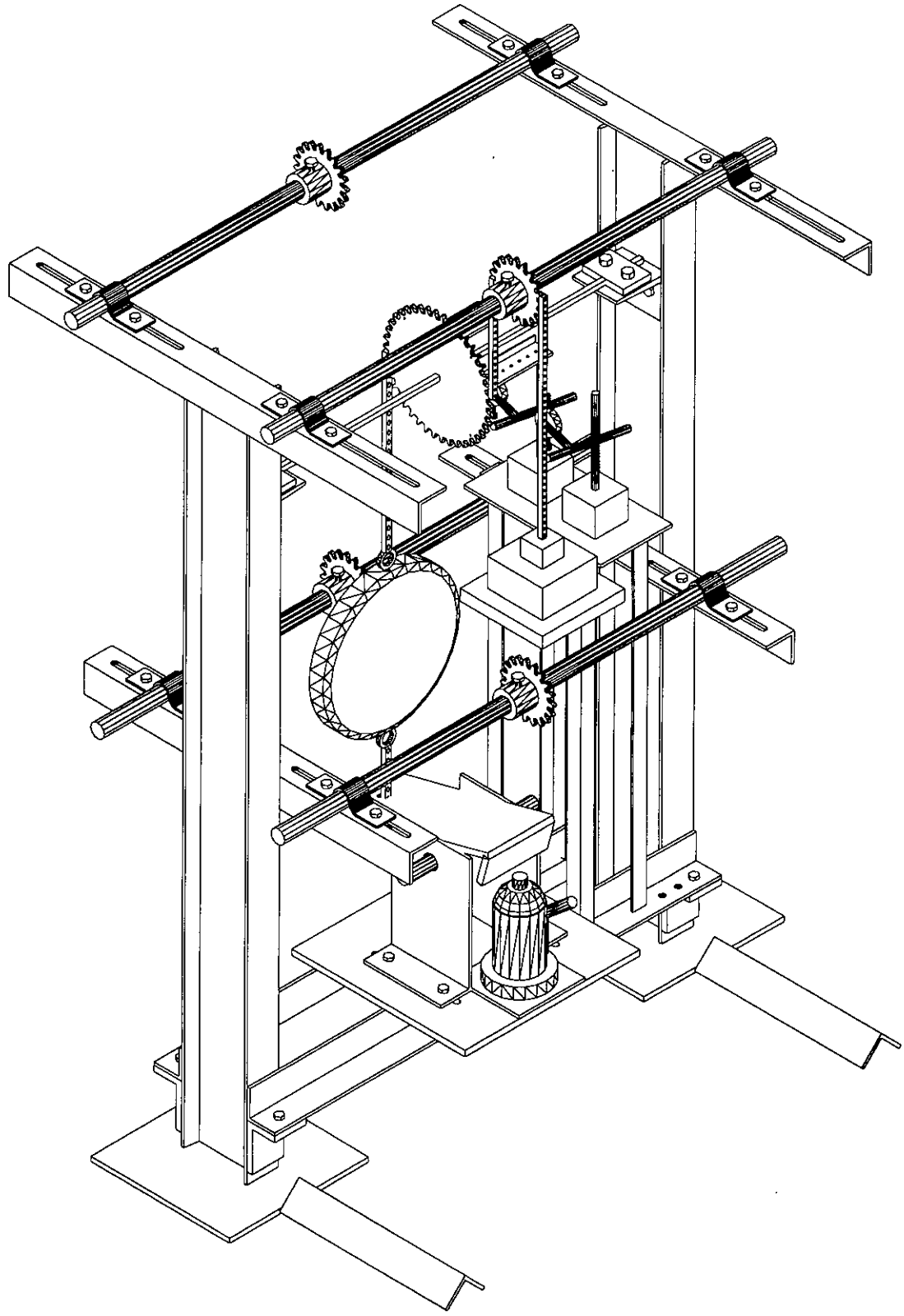

Figure 3.10: Schematic of the loading arrangement in the test rig for pure torsion

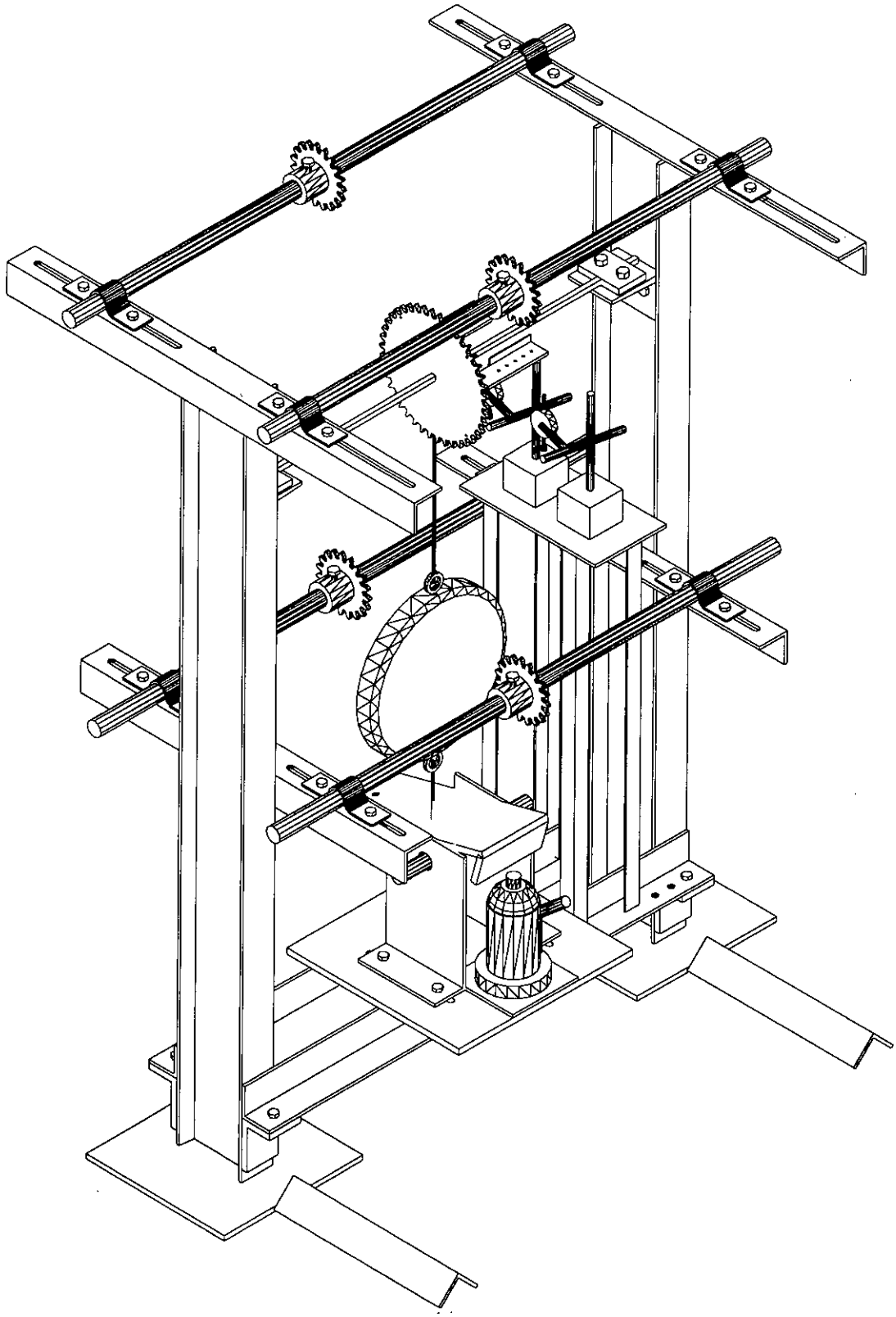

Figure 3.11: Schematic of the loading arrangement in the test rig for pure bending

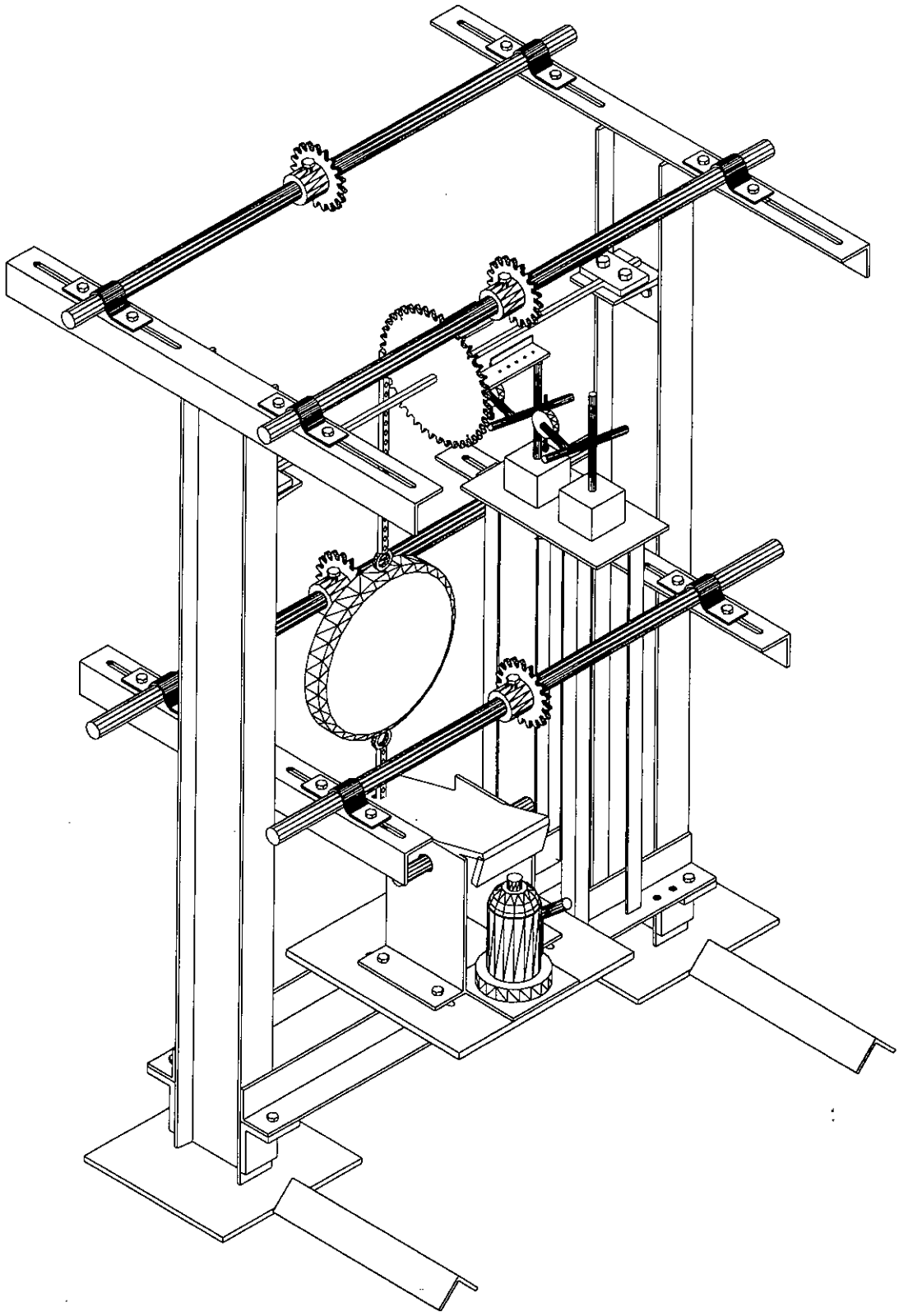

Figure 3.12: Schematic of the loading arrangement of M/T = 1.12

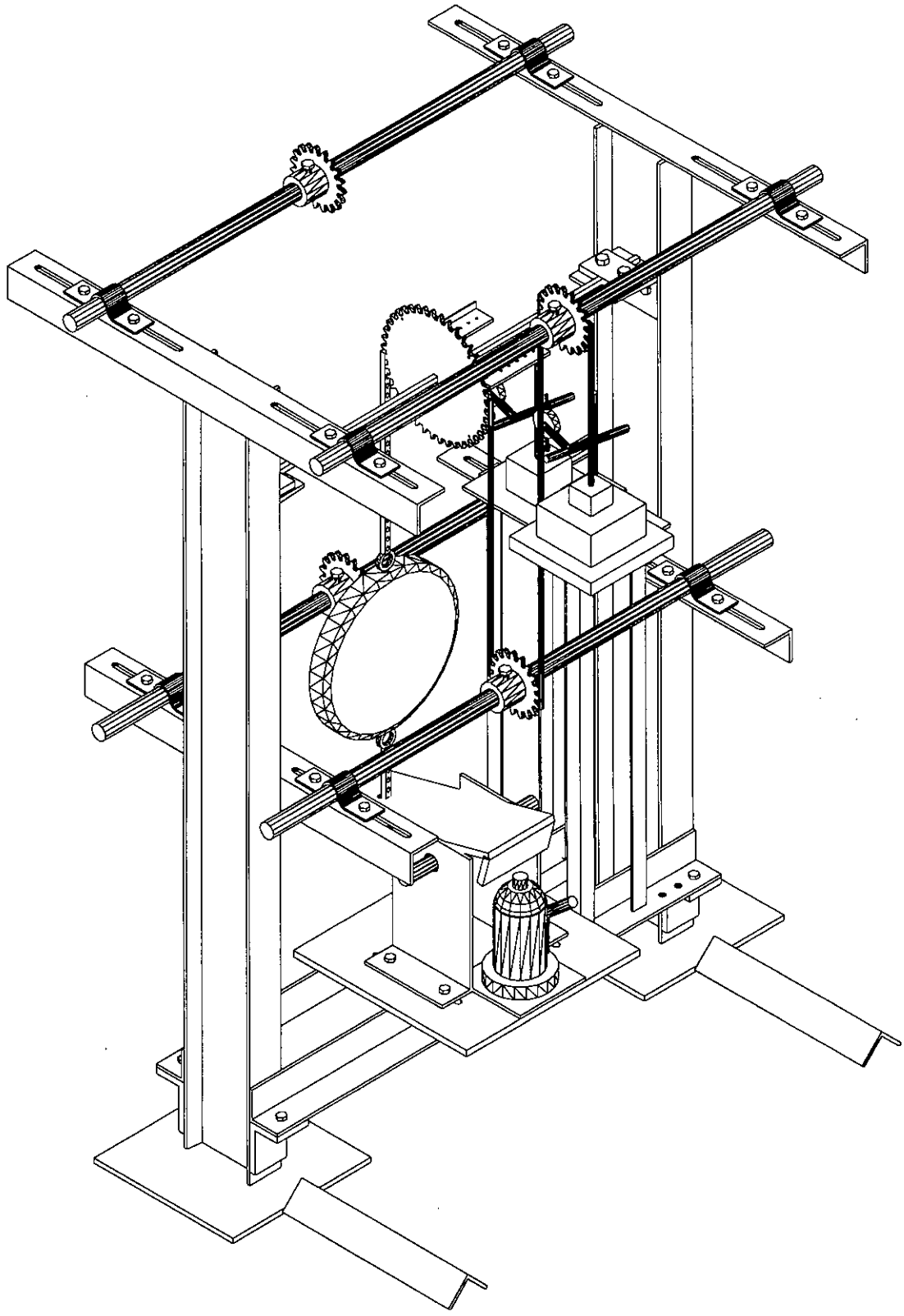

Figure 3.13: Schematic of the loading arrangement for M/T = 2.24 and M/T = 3.36

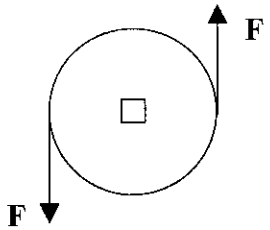

Figure 3.14: Loading pattern of M/T = 0 (Pure Torsion)

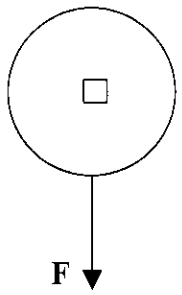

Figure 3.15: Loading pattern of M/T = ∝ (Pure Bending)

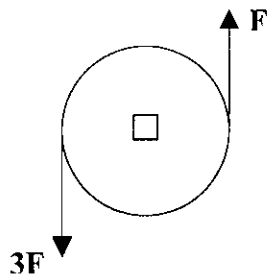

Figure 3.16: Loading pattern of M/T = 0.56

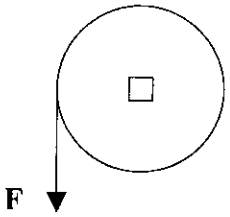

Figure 3.17: Loading pattern of M/T = 1.12

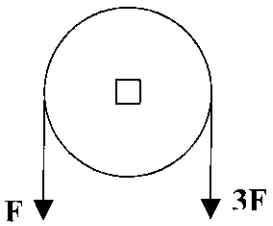

Figure 3.18: Loading pattern of M/T = 2.24

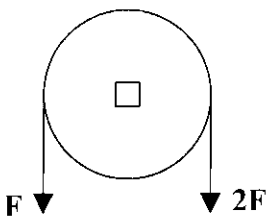

Figure 3.19: Loading pattern of M/T = 3.36

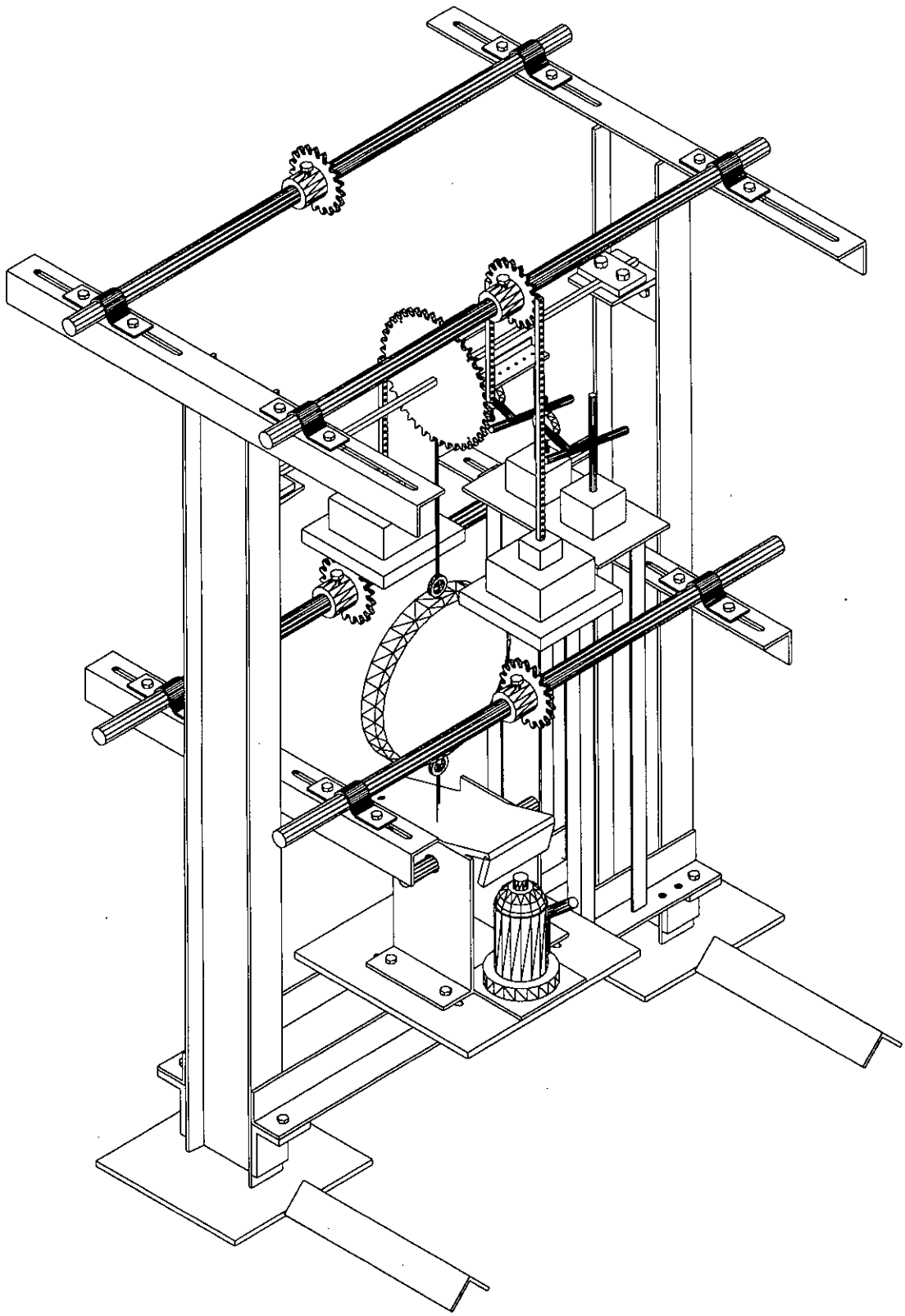

Figure 3.20: Schematic of the loading arrangment in the test rig for non-proportional loadings

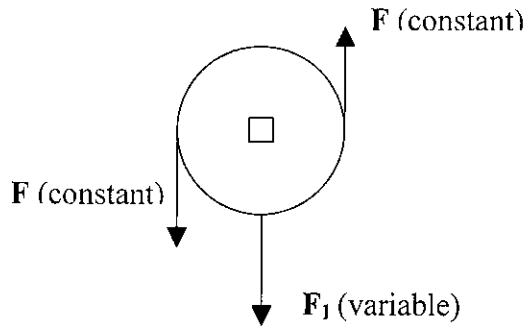

Figure 3.21: Loading pattern of combined loading with initial constant torque and different level of bending load

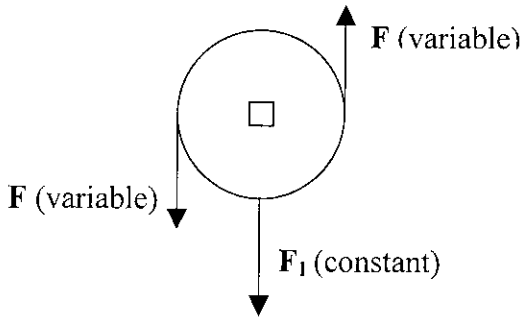

Figure 3.22: Loading pattern of combined loading with initial constant bending load and different level of torque

CHAPTER – 4
RESULTS AND DISCUSSION

4.1 GENERAL

Experimental setup and procedure of different loading arrangements have been discussed in the previous chapter. In order to find the basic mechanical properties of the test specimen investigated, a number of preliminary tests were conducted. Those were uniaxial tension test, pure torsion tests and pure bending test. Pure torsion and pure bending tests were conducted merely to justify the accuracy of the designed test rig and treated as calibration tests. In case of bending test, when concentrated transverse load was applied at the midpoint of the specimen it developed both flexural and shear stress. In this present investigation, the affect of shear stress in case of pure bending was considered negligible. After the preliminary tests, the specimens were subjected to combined bending and torsional loadings. Two types of combined loadings were carried out in this research work. One was proportional loading and the other was non-proportional loading. In proportional loading the ratio of bending moment to torque (i.e., M/T) was kept constant. In case of non-proportional loading, the ratio of bending moment to torque was not kept constant. Here two types of non-proportional loading paths were investigated. In the first type of non-proportional combined loading, different levels of torque were initially applied to the specimen and keeping each of those initial torques constant, bending load was gradually applied. In the second type of non-proportional combined loading, different levels of bending moment were initially applied to the specimen and keeping each of those initial bending moments constant, torsional load was gradually applied. In this chapter, results of the above-mentioned tests are discussed.

4.2 PRELIMINARY TEST

Uniaxial Tension Test

The uniaxial tension test of the specimen was carried out using a 100-ton capacity universal testing machine. The specimen was tested according to ASTM A 370-98 standard. The uniaxial tensile load versus elongation curve of the specimen is shown

in Figure 4.1 and the corresponding stress versus strain curve is shown in Figure 4.2. From Figure 4.1, yield load (F_y) at 0 % offset was measured and found to be 14.78 kN, whose corresponding yield stress (Y) was 522.70 MPa. The ultimate load and tensile strength of the specimen were 19.61 kN and 694.00 MPa respectively. Modulus of elasticity of the material of the specimen was calculated using the intial slope of the stress versus strain curve, whose value was equal to 195.00 GPa. It was observed that the difference between the ultimate and the yield load was comparatively small, which was due to over hardening of the material. It is worth mentioning here that all the specimens were tested from the as received materials.

Pure Torsion Tests

Two types of pure torsion tests were conducted in this research work. One was carried out using the torsion machine situated in the Applied Mechanics Laboratory of Mechanical Engineering Department of BUET, to know the shear yield stress and the modulus of rigidity of the material of the specimen. From the pure torsion test on the torsion machine, torque versus angle of twist curve of the specimen was plotted as shown in Figure 4.3. Yield torque was measured at the proportional limit, whose value was equal to 12.74 N.m and the corresponding shear yield stress was equal to 300.00 MPa. Using the initial slope of Figure 4.3 and equation (2.12), modulus of rigidity was calculated, which was equal to 80.20 GPa. From the uniaxial tension test of the specimen, the value of the yield stress in tension was equal to 522.70 MPa, whereas its corresponding yield stress in shear was 300.00 Mpa. Thus the ratio of the yield stress in shear to the yield stress in tension for the material of the specimen was 0.574.

Another pure torsion test was conducted using the newly designed test rig to justify the accuracy of the test rig in the torsion test. From that test, torsional load versus angle of twist curve was plotted as shown in Figure 4.4. From the figure, yield torsional load was measured at the proportional limit point, whose value was equal to 0.68 kN and the corresponding shear yield stress was equal to 279.66 MPa. Using the initial slope of Figure 4.4 and equation (2.14), the value of G was calculated which was equal to 79.69 GPa. On the other hand, the value of G found using the torsion

machine was 80.20 Gpa, which concludes the proper functioning of the designed test rig in case of torsion test.

Pure Bending Test

Pure bending test was carried out using the test rig in order to justify the accuracy of the test rig in case of bending loading. Here bending load versus midpoint deflection curve was plotted as shown in Figure 4.5. From this figure, yield bending load was measured at the proportional limit, which was equal to 0.44 kN, and the corresponding tensile yield stress was equal to 517.00 MPa. Using the initial slope of Figure 4.5 and equation (2.17), value of the modulus of elasticity E was calculated which was equal to 130.50 GPa. But from the uniaxial tension test it was found that the value of E was equal to 195.00 GPa, which was 1.5 times of 130.50 GPa. From the investigation, it was found that this discrepancy was due to the problem created in fixing the ends of the specimen. Equation (2.17) was for perfectly fixed ended beam. But in the present setup, the ends of the beam were not perfectly fixed. As a result, axial sliding of the specimen occurred in case of bending loading. Since it was not possible to fix the ends perfectly, magnitude of the restrained moments reduced and consequently midpoint bending moment of the specimen increased. So introducing a correction factor for the end condition in equations (2.16) and (2.17), equations (2.19) and (2.20) were obtained.

4.3 COMBINED LOADING

Two types of combined loading were studied to examine the behaviour of the material of the specimen in case of combined loading at elastic and plastic regions. One was proportional loading and the other non-proportional loading. In the proportional loading the ratio of bending moment to torque (i.e., M/T) was kept constant, while in the other case, the ratio was not constant. Furthermore, in case of non-proportional loading, two loading paths were investigated. In the first type of non-proportional loading, different levels of torque were initially applied and keeping each of those initial torques constant, bending load was gradually applied. In the second type of non-proportional loading, different levels of bending moment

were initially applied and keeping each of those initial bending moments constant, torsional load was gradually applied.

4.3.1 Proportional Loading

In proportional loading the ratio of bending moment to torque (i.e., M/T) was kept constant. In this work, six different ratios of proportional loading were studied, which were 0 (pure torsion), 0.56, 1.12, 2.24, 3.36 and ∞ (pure bending). Among these, ratios 0 and ∞ were considered as calibration tests to justify the accuracy of the test rig, which have already been discussed in section 4.2. However, for the other cases, i.e., when M/T ratio equals 0.56, 1.12, 2.24 and 3.36, the bending load versus midpoint deflection curves and torsional load versus angle of twist curves were plotted, which are shown in Figures 4.6 - 4.13.

Bending load versus midpoint deflection curve and torsional load versus angle of twist curve for the ratio of bending moment to torque (i.e., M/T) equals 0.56, are shown in Figures 4.6 and 4.7 respectively. From Figure 4.6, yield bending load (F_{by}) was measured, which was equal to 0.27 kN. The calculated yield flexural stress (σ_y) corresponding to the yield bending load was equal to 319.11 MPa. Using the initial slope of Figure 4.6 and equation (2.20), value of the modulus of elasticity E was calculated to be equal to 197.85 GPa. From Figure 4.7, yield torsional load (F_{ty}) was measured and its corresponding yield shear stress (τ_y) of the specimen was calculated, which were equal to 0.53 kN and 223.86 MPa respectively. Using the initial slope of Figure 4.7 and equation (2.14), value of the modulus of rigidity G was calculated to be equal to 80.19 GPa.

Bending load versus midpoint deflection curve and torsional load versus angle of twist curve for M/T = 1.12 are shown in Figures 4.8 and 4.9 respectively. From Figure 4.8, yield bending load (F_{by}) was measured, which was equal to 0.36 kN. The calculated yield flexural stress (σ_y) corresponding to the yield bending load was equal to 416.34 MPa. Using the initial slope of Figure 4.8 and equation (2.20), value of the modulus of elasticity E was calculated to be equal to 193.10 GPa. From Figure 4.9, yield torsional load (F_{ty}) was measured and its corresponding yield shear stress

(τ_y) was calculated, which were equal to 0.35 kN and 146.74 MPa respectively. Using the initial slope of Figure 4.9 and equation (2.14), value of the modulus of rigidity G was calculated to be equal to 79.28 GPa.

Bending load versus midpoint deflection curve and torsional load versus angle of twist curve for M/T = 2.24 are shown in Figures 4.10 and 4.11 respectively. Here yield bending load (F_{by}), yield torsional load (F_{ty}), yield flexural stress (σ_y), yield shear stress, modulus of elasticity E, and modulus of rigidity G were calculated, which were equal to 0.41 kN, 0.20 kN, 479.30 MPa, 85.00 MPa, 196.00 GPa and 79.96 GPa respectively.

Similarly bending load versus midpoint deflection curve and torsional load versus angle of twist curve for M/T = 3.36 are shown in Figures 4.12 and 4.13 respectively. Here yield bending load (F_{by}), yield torsional load (F_{ty}), yield flexural stress (σ_y), yield shear stress, modulus of elasticity E, and modulus of rigidity G were also calculated, which were equal to 0.42 kN, 0.14 kN, 490.74 MPa, 58.00 MPa, 190.20 GPa and 79.69 GPa respectively.

The numerical values of all the above-mentioned parameters are summarised in tabular form in Table 4.1A. From Figures 4.14 and 4.17, it is found that whatever was the level of M/T ratio, the initial slopes of the bending load versus deflection curves and torsional load versus angle of twist curves were similar to those of the pure bending and pure torsion test curves respectively, i.e., modulus of elasticity and modulus of rigidity did not vary considerably with the variation of M/T ratio and hence stiffness of the material of the specimen in the elastic region was nearly constant for all the ratios of M/T. Furthermore, with the increase of M/T ratio, yield bending load (F_{by}) increased while yield torsional load (F_{ty}) decreased.

Variation of the slopes of the bending load versus midpoint deflection curve with respect to the midpoint deflection of the beam for different M/T ratios is shown in Figure 4.15. From the figure it is found that up to the corresponding yield point the slopes were constant for all the M/T ratios and their values were nearly the same, but

there was a drastic change just after the yield point. From Figure 4.16 it was further observed that at the corresponding $1.50\delta_y$, $2.00\delta_y$ and $2.50\delta_y$ values, tangent modulus of elasticity was higher for the higher M/T ratio. So strain hardening was more noticeable in case of higher value of the M/T ratio. Numerical values of the tangent modulus of elasticity at the corresponding $1.50\delta_y$, $2.00\delta_y$ and $2.50\delta_y$ points are given in Table 4.1B

Similarly, variation of the slopes of the torsional load versus angle of twist curve with respect to the angle of twist for different M/T ratios is shown in Figure 4.18. From the figure it is found that up to the corresponding yield point the slopes were constant for all the M/T ratios and their values were nearly the same, but there was a drastic change just after the yield point. From Figure 4.19 it was further observed that at the corresponding $1.25\theta_y$, $1.50\theta_y$ and $2.00\theta_y$ values, tangent modulus of rigidity was higher for the higher M/T ratio. So strain hardening was more noticeable in case of higher value of the M/T ratio. Numerical values of the tangent modulus of rigidity at the corresponding $1.25\theta_y$, $1.50\theta_y$ and $2.00\theta_y$ points are given in the Table 4.1C

Table 4.1A: Results of Proportional Loading

M/T Ratio	F_b/δ $\times 10^3$ kN/mm	F_t/θ kN/rad	F_{by} kN	F_{ty} kN	σ MPa	τ MPa	E GPa	G GPa	σ/Y	τ/Y
0.00	-	3.43	-	0.68	-	279.66	-	79.69	0.00	0.54
0.56	40.81	3.45	0.27	0.53	319.11	223.86	197.85	80.19	0.61	0.43
1.12	39.83	3.41	0.36	0.35	416.34	146.74	193.10	79.28	0.80	0.28
2.24	40.42	3.44	0.41	0.20	479.30	85.00	196.00	79.96	0.92	0.16
3.36	39.24	3.43	0.42	0.14	490.74	58.00	190.20	79.69	0.94	0.11
∞	40.22	-	0.44	-	517.00	-	195.00	-	0.99	0.00

Table 4.1B: Results of Proportional Loading

					Value of E at				% Variation of E from		
M/T ratio	δ_y (mm)	$1.5\delta_y$ (mm)	$2\delta_y$ (mm)	$2.5\delta_y$ (mm)	δ_y GPa	$1.5\delta_y$ GPa	$2\delta_y$ GPa	$2.5\delta_y$ GPa	δ_y to $1.5\delta_y$	$1.5\delta_y$ to $2\delta_y$	$2\delta_y$ to $2.5\delta_y$
∞	10.50	15.74	20.98	26.22	195.00	70	50	40	23.8	13.8	9.9
3.36	9.38	14.00	18.76	23.45	197.85	56	40	34	28.6	16.0	11.1
2.24	8.50	12.75	17.00	21.25	193.10	44	32	25	35.8	19.4	13.4
1.12	8.37	12.56	16.74	20.93	196.00	33	22	19	38.3	20.4	13.9
0.56	5.77	8.66	11.54	14.43	190.20	30	20	17	58.2	30.8	20.9
0.00	-	-	-	-	-	-	-	-	-	-	-

Table 4.1C: Results of Proportional Loading

					Value of G at				% Variation of G from		
M/T ratio	θ_y (rad) $\times 10^2$	$1.25\theta_y$ (rad) $\times 10^2$	$1.5\theta_y$ (rad) $\times 10^2$	$2\theta_y$ (rad) $\times 10^2$	θ_y GPa	$1.25\theta_y$ GPa	$1.5\theta_y$ GPa	$2\theta_y$ GPa	θ_y to $1.25\theta_y$	θ_y to $1.5\theta_y$	θ_y to $2\theta_y$
∞	-	-	-	-	-	-	-	-	-	-	-
3.36	3.57	4.7	5.4	7.1	80.19	51	39	28	32.1	22.8	14.5
2.24	4.99	6.2	7.5	10.0	79.28	44	30	20	28.8	20.0	12.0
1.12	9.77	12.2	14.7	19.5	79.96	34	24	15	18.5	11.3	6.6
0.56	13.60	17.0	20.5	27.3	79.69	31	20	12	14.4	8.9	5.0
0.00	18.90	23.6	28.3	37.7	79.69	26	15	9	11.5	6.9	3.7

4.3.2 Non-proportional Loading

The purpose of this loading condition was to examine the behaviour of the material of the specimen at elastic and plastic regions in case of non-proportional loading. Two different loading paths were studied under non-proportional loading whose experimental procedures have already been discussed in chapter 3.

In the first type of non-proportional loading, different levels of torque were initially applied and keeping each of those initial torques constant, bending load was gradually applied. Three loading arrangements were studied in this case and the initial torques were 25 %, 50 % and 75 % of yield torque at pure torsion. For each loading arrangement bending load versus midpoint deflection curve was plotted, which are shown in Figures 4.20 - 4.22.

When the initially applied constant torque was equal to 25 % of yield torque of pure torsion, the corresponding bending load versus midpoint deflection curve is shown in Figure 4.20. From the figure, yield bending load (F_{by}) was measured, which was equal to 0.42 kN. The calculated yield flexural stress (σ_y) corresponding to the yield bending load was equal to 494.11 MPa. Using the initial slope of the figure and equation (2.20), value of the modulus of elasticity was calculated to be equal to 192.62 GPa.

Bending load versus midpoint deflection curve for initially applied constant torque of 50 % of yield torque of pure torsion is shown in Figure 4.21. From the figure, yield bending load (F_{by}) was measured, which was equal to 0.36 kN and the corresponding calculated yield flexural stress (σ_y) was equal to 425.50 MPa. Using the initial slope of the figure and equation (2.20), value of the modulus of elasticity was calculated to be equal to 195.00 GPa.

Similarly, bending load versus midpoint deflection curve for initial 75 % of yield torque of pure torsion is shown in Figure 4.22. Here yield bending load, yield flexural stress and modulus of elasticity were measured and calculated, which were equal to 0.28 kN, 322.55 MPa and 193.57 GPa respectively.

The numerical values of all the above-mentioned parameters are summarised in tabular form in Table 4.2A. From Figure 4.23, it is found that whatever was the level of initially applied constant torque, the initial slopes of the bending load versus midpoint deflection curves were similar to that of the pure bending test curve, i.e., modulus of elasticity did not vary considerably with the variation of the level of the

initially applied constant torque and hence stiffness of the material of the specimen in the elastic region was almost constant. Furthermore, with the increase of the initially applied constant torsional load (i.e, torque), yield bending load (F_{by}) decreased.

Variation of the slopes of the bending load versus midpoint deflection curve with respect to the midpoint deflection of the beam for the above three loading arrangements is shown in Figure 4.24. From the figure it is found that up to the corresponding yield point the slopes were constant for all the three cases and their values were almost the same, but there was a drastic change just after the yield point. From Figure 4.25, it is further observed that at the corresponding $1.50\delta_y$, $2.00\delta_y$ and $2.50\delta_y$ values, tangent modulus of elasticity was higher for the smaller value of the initially applied constant torsional load. This means strain hardening was more noticeable in case of the smaller value of the initially applied constant torsional load. Numerical values of the tangent modulus of elasticity at the corresponding $1.50\delta_y$, $2.00\delta_y$ and $2.50\delta_y$ points for the above three cases are given in Table 4.2B.

In the second type of non-proportional loading, different levels of constant bending moment were initially applied to the specimen and keeping each of those moments constant, torque was gradually applied. Three loading arrangements were also studied in this case and the three initially applied constant bending moments were 25 %, 50 %, and 75 % of yield bending moment at pure bending. For each loading arrangement torsional load versus angle of twist curve was plotted, which are shown in Figures 4.26 - 4.28.

Torsional load versus angle of twist curve for initially applied constant bending moment of 25 % of yield bending moment at pure bending is shown in Figure 4.26. From the figure, yield torsional load (F_{ty}) was measured, which was equal to 0.64 kN. The calculated yield shear stress (τ_y) corresponding to the yield torsional load was equal to 269.44 MPa. Using the initial slope of the figure and equation (2.14), value of the modulus of rigidity was calculated to be equal to 79.69 GPa.

Torsional load versus angle of twist curve for initial 50 % of yield bending moment at pure bending is shown in Figure 4.27. From the figure, yield torsional load (F_{ty}) was measured, and the corresponding yield shear stress (τ_y) was calculated which were equal to 0.55 kN and 232.13 MPa respectively. Using the initial slope of the figure and equation (2.14), value of the modulus of rigidity was calculated to be equal to 79.00 GPa.

Similarly, torsional load versus angle of twist curve for initially applied constant bending moment of 75 % of yield bending moment at pure bending is shown in Figure 4.28. Here yield torsional load, yield shear stress and modulus of rigidity were also measured and calculated, which were equal to 0.43 kN, 182.39 MPa and 78.55 GPa respectively.

The numerical values of all the above-mentioned parameters are also summarised in tabular form in Table 4.2A. From Figure 4.29, it is found that whatever was the level of the initially applied constant bending moment, the initial slopes of the torsional load versus angle of twist curves were similar to that of the pure torsion curve, i.e., modulus of rigidity did not vary considerably with the variation of the level of the initially applied constant bending moment and hence stiffness of the material of the specimen in the elastic region was almost constant. Furthermore, with the increase of the initially applied bending moment, yield torsional load (F_{ty}) decreased.

Table 4.2A: Results of Non - proportional Loading

Initially Applied Constant Load	F_b/δ $\times 10^3$ kN/mm	F_t/θ kN/rad	F_{by} kN	F_{ty} kN	σ MPa	τ MPa	E GPa	G GPa	σ/Y	τ/Y
25% of YTL	39.73	-	0.42	-	494.11	69.62	192.62	-	0.95	0.13
50% of YTL	40.22	-	0.36	-	425.50	139.83	195.00	-	0.81	0.29
75% of YTL	39.93	-	0.28	-	322.55	209.75	193.57	-	0.62	0.40
25% of YBL	-	3.43	-	0.64	129.25	269.44	-	79.69	0.25	0.49
50% of YBL	-	3.40	-	0.55	258.50	232.13	-	79.00	0.50	0.44
75% of YBL	-	3.38	-	0.43	387.75	182.39	-	78.55	0.74	0.35

Variation of the slopes of the torsional load versus angle of twist curve with respect to the angle of twist of the beam is shown in Figure 4.30 for the above three loading arrangements. From the figure it is found that up to the corresponding yield point the slopes were constant for all the three cases and their values were almost the same, but there was a drastic change just after the yield point. It is further observed from Figure 4.31, that at the corresponding $1.25\theta_y$, $1.50\theta_y$ and $2.00\theta_y$ values, tangent modulus of rigidity was higher for the smaller value of the initially applied constant bending load. This means strain hardening was more noticeable in case of smaller value of the initially applied constant bending load. Numerical values of the tangent modulus of rigidity at the corresponding $1.25\theta_y$, $1.50\theta_y$ and $2.00\theta_y$ points are given in Table 4.2C.

Table 4.2B: Results of Non - proportional Loading

					Value of E at				% Variation of E from		
Initially applied constant load	δ_y (mm)	$1.5\delta_y$ mm	$2\delta_y$ mm	$2.5\delta_y$ mm	δ_y GPa	$1.5\delta_y$ GPa	$2\delta_y$ GPa	$2.5\delta_y$ GPa	δ_y to $1.5\delta_y$	$1.5\delta_y$ to $2\delta_y$	$2\delta_y$ to $2.5\delta_y$
25% of YTL	10.12	15.2	20.2	25.3	192.6	50.0	34.0	28.0	28.2	15.7	10.8
50% of YTL	8.54	12.8	17.0	21.4	195.0	45.0	29.0	21.0	35.1	19.4	13.6
75% of YTL	6.39	9.6	12.8	16.0	193.6	41.0	27.0	18.0	47.7	26.0	18.3

Table 4.2C: Results of Non - proportional Loading

					Value of G at				% Variation of G from		
Initially applied constant load	θ_y (rad) $\times 10^2$	$1.25\theta_y$ (rad) $\times 10^2$	$1.5\theta_y$ (rad) $\times 10^2$	$2\theta_y$ (rad) $\times 10^2$	θ_y (GPa)	$1.25\theta_y$ (GPa)	$1.5\theta_y$ (GPa)	$2\theta_y$ (Gpa)	θ_y to $1.25\theta_y$	θ_y to $1.5\theta_y$	θ_y to $2\theta_y$
25% of YBL	17.7	22.1	26.6	35.4	79.69	19.00	12.00	7.00	13.70	7.60	4.10
50% of YBL	15.3	19.0	22.9	30.5	79.00	16.50	11.30	6.20	16.40	8.90	4.80
75% of YBL	11.9	14.9	17.8	23.8	78.55	14.00	10.00	5.60	21.70	11.50	6.10

4.4 COMPARISON OF THE EXPERIMENTAL RESULTS WITH THEORY

Using the yield flexural stress and yield shear stress of different loading arrangements dimensionless interaction curves are drawn, which are shown in Figures 3.32-3.34. The solid lines represent the theoretical results and the points, the experimental results. From these figures it is found that maximum experimental points are lay nearby the Tresca line and below the von Mises line. One thing is clear from these figures that the experimental results were more conservative. This may be due to defining the yield point in bending load versus midpoint deflection and torsional load versus angle of twist curves. In this research work, proportional limit and yield point were assumed to be the same point. Offset or any other methods were not used to find the yield point. As a result, the experimental yield points were conservative.

Investigating the interaction curves it can be said that, prediction of the plastic yielding of the square solid bar under combined bending and torsion can be made fairly according to Tresca yield Criterion.

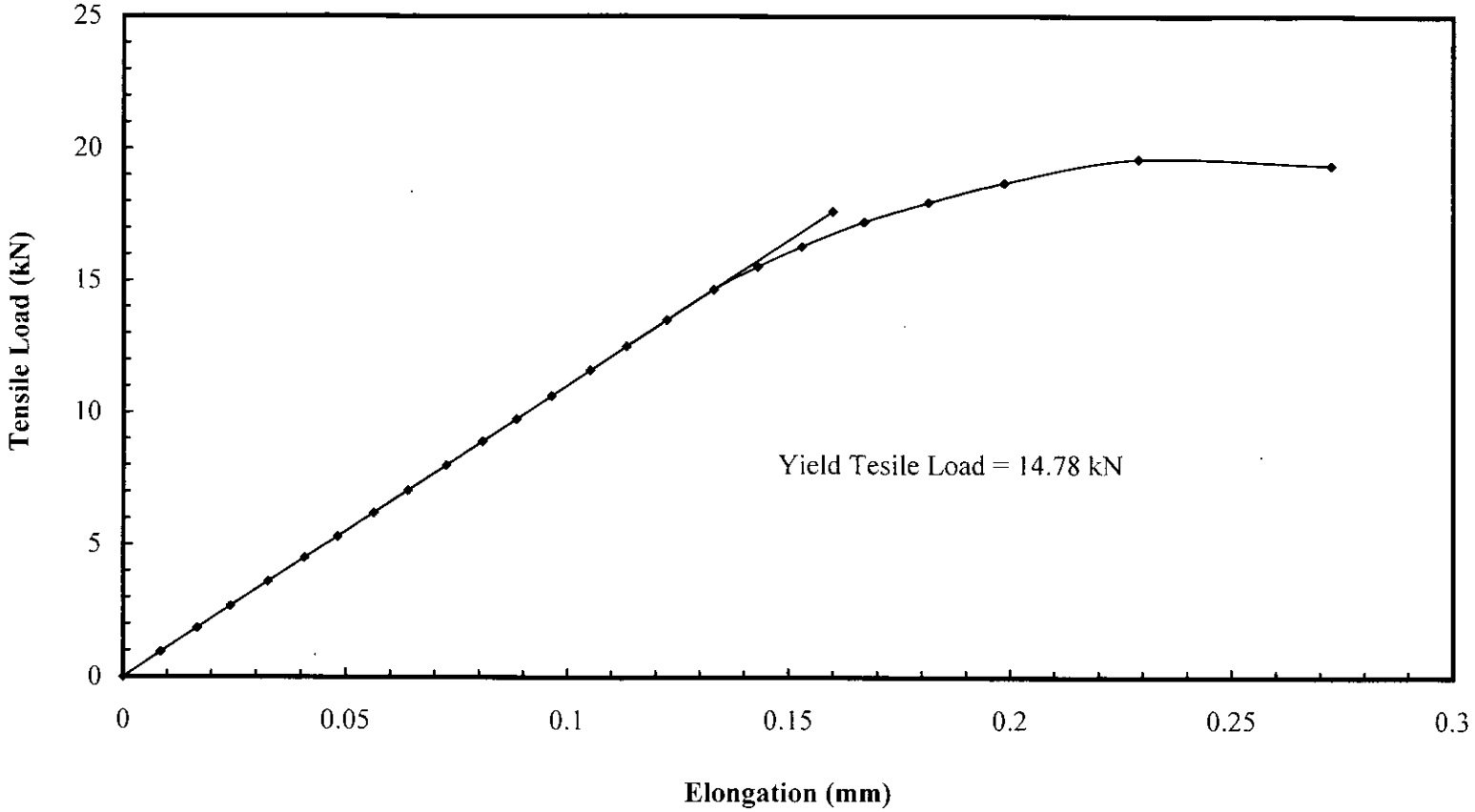

Figure 4.1: Tensile load versus elongation curve for the uniaxial tesion test

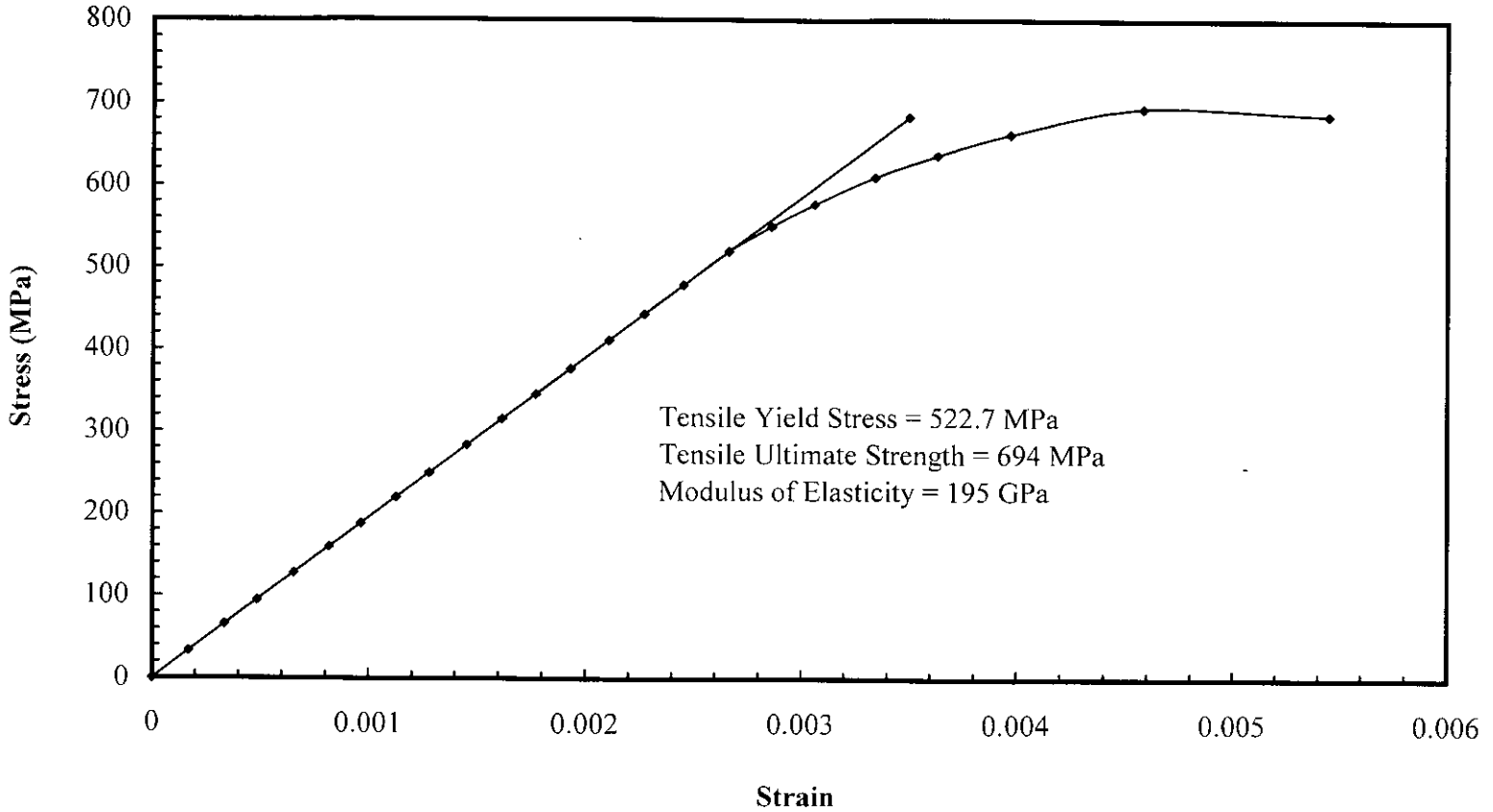

Figure 4.2: Axial stress versus axial strain curve for the uniaxial tension test

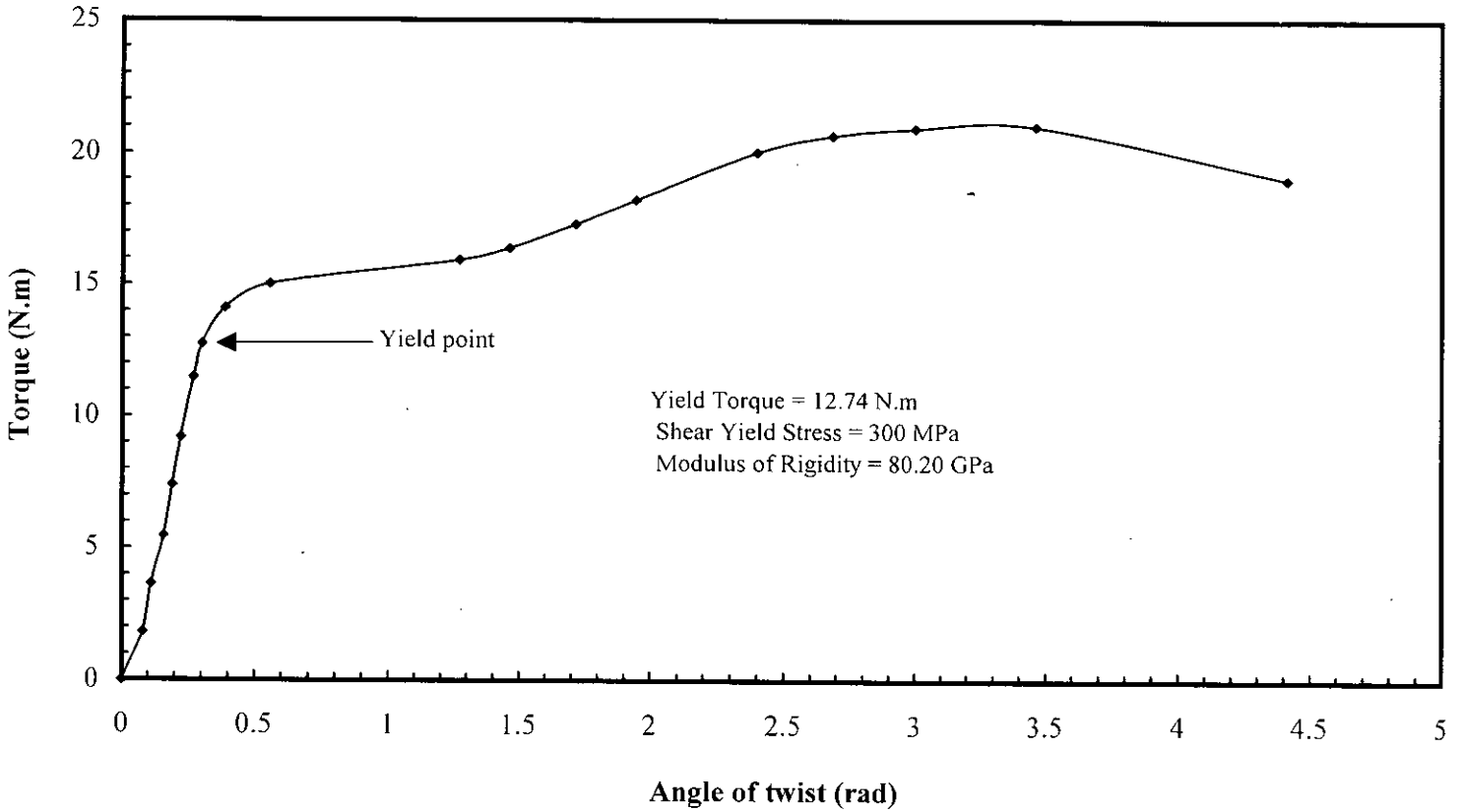

Figure 4.3: Torque versus angle of twist curve for torsion test in the torsion machine

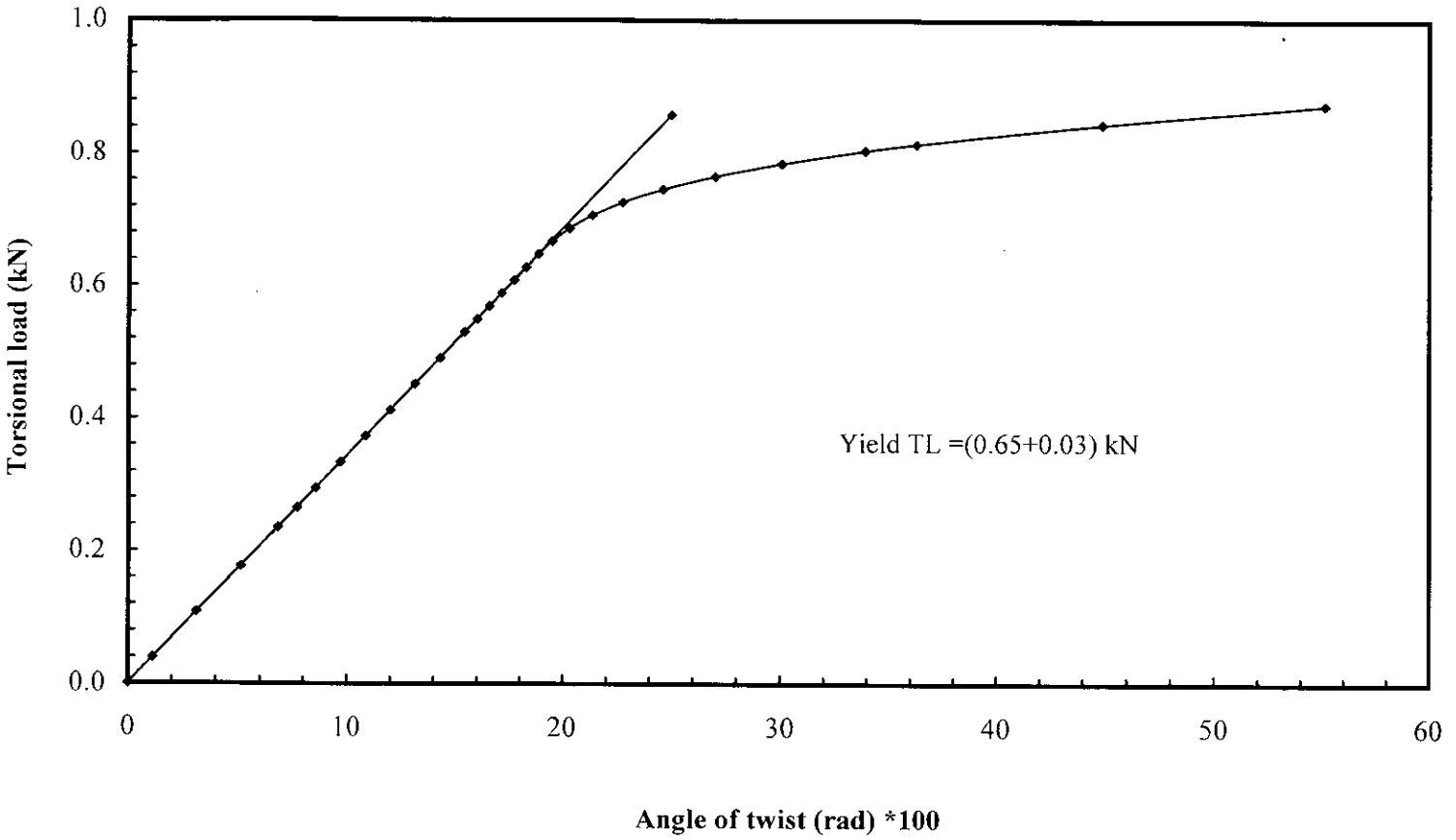

Figure 4.4: Torsional load versus angle of twist curve for pure torsion on test rig

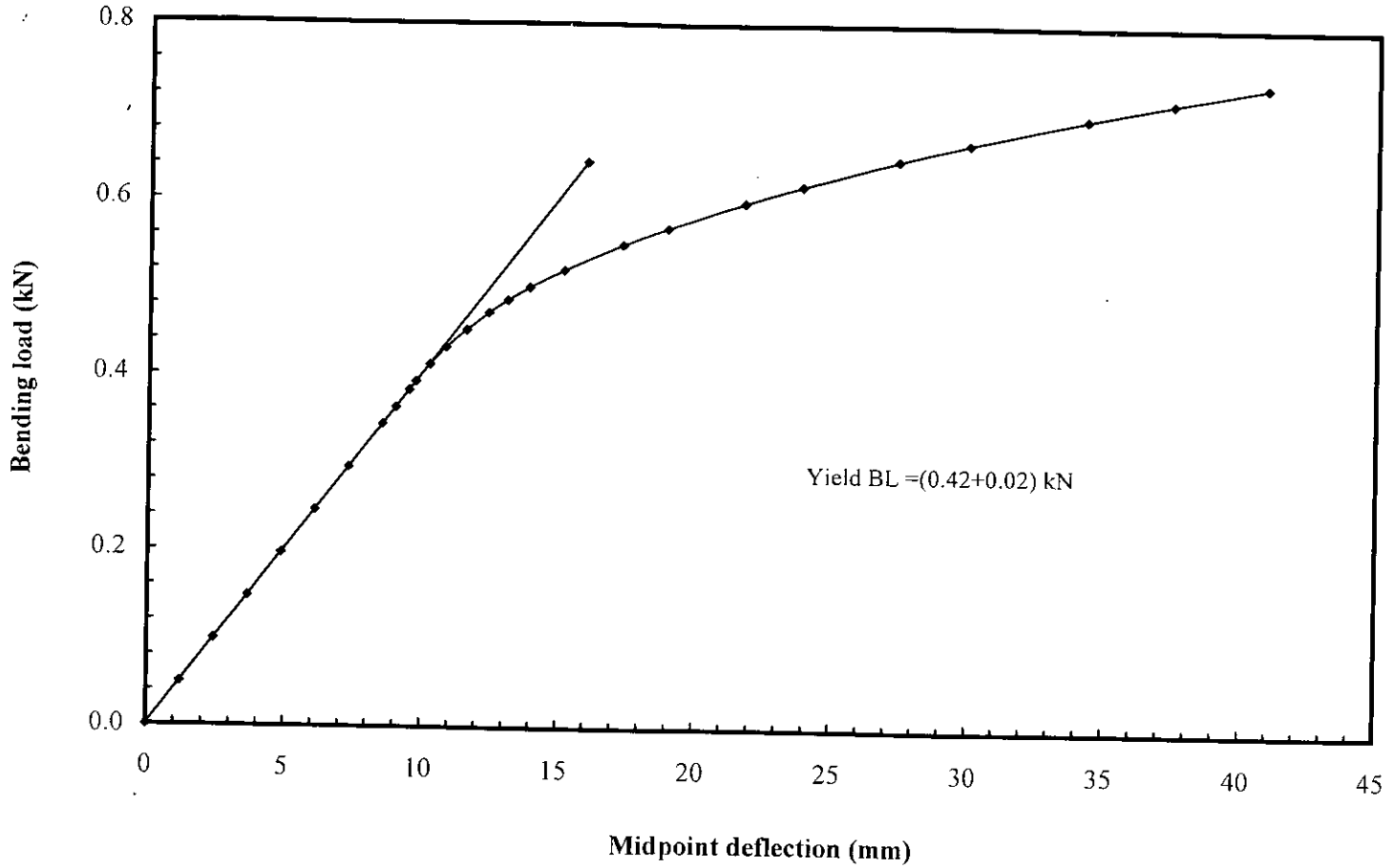

Figure 4.5: Bending load versus midpoint deflection for pure bending

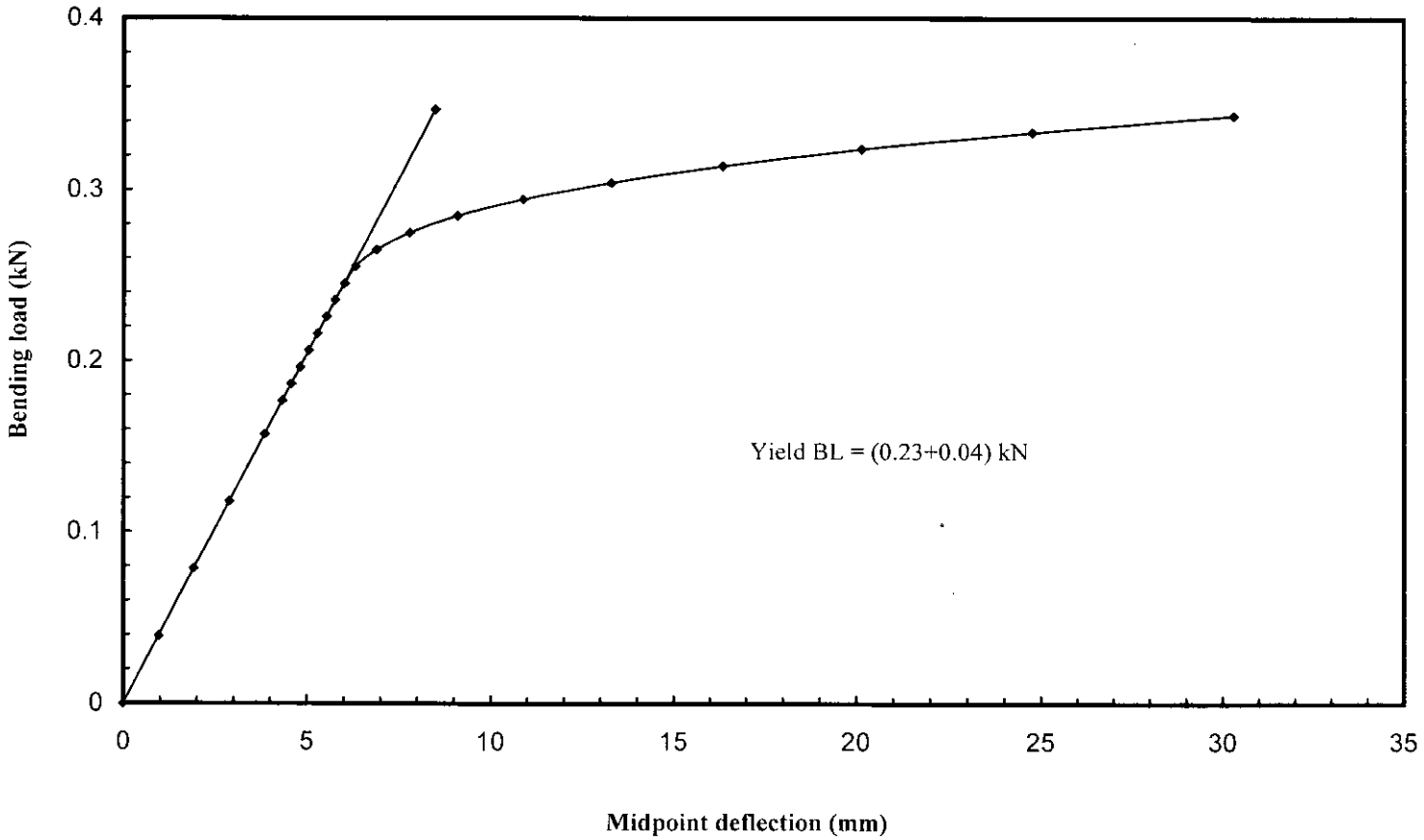

Figure 4.6: Bending load versus midpoint deflection curve for M/T = 0.56

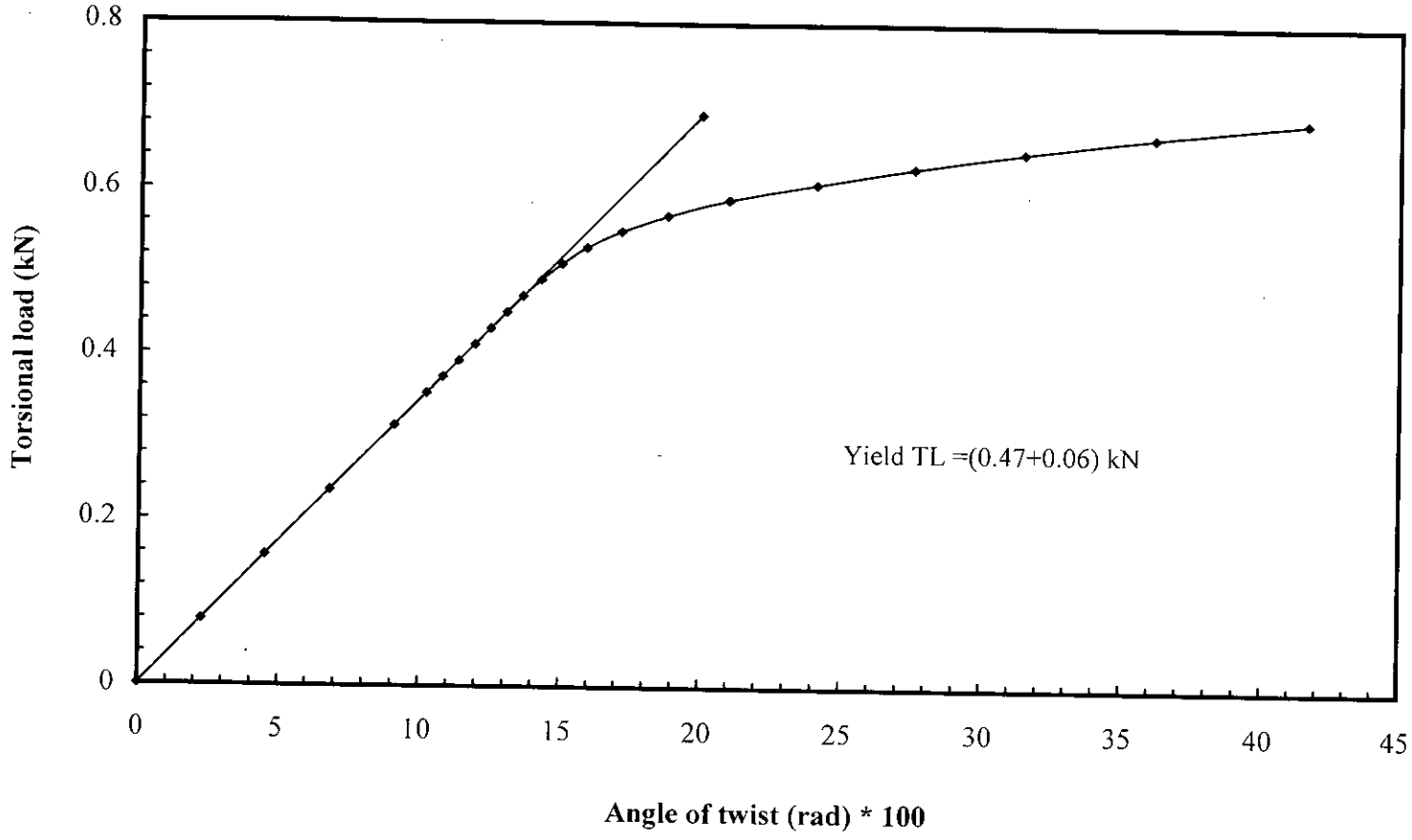

Figure 4.7: Torsional load versus angle of twist curve for M/T = 0.56

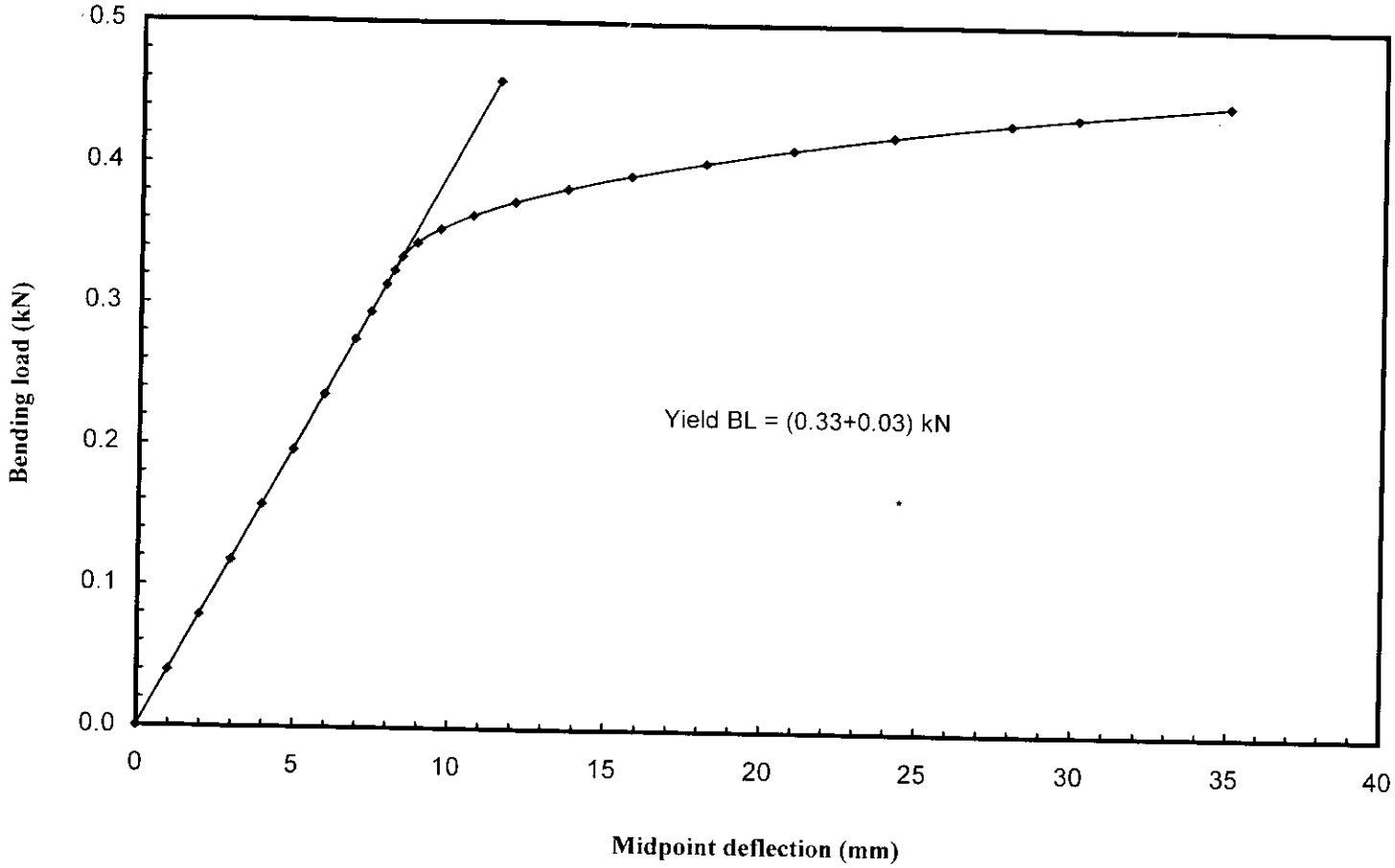

Figure 4.8: Bending load versus midpoint deflection curve for M/T=1.12

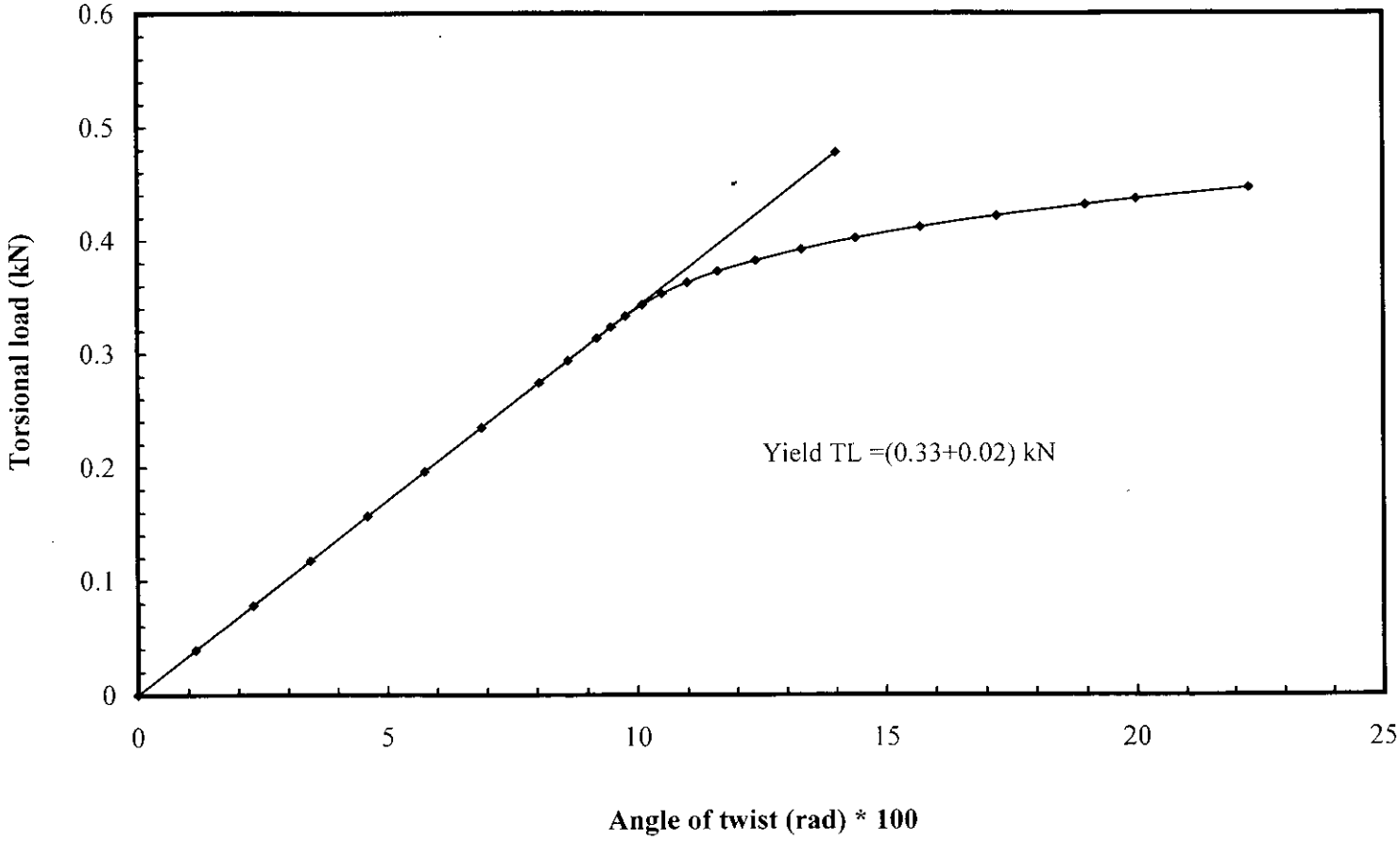

Figure 4.9: Torsional load versus angle of twist curve for M/T = 1.12

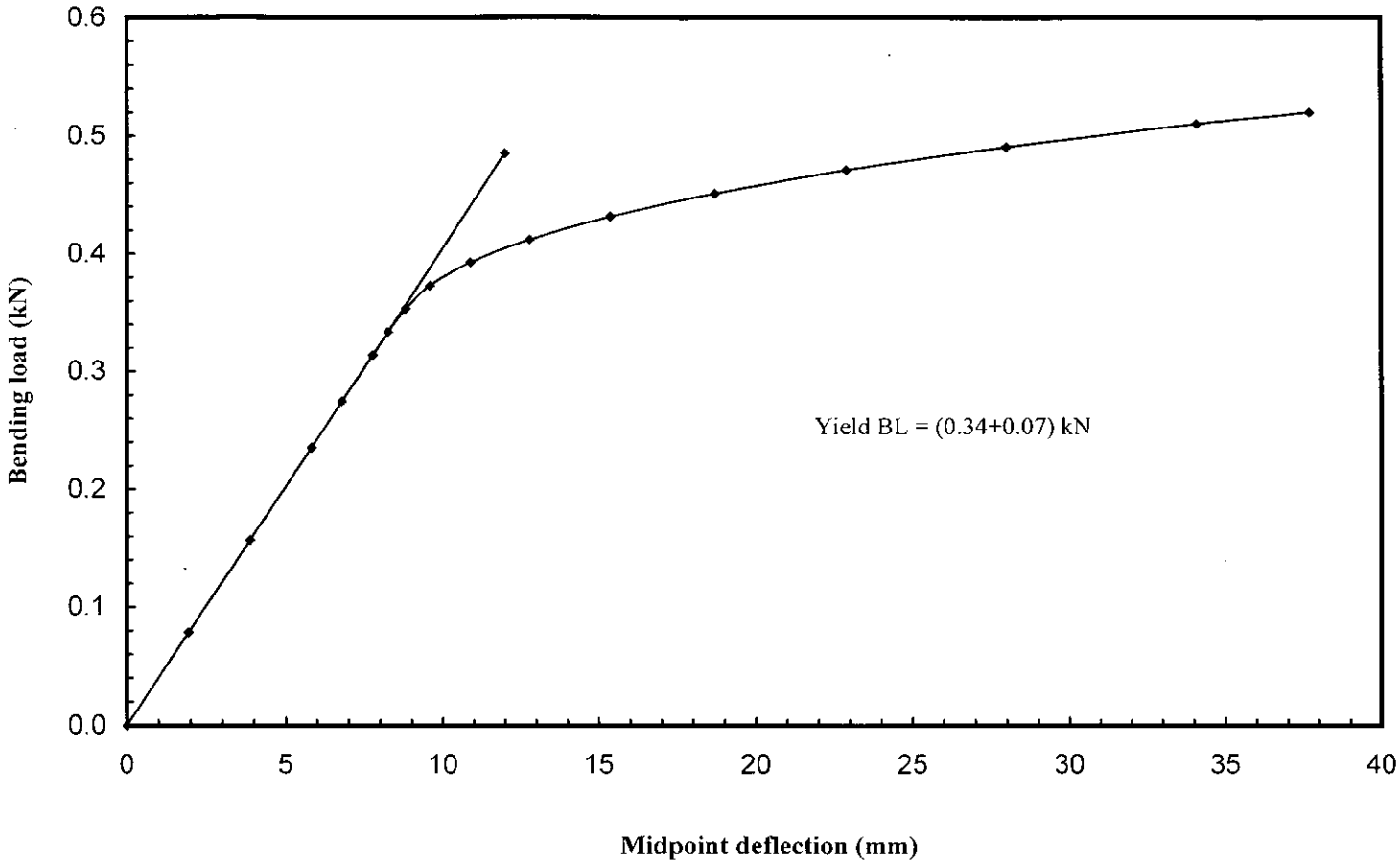

Figure 4.10: Bending load versus midpoint deflection curve for M/T=2.24

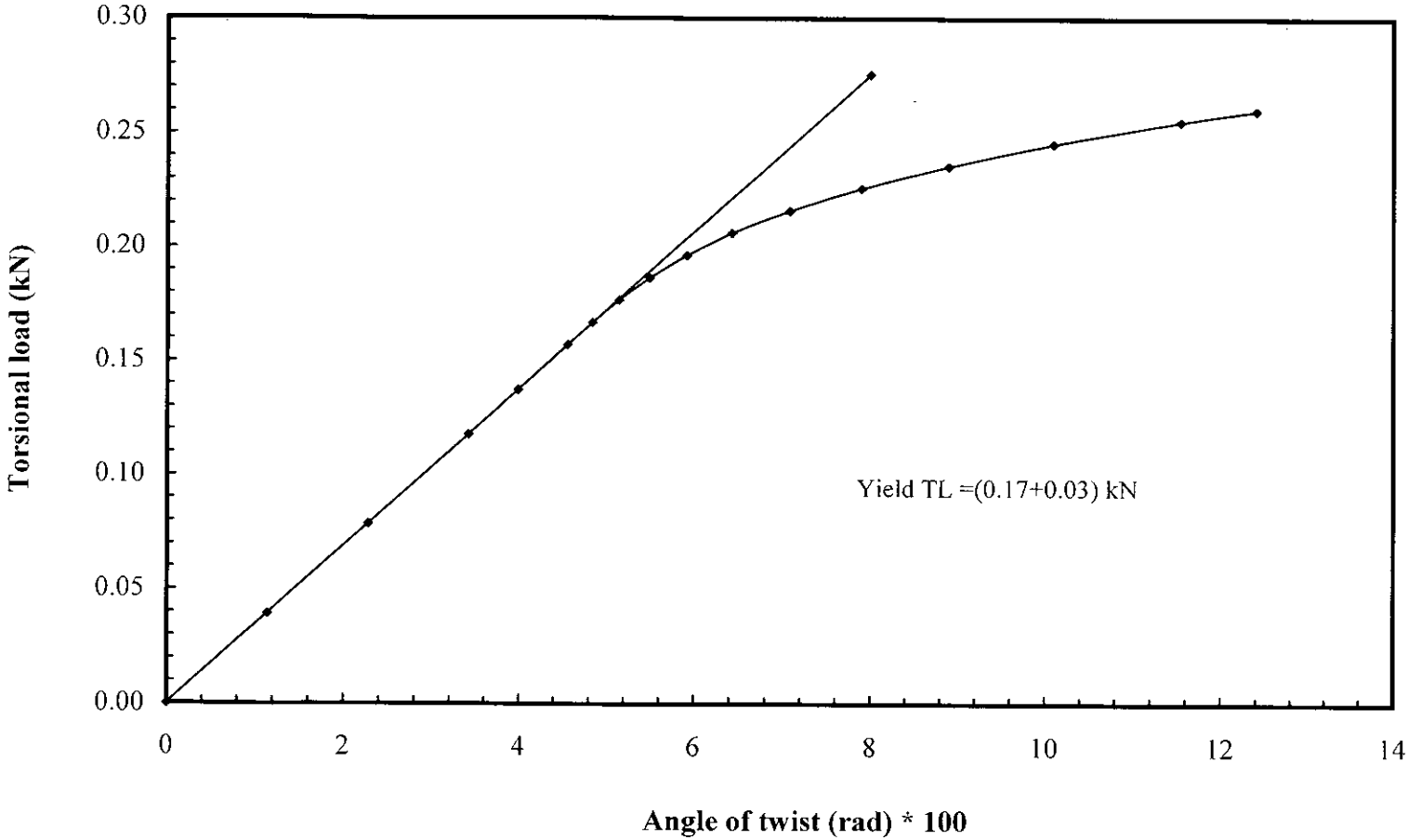

Figure 4.11: Torsional load versus angle of twist curve for M/T = 2.24

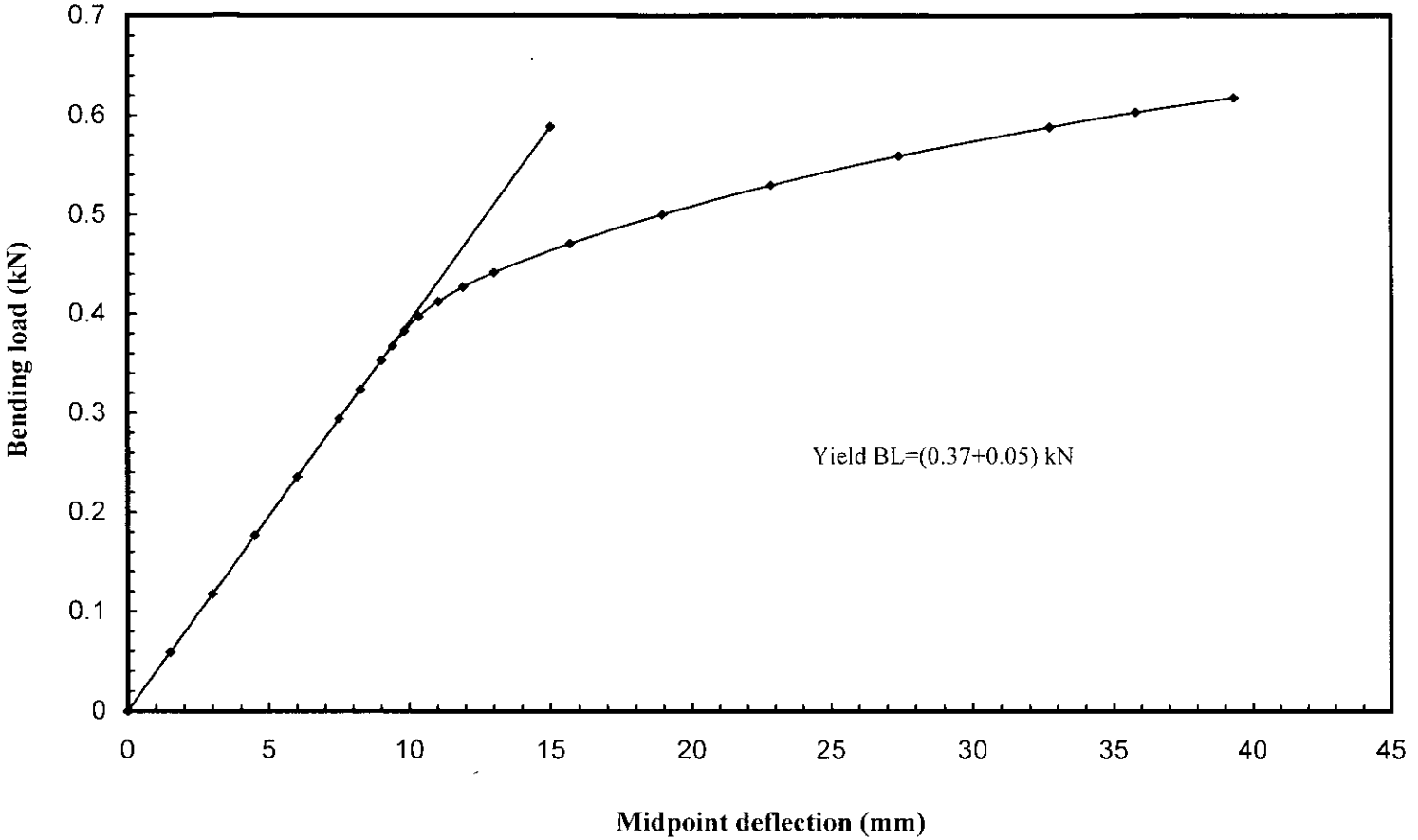

Figure 4.12: Bending load versus midpoint deflection curve for M/T = 3.36

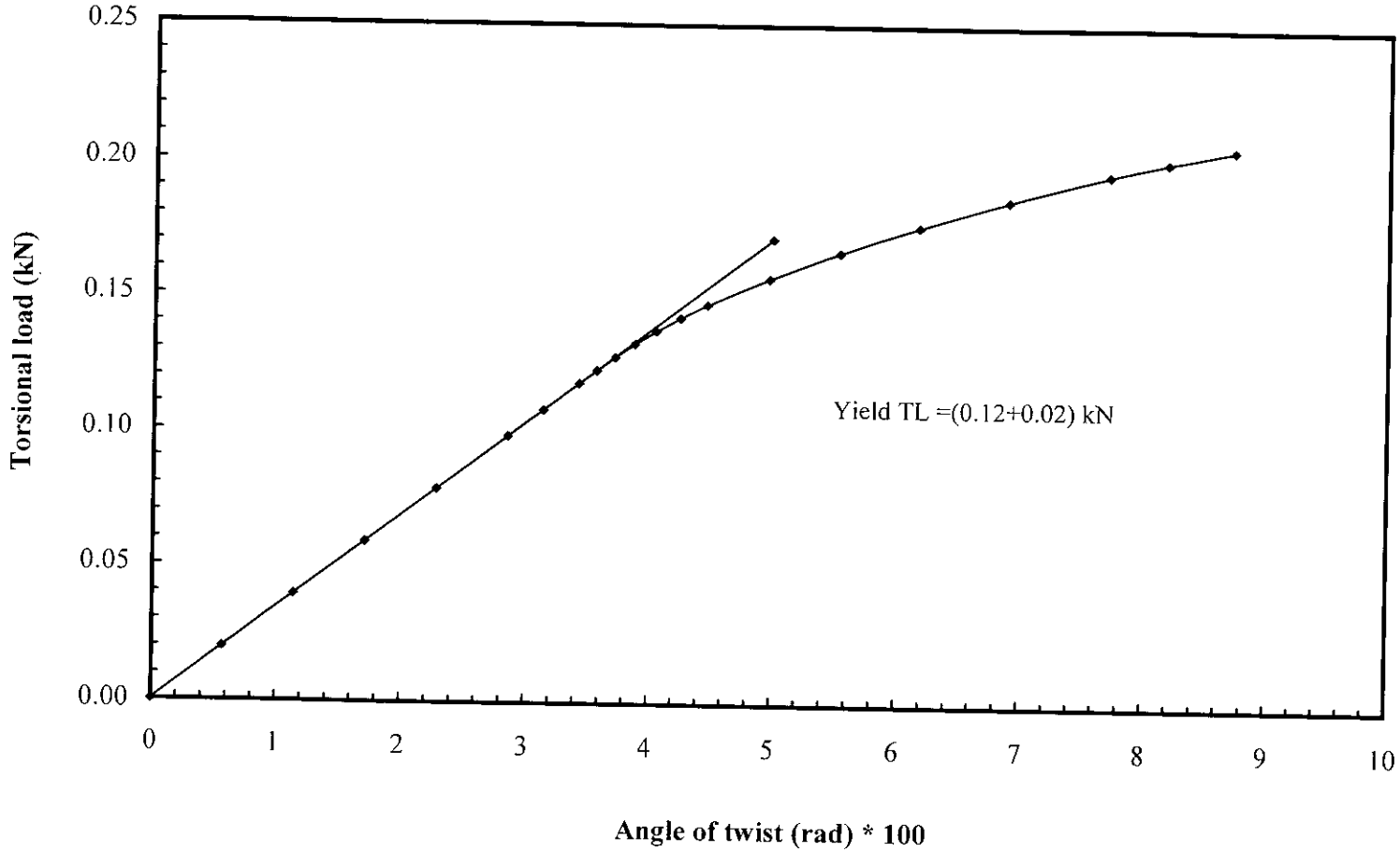

Figure 4.13: Torsional load versus angle of twist curve for M/T = 3.36

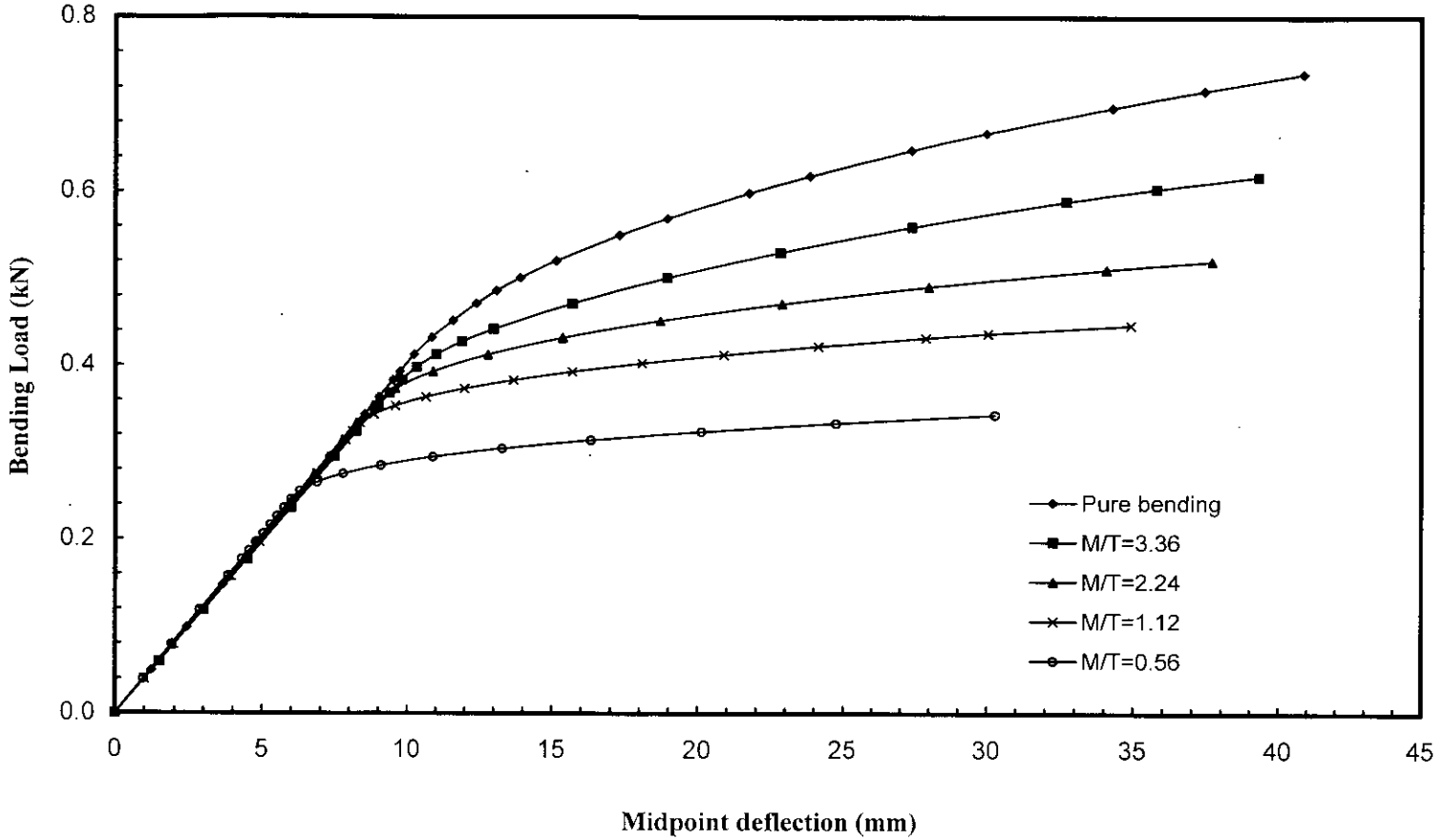

Figure 4.14: Bending load versus midpoint deflection curve for different M/T ratios (Proportional loading)

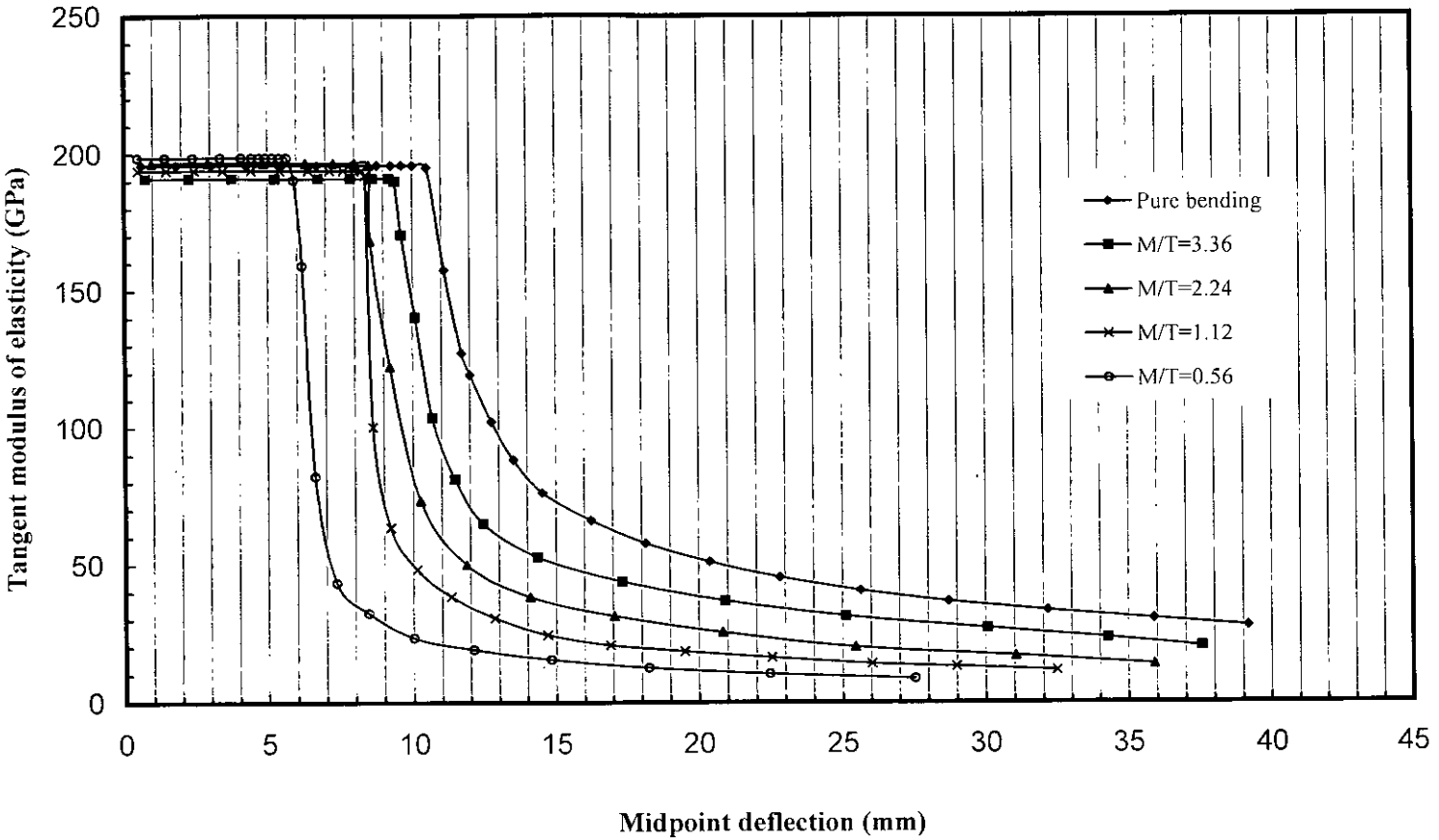

Figure 4.15: Variation of the tangent modulus of elasticity with respect to the midpoint deflection of the beam for different M/T ratios (Proportional loading)

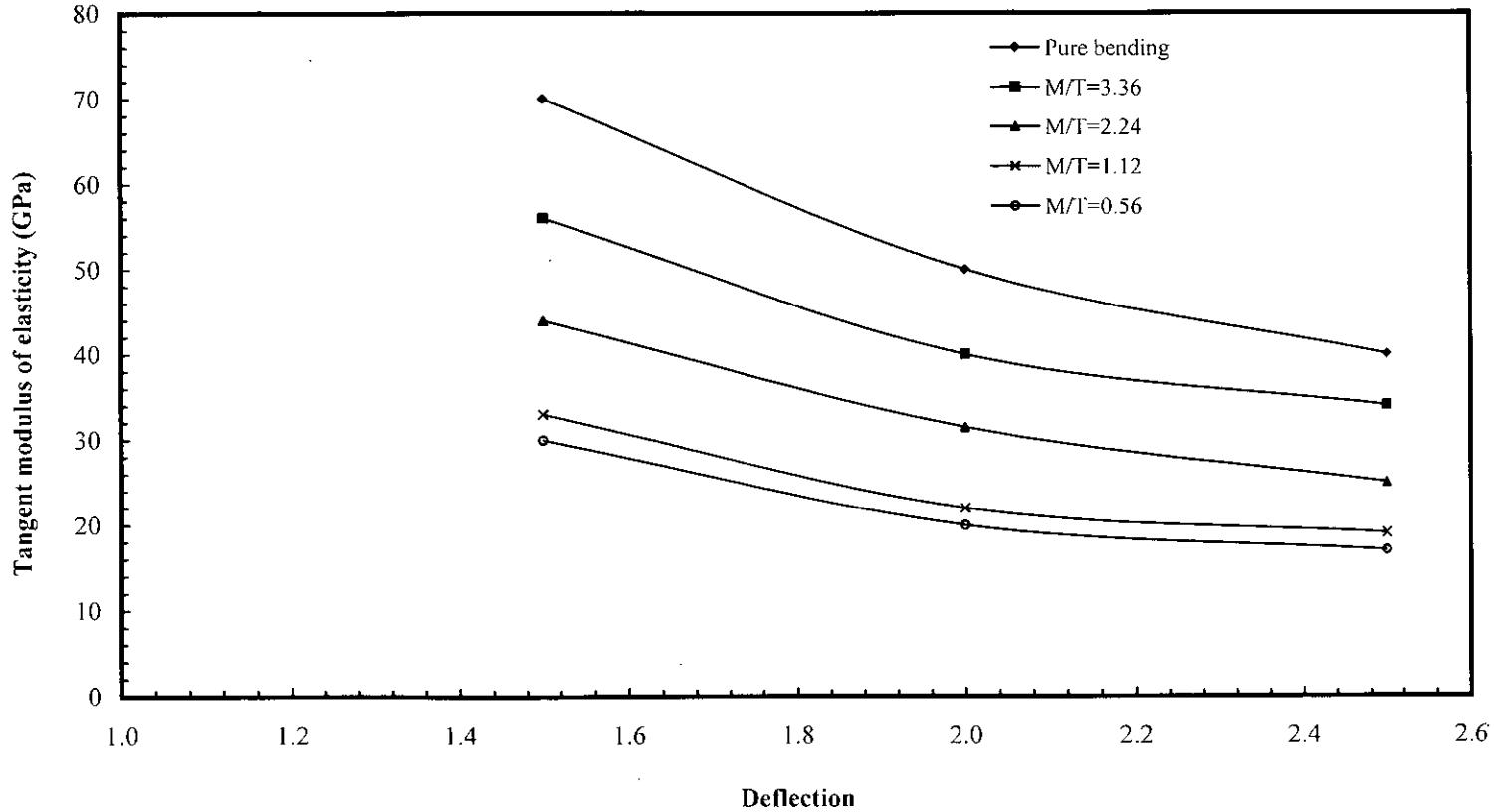

Figure 4.16: Variation of the tangent modulus of elasticity at 1.5, 2, 2.5 times of the corresponding midpoint deflection for different M/T ratios (Proportional loading)

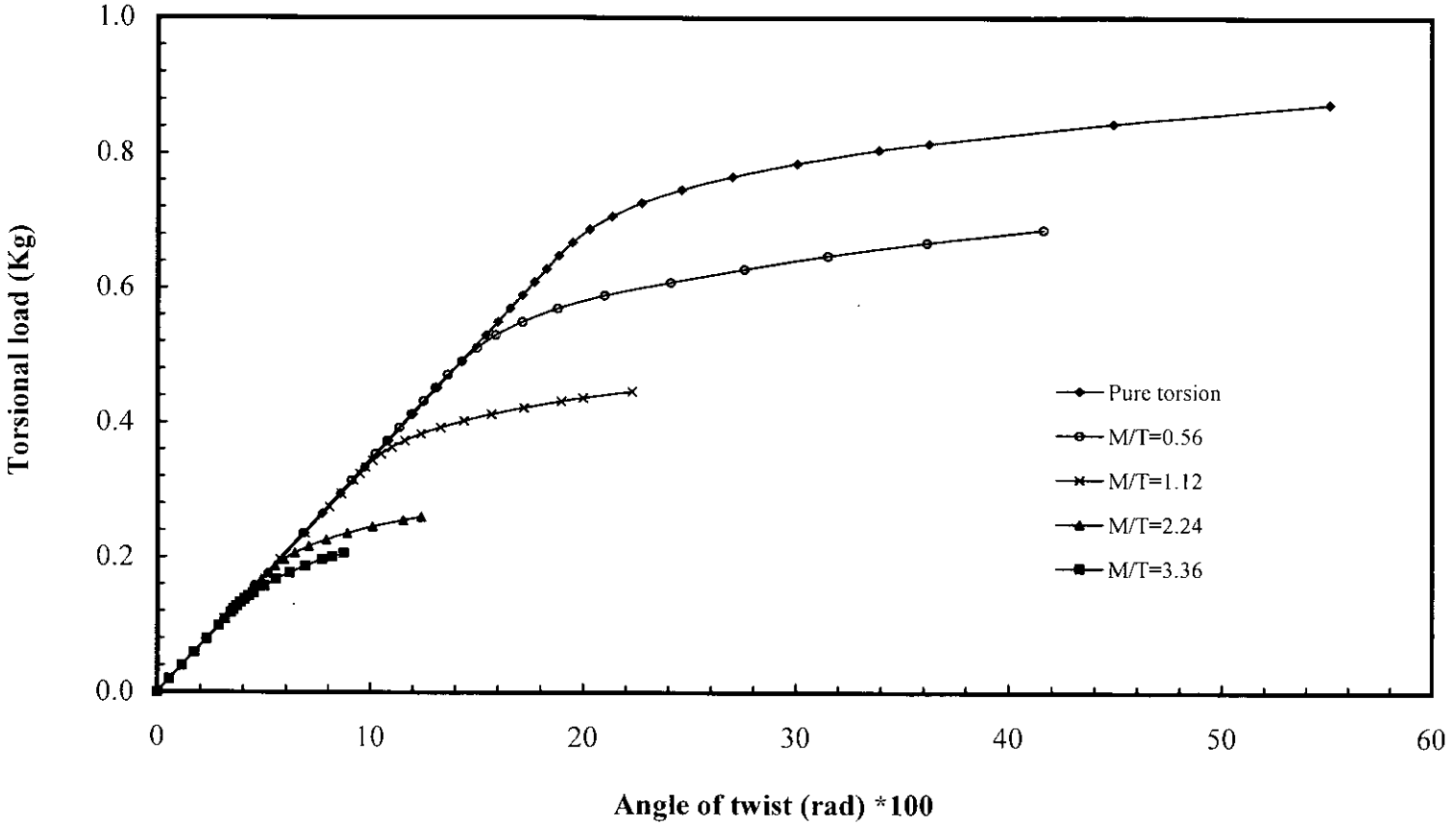

Figure 4.17: Torsional load versus angle of twist curves for different M/T ratios (Proportional loading)

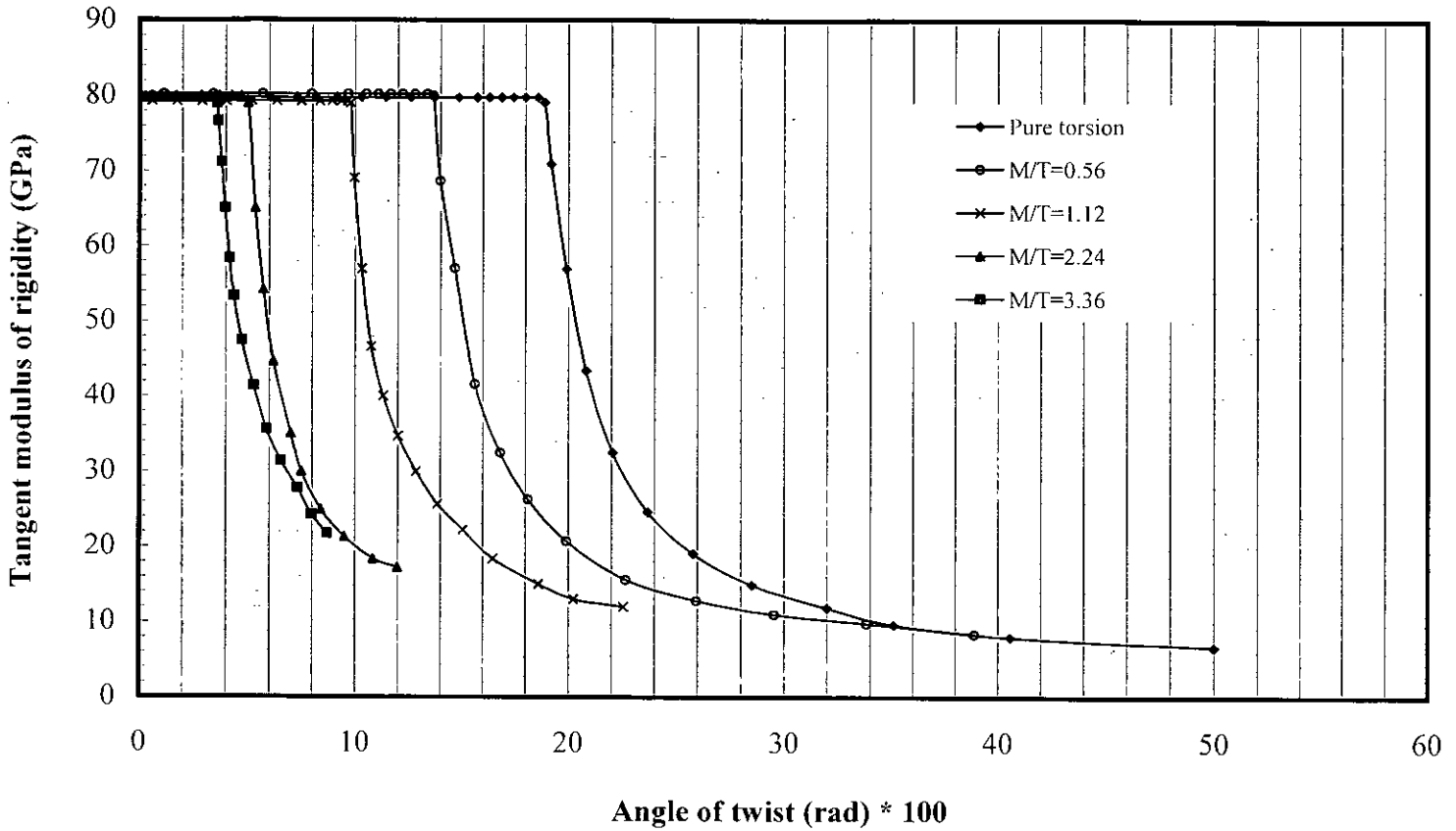

Figure 4.18: Variation of the tangent modulus of rigidity with respect to angle of twist for different M/T ratios (Proportional loading)

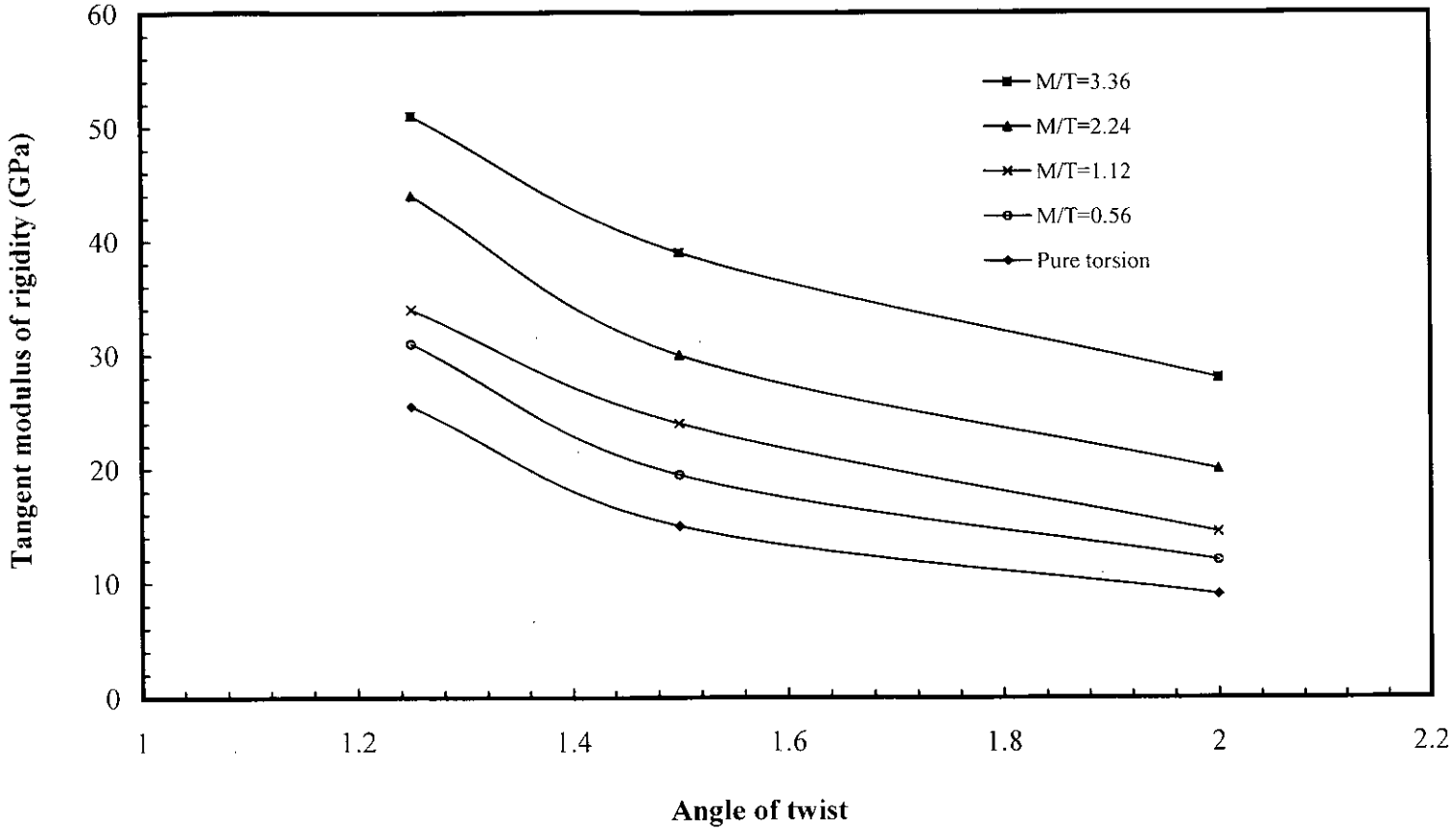

Figure 4.19: Variation of the tangent modulus of rigidity at the 1.25, 1.5 and 2 times of the corresponding yield angle of twist for different M/T ratios (Proportional loading)

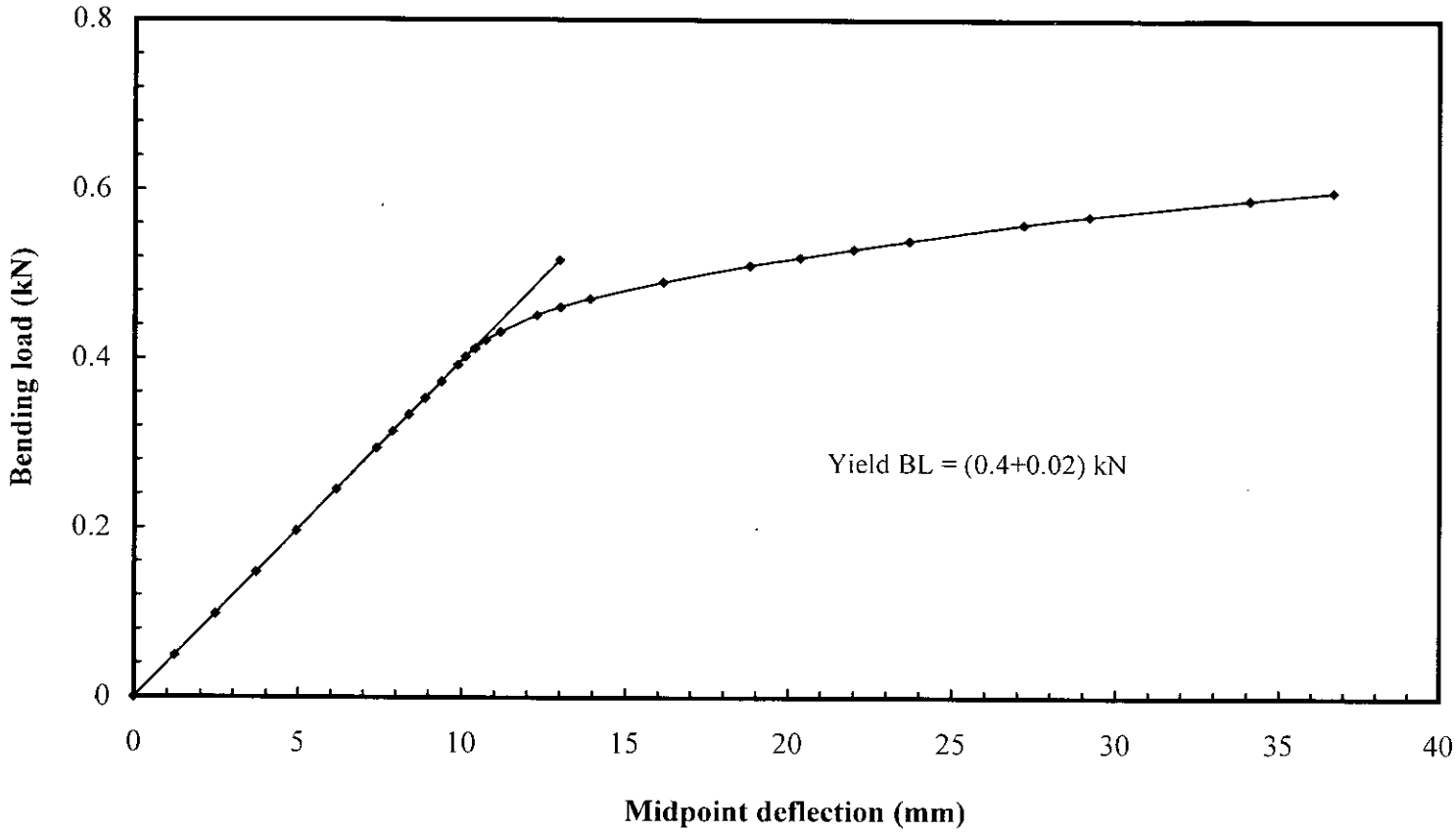

Figure 4.20: Bending load versus midpoint deflection curve for initial 25% of YTL of pure torsion

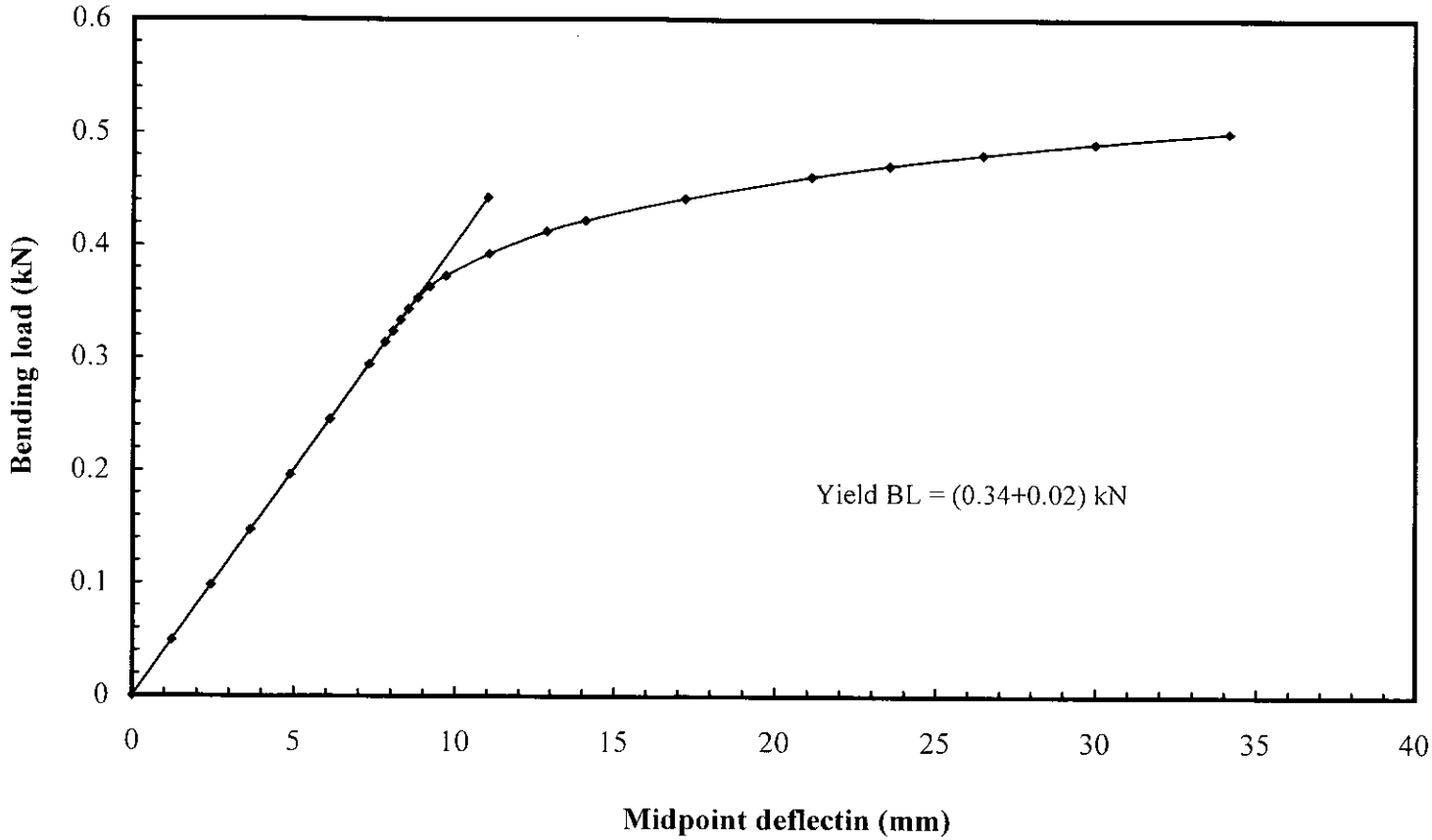

Figure 4.21: Bending load versus midpoint deflection curve for initial 50% of YTL of pure torsion

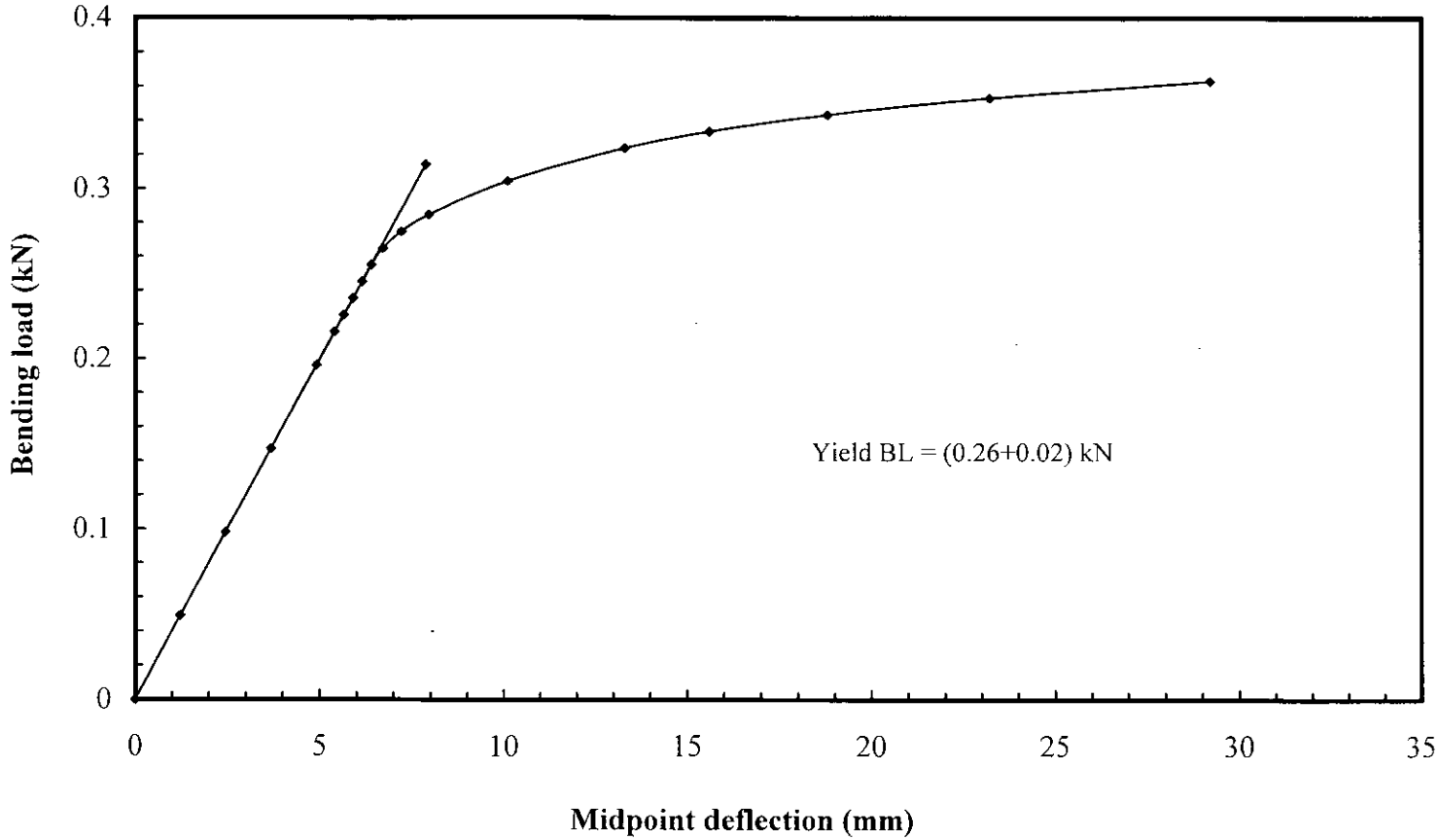

Figure 4.22: Bending load versus midpoint deflection curve for initial 75% of YTL of pure torsion

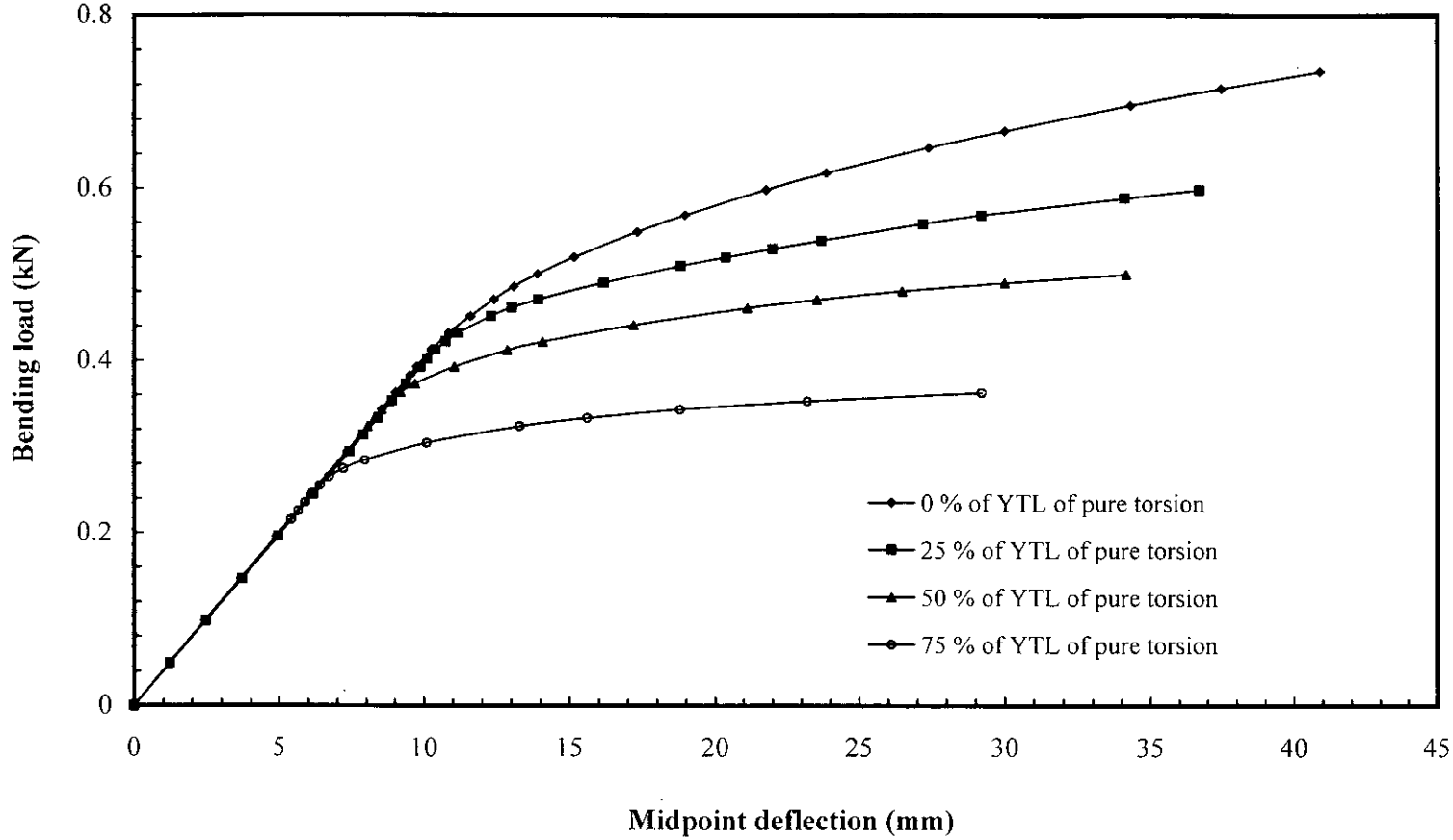

Figure 4.23: Bending load versus midpoint deflection curves for different levels of initially applied constant torsional loads (Non-proportional loading)

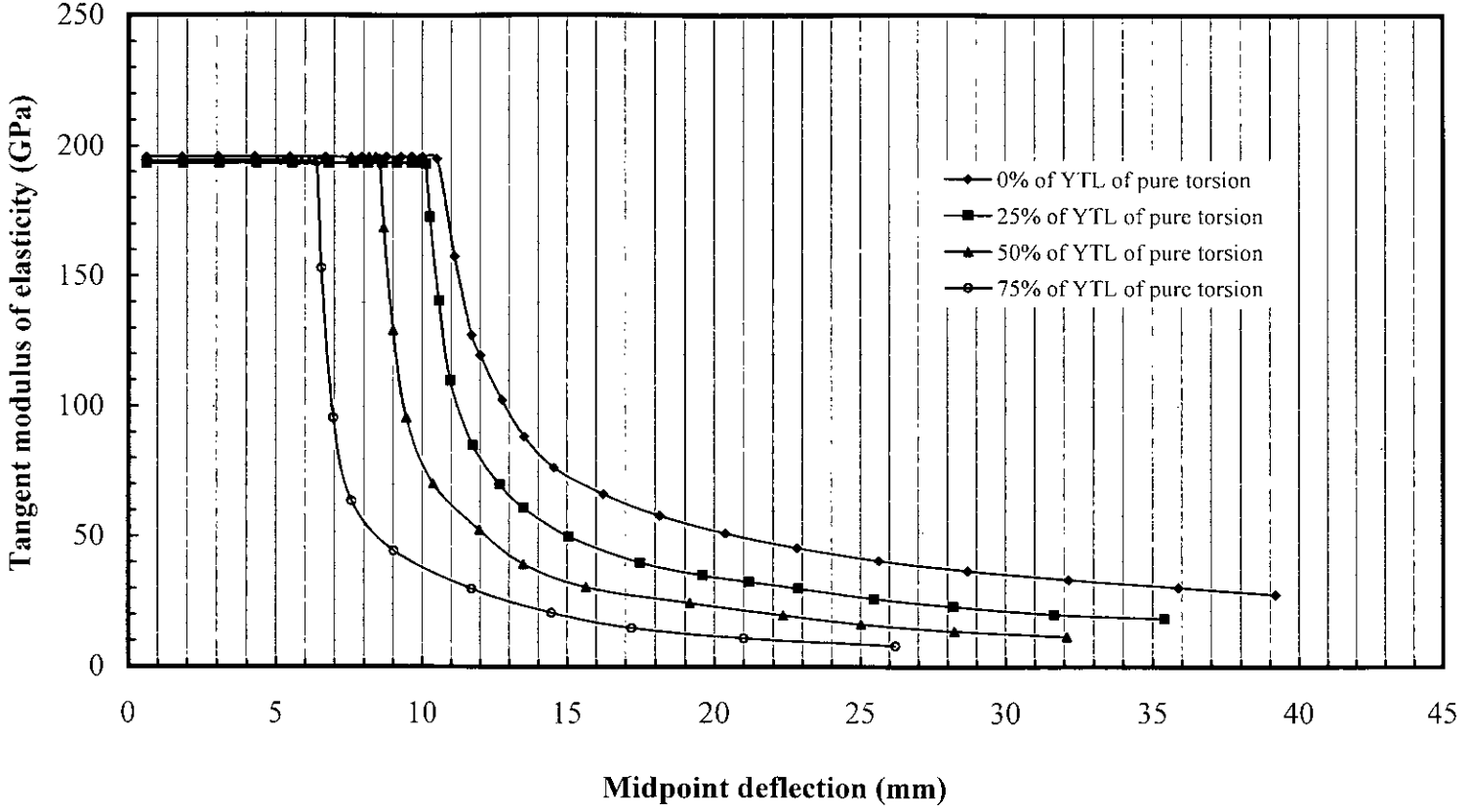

Figure 4.24: Variation of the tangent modulus of elasticity with respect to the midpoint deflection for different levels of initially applied constant torsional loads (Non-proportional loading)

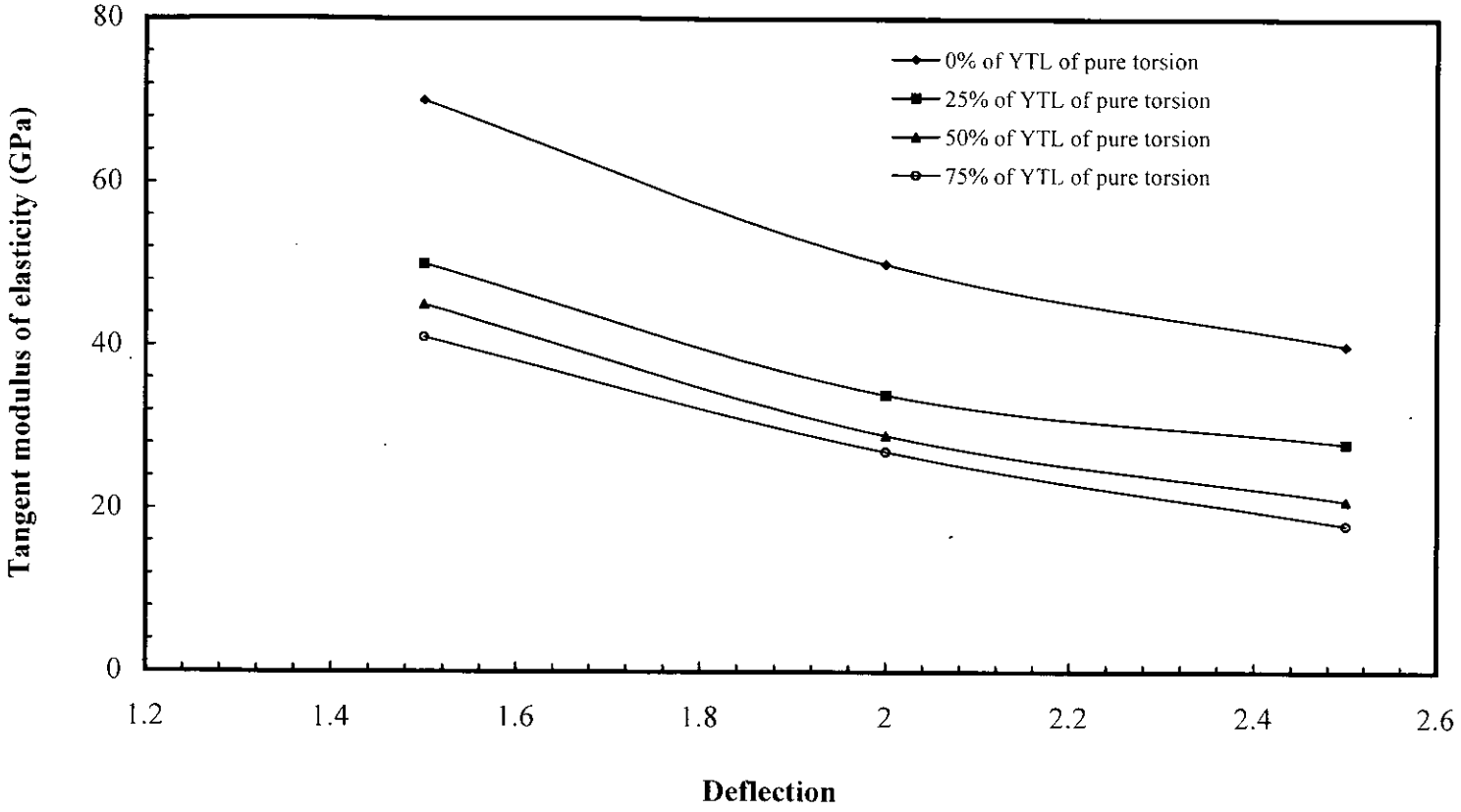

Figure 4.25: Variation of the tangent modulus of elasticity at 1.5, 2, and 2.5 times of the corresponding yield deflection for different levels of initially applied constant torsional loads (Non-proportional loading)

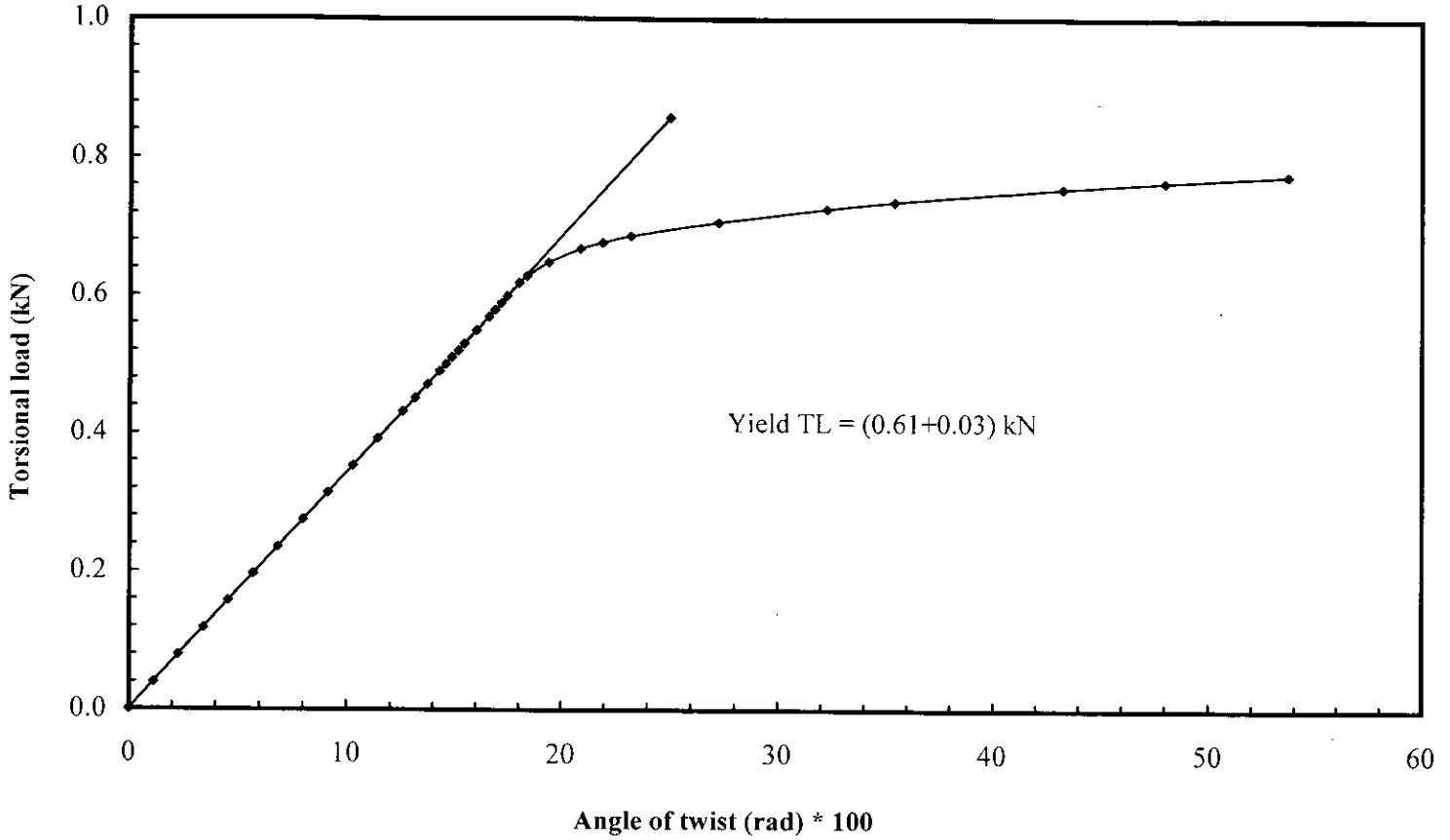

Figure 4.26: Torsional load versus angle of twist curve for initial 25% of YBL of pure bending

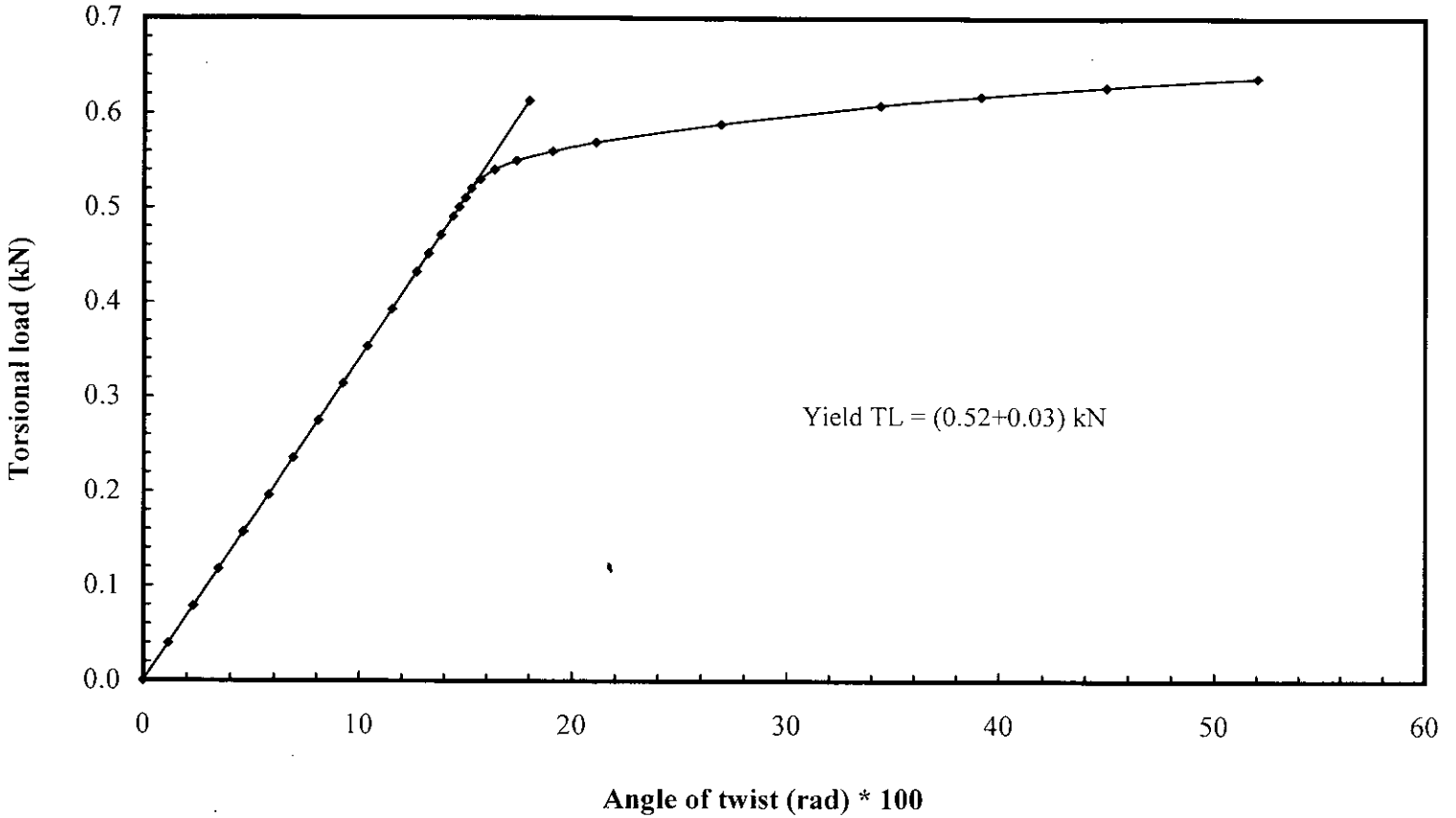

Figure 4.27: Torsional load versus angle of twist curve for initial 50% of YBL of pure bending

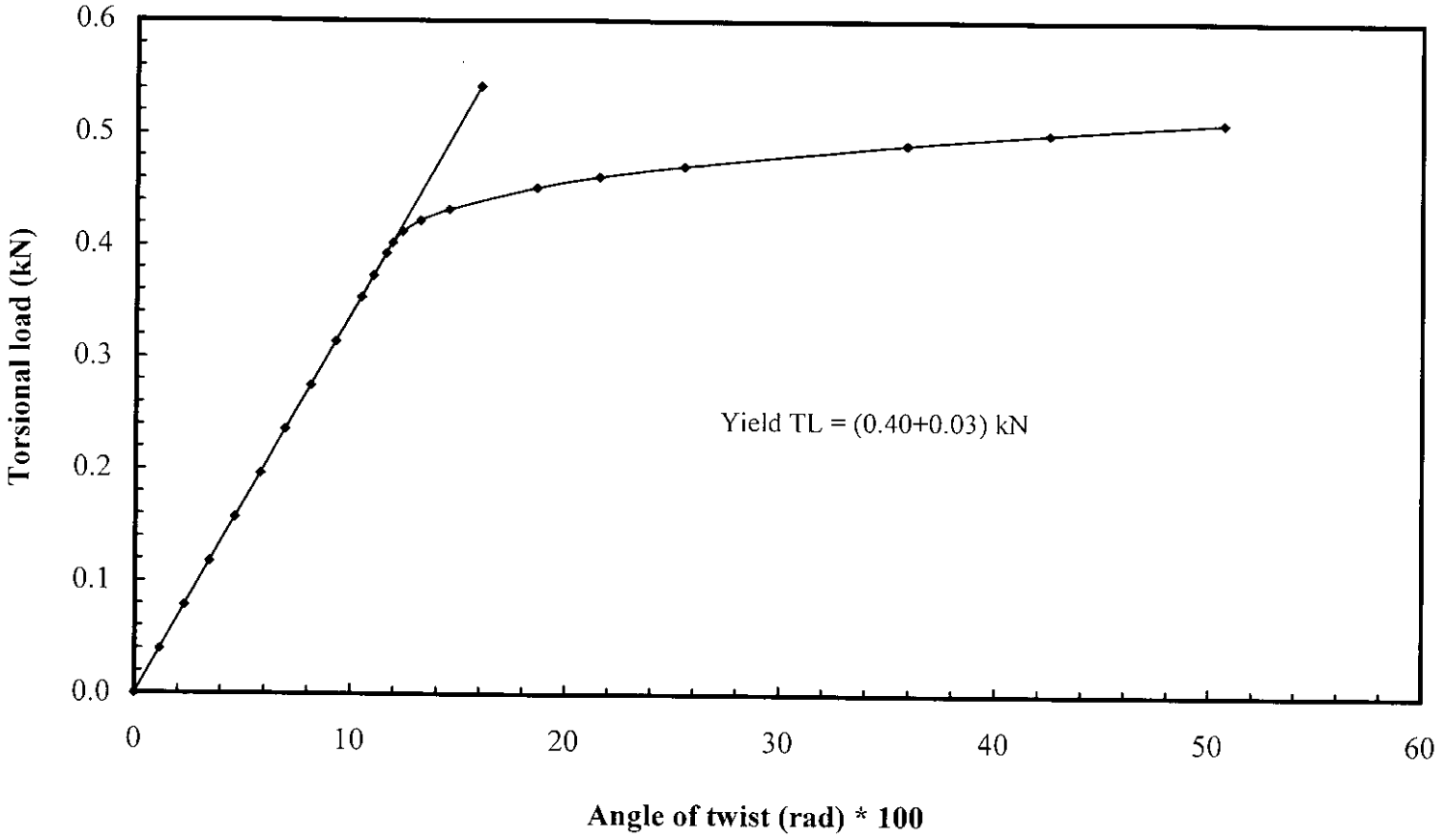

Figure 4.28: Torsional load versus angle of twist curve for initial 75% of YBL of pure bending

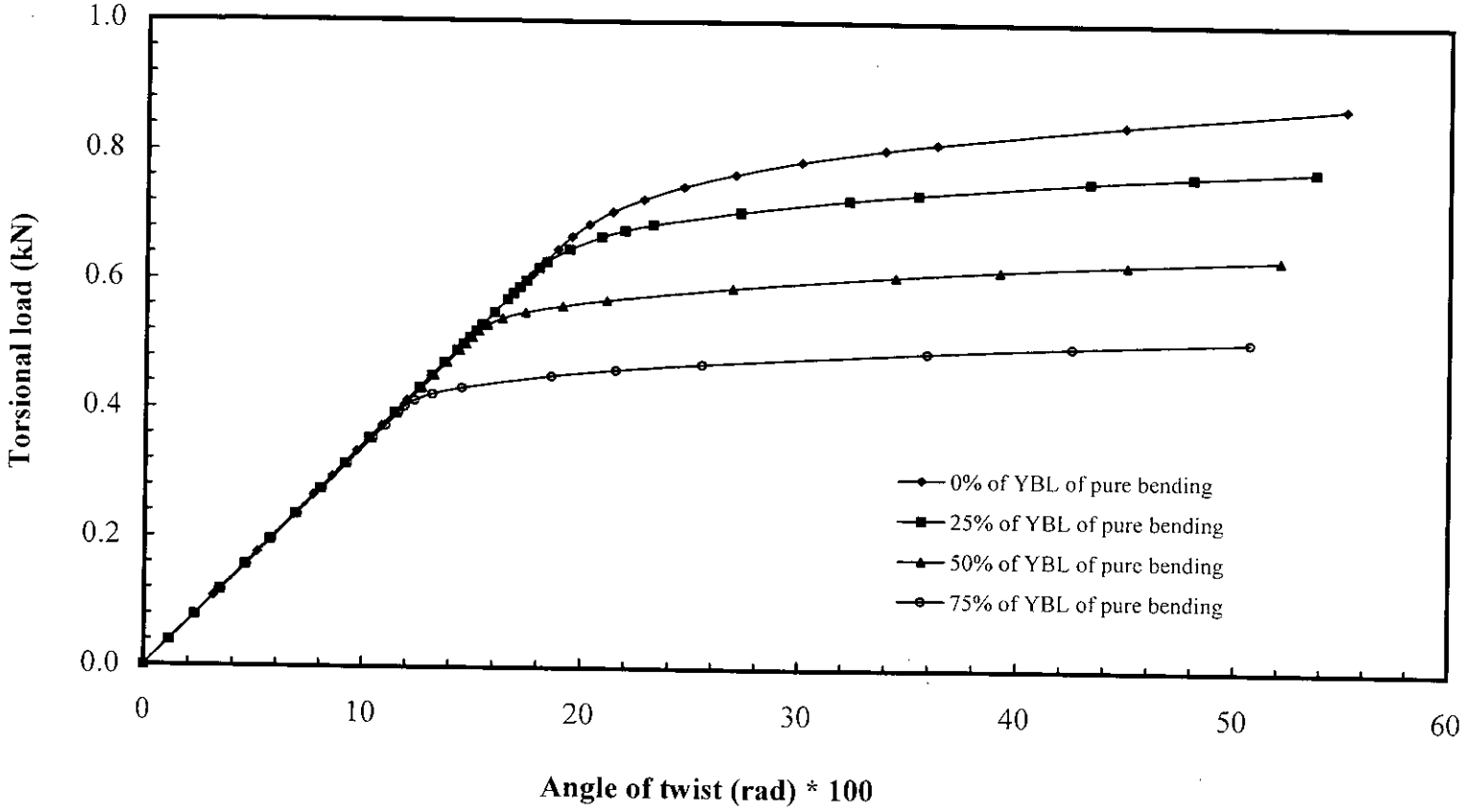

Figure 4.29: Torsional load versus angle of twist curves for different levels of initially applied constant bending loads (Non-proportional loading)

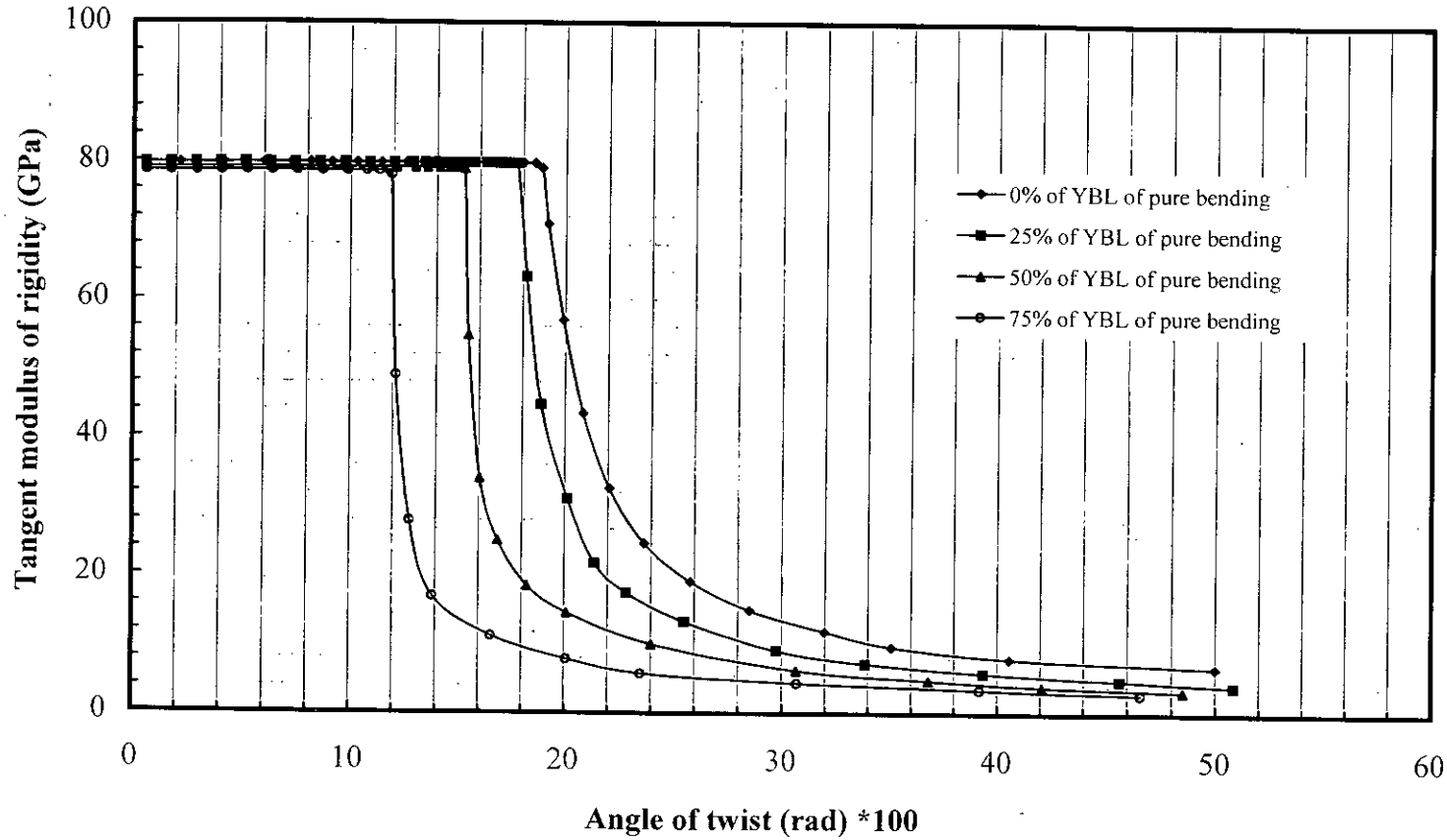

Figure 4.30: Variation of the tangent modulus of rigidity with respect to the angle of twist for different levels of initially applied constant bending loads (Non-proportional loading)

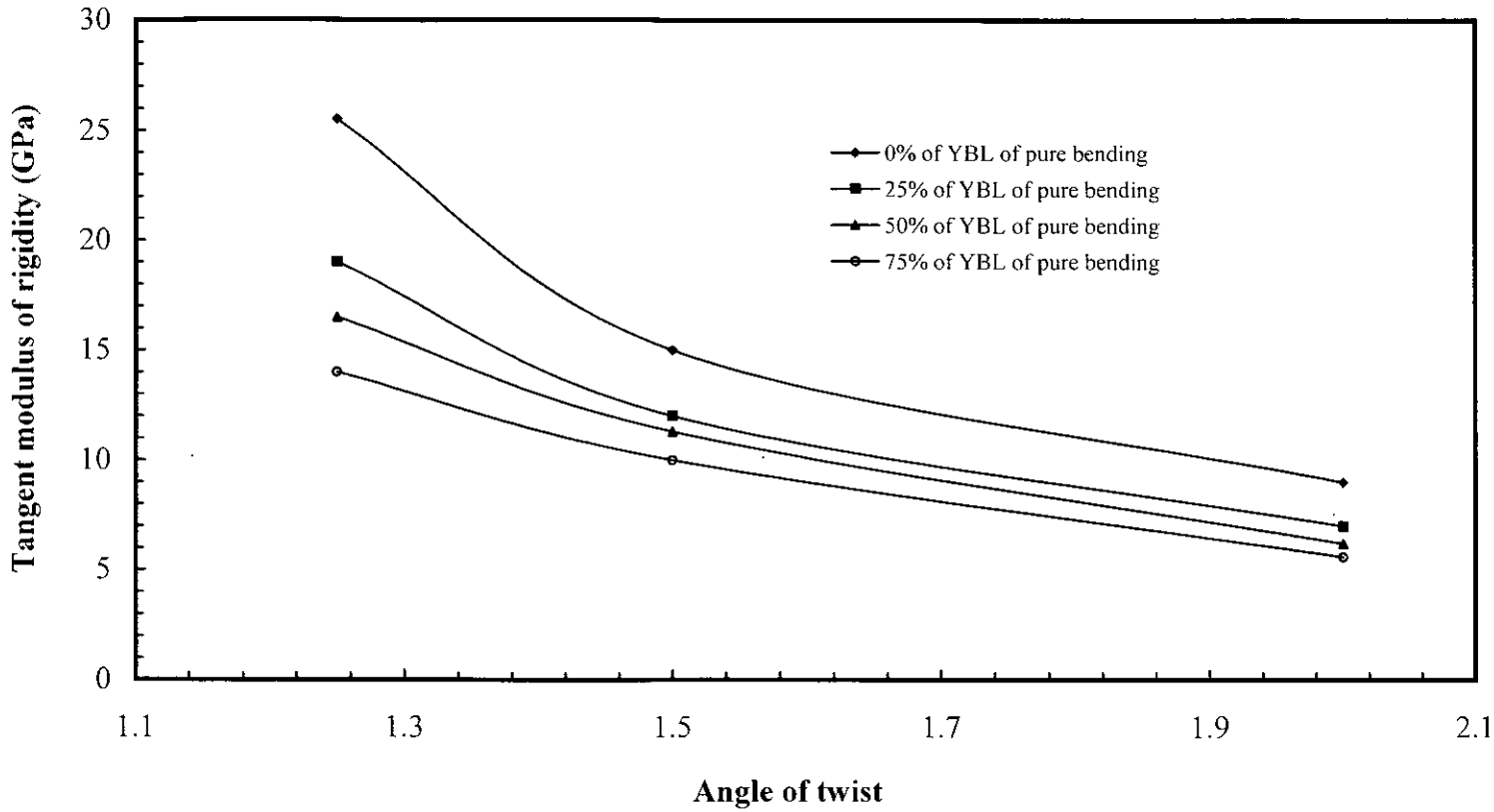

Figure 4.31: Variation of the tangent modulus of rigidity at 1.25, 1.5, and 2 times of the corresponding yield angle of twist for different levels of initially applied constant bending loads (Non-proportional loading)

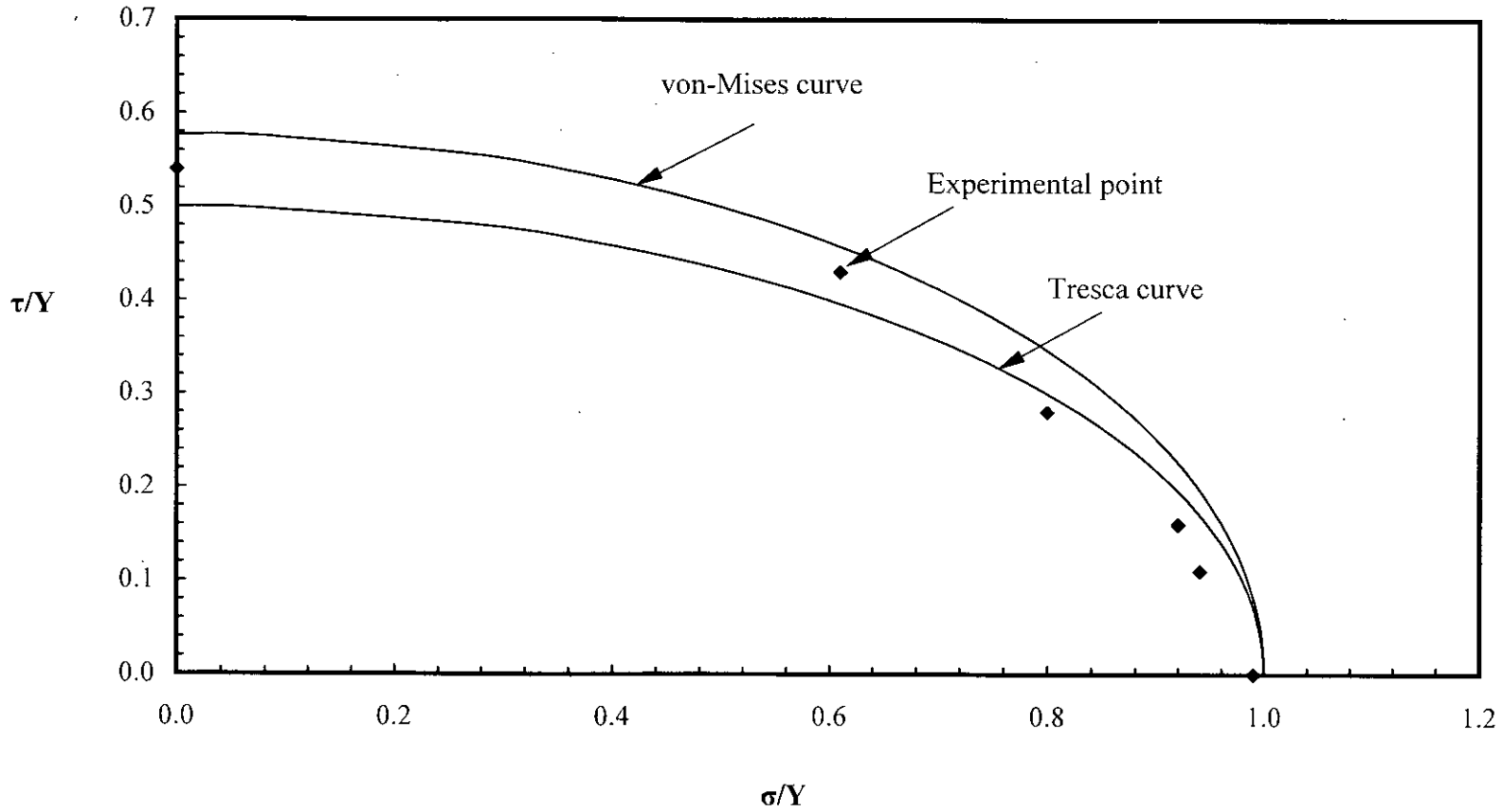

Figure 4.32: Interaction curves and experimental points for proportional loadings

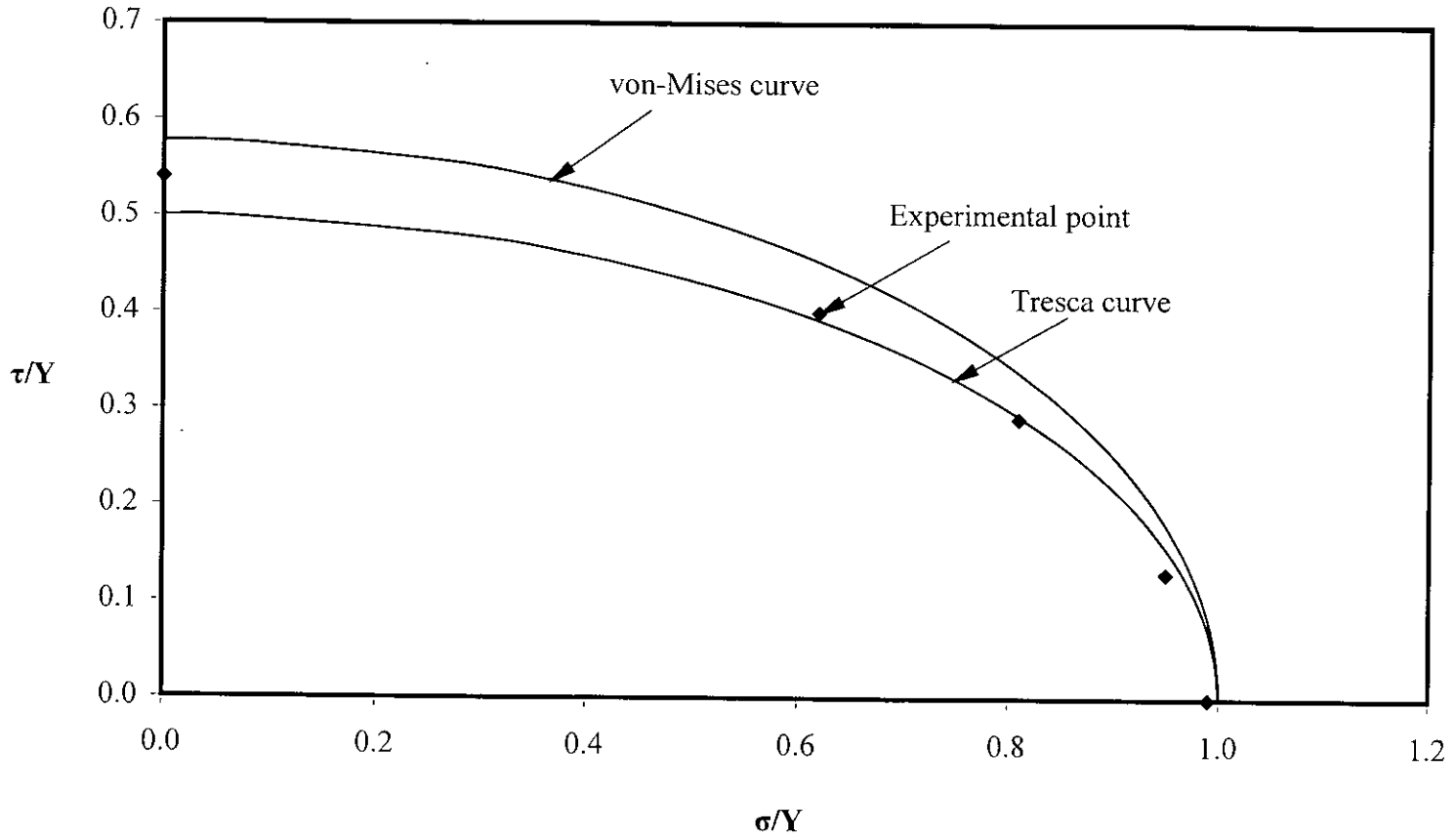

Figure 4.33: Interaction curves and experimental points for non-proportional loading (Variable bending load with constant initial torsional load)

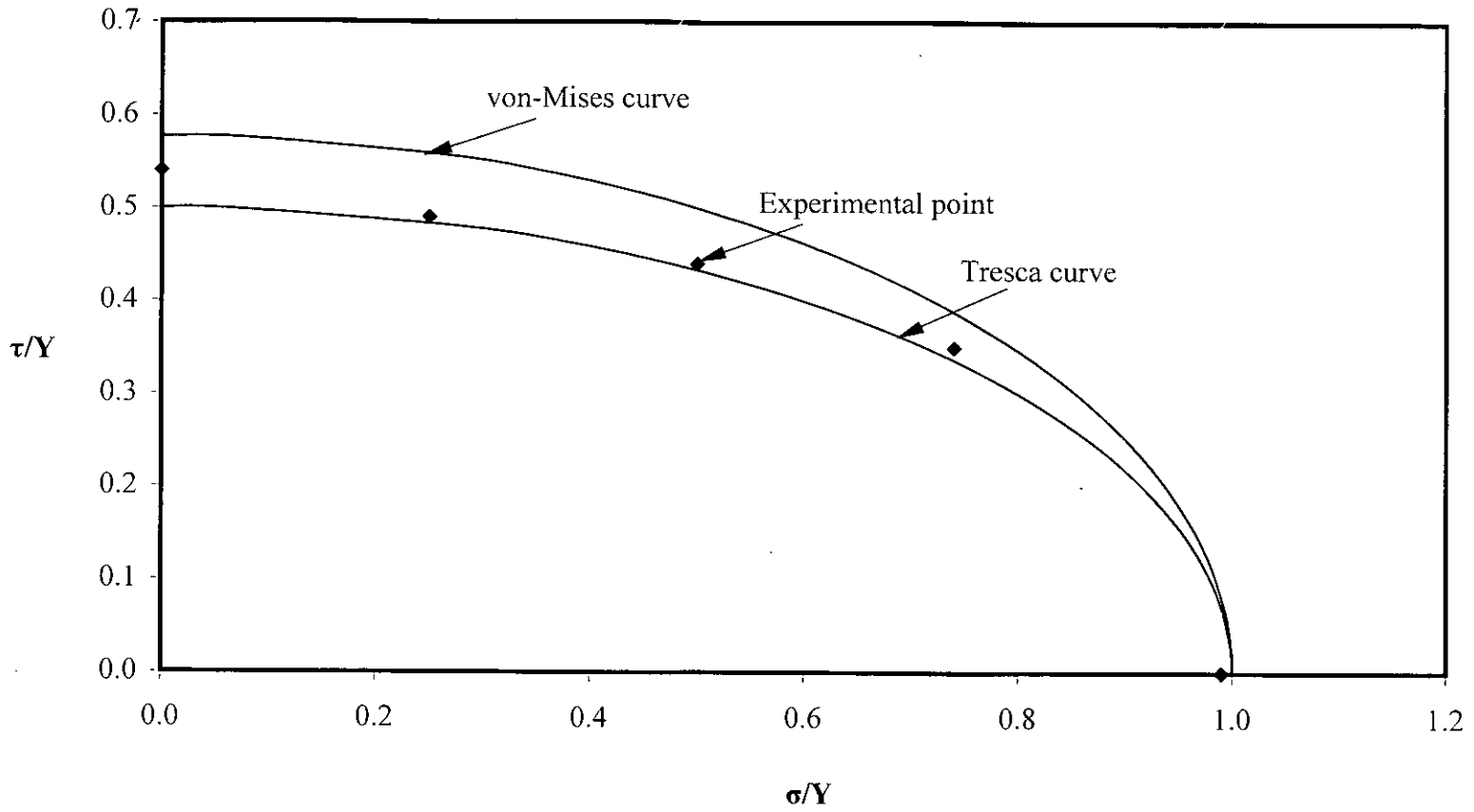

Figure 4.34: Interaction curves and experimental points for non-proportional loading (Variable torsional load with constant initial bending load)

CHAPTER – 5
CONCLUSIONS AND RECOMMENDATIONS

5.1 INTRODUCTION

An experimental investigation has been carried out in this research work where square solid bars are subjected to different types of combined loading arrangement- both proportional and nonproportional loading. In order to carry out the investigation a purpose-built test rig has been designed and constructed. Details of the experimental set up and procedures have been discussed in Chapter 3 whereas results have been presented in Chapter 4. Main findings and recommendations are given in the present chapter.

5.2 GENERAL CONCLUSION

5.2.1 Test Rig

A purpose-built test rig, which is capable of applying bending and torsional loads either separately or simultaneously has been designed and fabricated.

5.2.2 Conclusions

The following major conclusions can be drawn from the present investigation:

1. In case of proportional loading, with the increase of the ratio of bending moment to torque (i.e, M/T ratio), yield bending load increases while yield torsional load decreases. It is further observed that yield torsional load does not decrease by the same magnitude as the yield bending load increases. As for example, when the M/T ratio increased from 0.56 to 1.12, yield bending load increased by 33.33% whereas yield torsional load decreased by 33.96 %.

2. In case of proportional loading, it is also observed that whatever be the level of M/T ratio, the initial slopes of the bending load versus midpoint deflection curves and torsional load versus angle of twist curves are similar to those of

pure bending and pure torsion curves respectively, i.e., modulus of elasticity and modulus of rigidity don't vary with the variation of M/T ratio and hence stiffness of the material of the specimens in the elastic region is nearly constant for all the ratios of M/T.

3. It is found that in case of proportional loading, whatever be the level of M/T ratio, tangent modulus of elasticity beyond the yield point steadily decreases with the increase of load and at the same corresponding deflection its value is higher for the higher value of M/T ratio. Similarly, whatever be the level of M/T ratio, tangent modulus of rigidity beyond the yield point steadily decreases with the increase of load and at the same corresponding angle of twist its value is higher for the higher value of M/T ratio. This means, when bending moment dominates in the combined loading, strain hardening and stiffness of the material in the inelastic region become more noticeable. It is also observed that percentage variation of the tangent modulus of elasticity is smaller for higher value of M/T ratio whereas percentage variation of the tangent modulus of rigidity is higher for higher value of M/T ratio.

4. In case of non-proportional loading, it is found that, the higher the level of initially applied constant torque, the lower the level of bending moment for which the square solid bar yields plastically and the higher the level of initially applied constant bending moment, the lower the level of torque for which the square solid bar yields plastically. As for example, when the initially applied constant torque increased by 25 %, bending moment decreased by 18.25 % and when the initially applied constant bending moment increased by 25 % torque decreased by 17.93 %.

5. In case of non-proportional loading, it is also observed that whatever be the level of initial torque or bending moment, the initial slopes of the bending load versus midpoint deflection curves and torsional load versus angle of twist curves are similar to those of pure bending and pure torsion curves respectively, i.e., modulus of elasticity and modulus of rigidity are nearly

constant for all levels of initially applied constant bending moment and torque respectively. Hence stiffness of the material of the specimens is nearly constant in the elastic region for all levels of initially applied constant bending moment or torque.

6. For non-proportional loading, whatever be the level of initially applied constant torque, tangent modulus of elasticity beyond the yield point steadily decreases with the increase of load and at the same corresponding deflection its value is higher for the smaller level of initial torque. Similarly, whatever be the level of initially applied constant bending moment, tangent modulus of rigidity beyond the yield point steadily decreases with the increase of load and at the same corresponding angle of twist its value is higher for the smaller level of initial bending moment. This means, when the initially applied constant bending moment or torque comparatively less dominates in the combined loading, strain hardening and stiffness of the material in the inelastic region become more noticeable. It is also observed that percentage variation of the tangent modulus of elasticity and tangent modulus of rigidity is higher for higher value of initially applied torque and bending moment respectively.

7. From the comparision of the experimental data with von-Mises and Tresca results, it is seen that experimental results have better agreement with Tresca yield criterion.

5.3 RECOMMENDATIONS

To increase the flexibility and accuracy of the set up and experimental procedures to get the best possible results, the following points are recommended for future works:

1. Digital stepper motor can be used to apply torque to the specimen

2. Transducers along with a spectra automatic data-acquisition system can be used to measure the deflection and twisting angle of the specimen.

3. After the limit of proportionality there will, of course be some creep. So standardised time gap should be applied between successive increments of loads.

4. In this experiment it has been considered that all the members of the test rig are perfectly rigid. But ideally, it is not so. Hence due consideration should be given to obtain the highest possible rigidity of the test rig.

5. It has been considered that the test specimen is completely homogeneous throughout its length and cross section. But ideally, it is not possible to get one such. Hence non-homogeneous materials may have some effects on its results. This point needs to be considered to obtain the best possible results.

6. The experimental results presented in this work were not verified theoretically. So a theoretical model could be developed and should be compared with the experimental results.

REFERENCES

[1] Hill. R. "The Mathematical Theory of Plasticity", Oxford University Press, London, 1950.

[2] Westergaard, B.W., "Theory of Elasticity and Plasticity", Harvard University Press, Cambridge, 1952.

[3] Siebel, M. P. L. "The combined bending and twisting of thin cylinders in the plastic range" Jour. Mech. and Phys. Solids, Vol. I, 1953, pp. 189-206.

[4] Hill, R and Siebel, M. P. L., "On the combined bending and twisting of thin tubes in the plastic range", Philosophical Mag., Vol. 42(7), 1951, pp. 722-33.

[5] Imegwu, E. O., "Plastic flexture and torsion of thin tubes", Jour. Mech. and Phys. Solids, Vol. 3, 1954, pp 156-66.

[6] Banerjee, J. K., "Plastic instability in tubes of finite length", ibid, vol. – 17, 1975, pp. 659

[7] Menkin, C. M. and Veldpavs, F. E., "The non linear flexural-torsional behaviour of straight slender elastic member with arbitrary cross sections", Thin walled Structure, Vol – 6 (5), 1988, pp. 385-404.

[8] Bathe, K. J. and Wieser. P. M., "On elastic-plastic analysis of I beam in bending and torsion", J. of Struc. Engineering, Vol- 17, 1983, pp. 711-718.

[9] Pi, Y. L. and Trahair, N. S., "Inelastic bending and torsion of steel I beams", Journal of Structural Engineering, Vol-120 (12), 1994, pp. 3397-3417.

[10] Zhao, X. L. and Hancock, G. J., "Square and Rectangular Hollow Sections Subjected to Combined Actions", Journal of Structural Engineering, Vol-118, No. 3, March 1992, pp. 648-668.

[11] Drucker, D. C., "Relations of Experiments to Mathematical Theories of Plasticity", ASME Journal of Applied Mechanics, vol. 71, 1949, pp. 349 – 357.

[12] Drucker, D. C., "The Significance of the Criterion for Additional Plastic Deformation of Metals", Journal of Colloid Science, vol. 4, 1949, pp. 299 – 311.

[13] Edelman, F. and Drucker, D.C. "Some Extensions of Elementary Plasticity Theory", Journal of the Franklin Institute, vol. 251, 1951, pp. 581– 605.

[14] Prager, W. and Hodge, P.G., "Theory of Perfectly Plastic Solids", John Wiley, New York, 1951.

[15] Chakrabarty, J., "Theory of Plasticity", McGraw-Hill, Inc., 1987.

[16] Mendelson, A., "Plasticity: Theory and Application", The MacMillan Company, New York, 1968.

[17] Argon, editor., "Constitutive Equation in Plasticity", The MIT Press, Cambridge, London, 1975.

[18] Das, P. K., " Elastic-Plastic Behaviour of a Circular Rod under Combined Tension and Torque", M. Sc Engg. Thesis, 2001, Dept. of Mechanical Engineering, BUET, Dhaka.

[19] Bowes, W. H.; Russell, L. T. and Suter, G.T., "Mechanics of Engineering Materials", John Wiley & Sons, New York.

[20] Boresi, A. P.; Sidebottom, O. M. and Seely, F. B., "Advanced Mechanics of Materials", 3rd Edition, John Wiley & Sons, New York.

[21] Olsen, G. A., "Elements of Mechanics of Materials", 4th Edition, Prentice-Hall, Inc., New Jersey.

APPENDIX – A
CHEMICAL COMPOSITION OF THE SPECIMEN

Chemical Composition of the Material of the Specimen

Chemical composition and heat treatment have a great influence on the mechanical behaviour of the materials both in the elastic and plastic regions. Brittleness of the material has a great impact on the strength of the material. Brittleness of the material depends on the percentage of carbon present in it. If percentage of carbon is more then brittleness will be more and vice versa. The chemical treatment of several virgin specimens is conducted in Metal Treatment Laboratory of Materials and Metallurgical Engineering Department of Bangladesh University of Engineering and Technology (BUET). The chemical composition of the material of the specimen is given below:

Components	Percentage
Carbon	0.15
Manganese	0.90
Phosphorous	0.03
Sulfur	0.03
Silicon	0.20

APPENDIX – B
SAMPLE CALCULATION

Sample Calculation

Uniaxial Tension Test

Ultimate strength, S_{ut} = 694.00 MPa (From stress versus strain curve)

Yield strength, σ_Y = 522.70 MPa. (From stress versus strain curve using 0 % offset)

Modulus of elasticity, E = 195.00 MPa. (From initial slope of the tangent of the stress versus strain curve)

Torsion Test on Torsion Machine:

Equivalent gauge length of the specimen, L = 259.50 mm

Diameter of the specimen, d = 6 mm

From torque versus angle graph it was found that

$$\frac{T}{\theta} = 39.32 N/rad$$

And yield torque T_Y =12.74 N.m

From equation (2.12) it was found that

$$\theta = \frac{TL}{GJ}$$

Or $$G = \frac{39.32 \times 0.2595 \times 32}{3.14 \times 0.006^4} = 80.20 GPa$$

From equation (2.13) it was found that

Yield shear strength, $\tau_Y = \frac{T_Y r}{J} = \frac{12.74 \times 0.003 \times 32}{3.14 \times 0.006^4} = 300 MPa$

So ratio of the yield shear stress to the yield tensile stress, $\frac{\tau_Y}{\sigma_Y} = \frac{300}{522.7} = 0.574$

Pure Bending on Test Rig

From equation (2.17) it was found that for both ends fixed beam, midpoint deflection

$$\delta = \frac{F_b L^3}{192EI}$$

Or $$E = \frac{L^3}{192I} \times \frac{F_b}{\delta}$$

where E = Modulus of elasticity of the material of beam

L = Suspended length of beam

= 597 mm

I = Moment of inertia

$$= \frac{1}{12} ab^3$$

$$= \frac{1}{12}(0.008)(0.008)^3$$

$$= 3.413 \times 10^{-10} \text{ m}^4$$

F_b = Concentrated load applied at midspan of the beam

δ = Midpoint deflection of the beam

From bending load versus midpoint deflection curve for pure bending test it was found that $\frac{F_b}{\delta} = 40.22 kN/mm$

So $$E = \frac{0.597^3}{192 \times 3.413 \times 10^{-10}} \times 40220$$

= 130.50 GPa

But from the stress versus strain curve of uniaxial tension test, it was found that value of the modulus of elasticity E was equal to 195 GPa, which was 1.5 times of 130.50 GPa.

From the investigation, it is found that this discrepancy was due to the problem created in fixing the ends of the specimen. Equation (2.17) is for perfectly fixed ended beam. But in the present setup, the ends of the beam were not perfectly fixed. So it was a partially restrained beam and as a result, axial sliding of the specimen occurs in case of bending loading. Equation (2.20) was obtained from equation (2.17) by introducing a correction factor so that the value of E obtained from the modified equation (2.20) could have a good agreement with that obtained from uniaxial tension test. The value of the correction factor, x was equal to 195.00/130.50 = 1.5. Since it was not possible to fix the ends perfectly, magnitude of the restrained moments reduced and consequently midpoint bending moment of the specimen increased. Modified equation (2.19) for the maximum moment (midpoint momemt) was derived as follows:

Midpoint moment = Resisting moment at the end + Moment due to vertical reaction force at the end.

Or $$M_{max} = -\frac{FL}{8x} + \frac{FL}{4}$$

Or $$M_{max} = \frac{FL}{6}$$

From bending load versus midpoint deflection curve of pure bending test on the test rig, it was found that the yield bending load

$$F_{by} = 0.44 \text{ kN}$$

So yield bending moment

$$M_y = \frac{F_{by}L}{6}$$

$$= \frac{0.44 \times 1000 \times 0.597}{6}$$

$$= 43.78 \text{ N.m.}$$

Corresponding flexural yield stress

$$\sigma_y = \frac{M_y c}{I}$$

Or $$\sigma_Y = \frac{43.78 \times 0.004}{3.413 \times 10^{-10}}$$

$$= 517.00 \text{ MPa.}$$

Pure Torsion on Test Rig:

If a circular shaft is subjected to torsional force in such a way that it's one end is fixed and torsional force is applied at the other free end then twisting angle

$$\theta = \frac{TL}{GJ}$$

But if the circular shaft is subjected to torsional force in such a way that it's both ends are fixed and torsional force is applied at the midpoint of it then twisting angle

$$\theta = \frac{TL}{4GJ}$$

Similarly when square cross section bar is subjected to torsional force in such a way that it's both ends are fixed and torsional force is applied at the midpoint of it then twisting angle

$$\theta = \frac{TL}{4Gk_1a^4}$$

Or $$G = \frac{L}{4k_1a^4} \times \frac{T}{\theta}$$

Here G = Modulus of rigidity

L = Twisted length of the beam

= 609 mm

$k_1 = 0.141$

a = Dimension of the sides of the cross section of the beam

= 8 mm

T = Applied torque at the midspan of the beam

θ = Twisting angle of the the beam

From the torsional load versus angle of twist curve of pure torsion test on the test rig it is found that the value of the F_b/θ up to the yield point was equal to 3.43 kN/rad. Since torque arm length of the loading wheel was 88 mm

So $$\frac{T}{\theta} = 3.43 \times 1000 \times 0.088 = 302 N.m/rad$$

So $$G = \frac{0.609 \times 302}{4 \times 0.141 \times 0.008^4} = 79.69 GPa$$

From torsion test on the torsion machine, it is found that G = 80.20 GPa which was very close to 79.69 GPa. So no modification was needed in the equation of the modulus of rigidity.

From the torsional load versus angle of twist curve of pure torsion in the test rig, it is found that yield torsional load was equal to 0.68 kN. So corresponding yield torque was

$$T_y = 0.68 \times 1000 \times 0.088$$

$$= 59.57 \text{ N.m}$$

Maximum shear yield stress

$$\tau_{max} = \frac{T_y}{2k_2 a^3}$$

$$= \frac{59.57}{2 \times 0.208 \times 0.008^3}$$

$$= 279.66 \text{ MPa}$$

Calculation of the Deflection and the Angle of Twist from Dial Gauge Readings

Pure Bending

In case of pure bending test, only downward movement of the loading wheel was present. So in that case twisting angle was zero and midpoint deflection was equal to l, which had been calculated from the dial gauge reading.

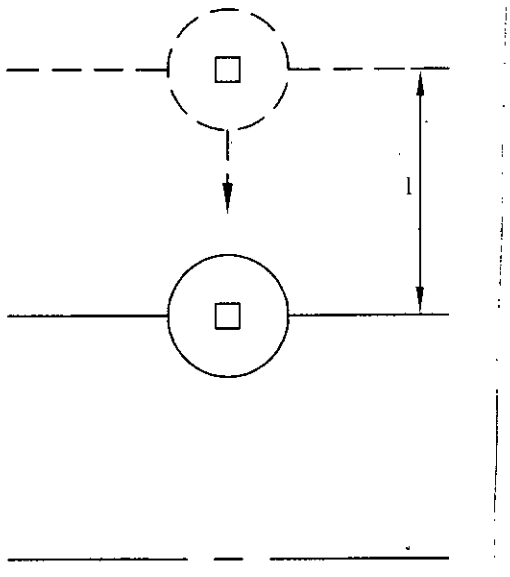

Figure B.1: Schematic diagram of dial gauge position in pure bending loading

Pure Torsion

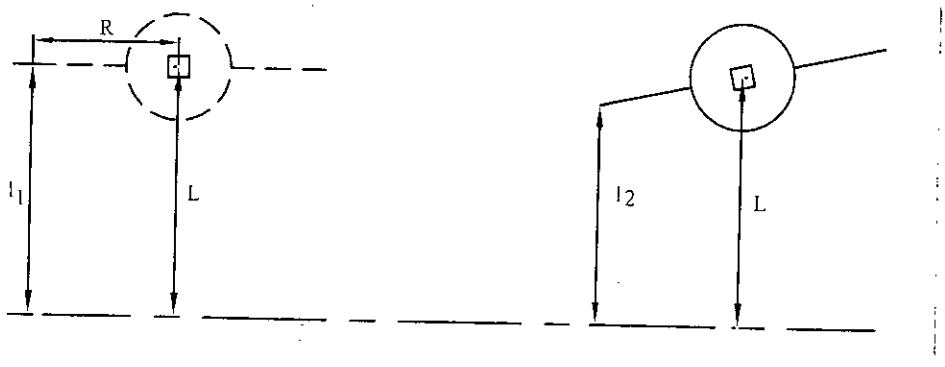

Figure C. 2: Schematic diagram of dial gauge position in pure torsion loading

In case of pure torsion, only twisting of the beam was present and its value was calculated as follows:

Angle of twist, $\theta = \tan^{-1}\left[\frac{l_1 - l_2}{R}\right]$

Here R was the radial distance of the tip of the needle of dial gauge from the center of the loading wheel and its value was 57 mm.

Combined Loading

In this loading condition both downward deflection and twisting of the specimen were present. When second dial gauge's needle moved downward from its initial position, then

Midpoint deflection, $y = \frac{l_1 + l_2}{2}$

And angle of twist, $\theta = \tan^{-1}\left(\frac{l_1 - l_2}{2R}\right)$

But when second dial gauge's needle moved upward from its initial position, then

Midpoint deflection, $y = \frac{l_1 - l_2}{2}$

And angle of twist, $\theta = \tan^{-1}\left(\frac{l_1 + l_2}{2R}\right)$

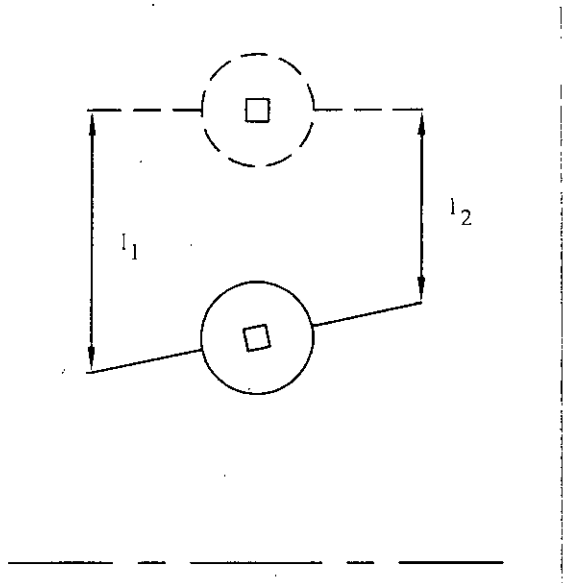

Figure C. 3: Schematic diagram of dial gauges' deflection in combined loading

APPENDIX – C
PHOTOGRAPHS OF THE TEST RIG

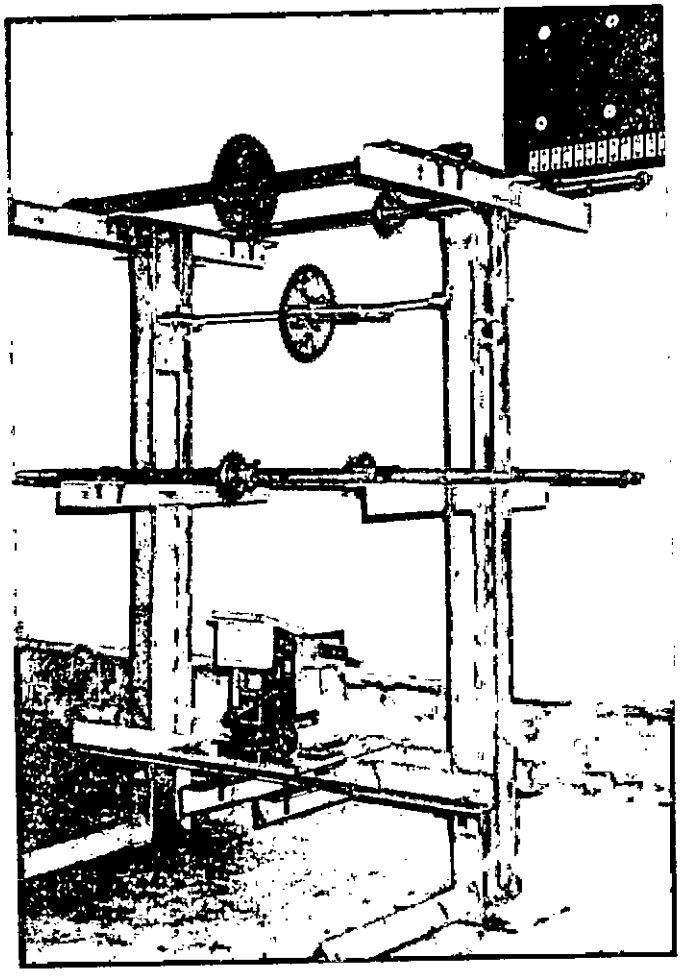

Photograph 1: Main components of the test rig

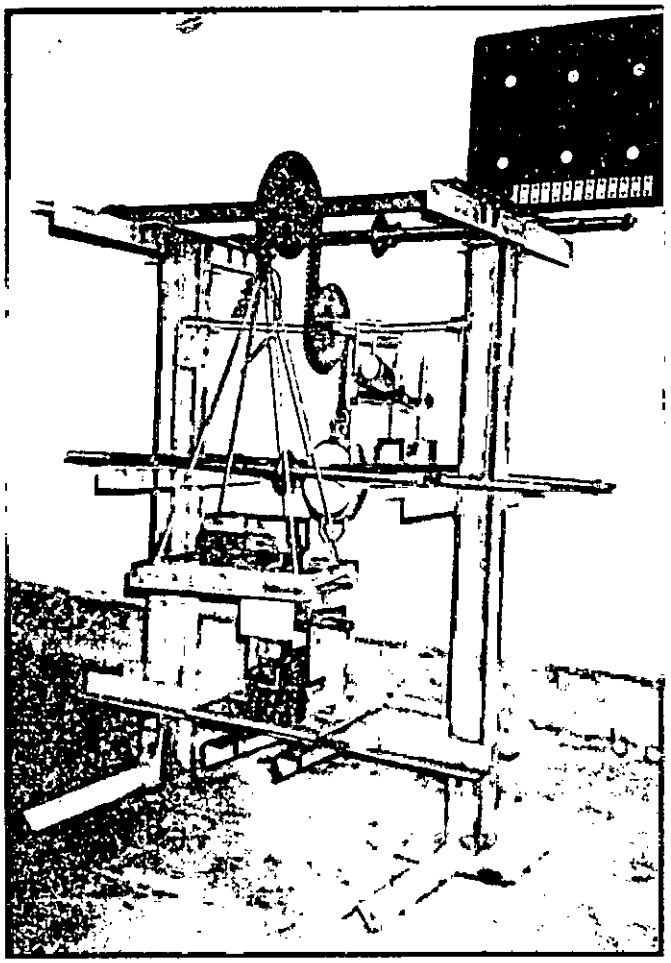

Photograph 2: Loading arrangement for pure torsion and M/T = 0.56

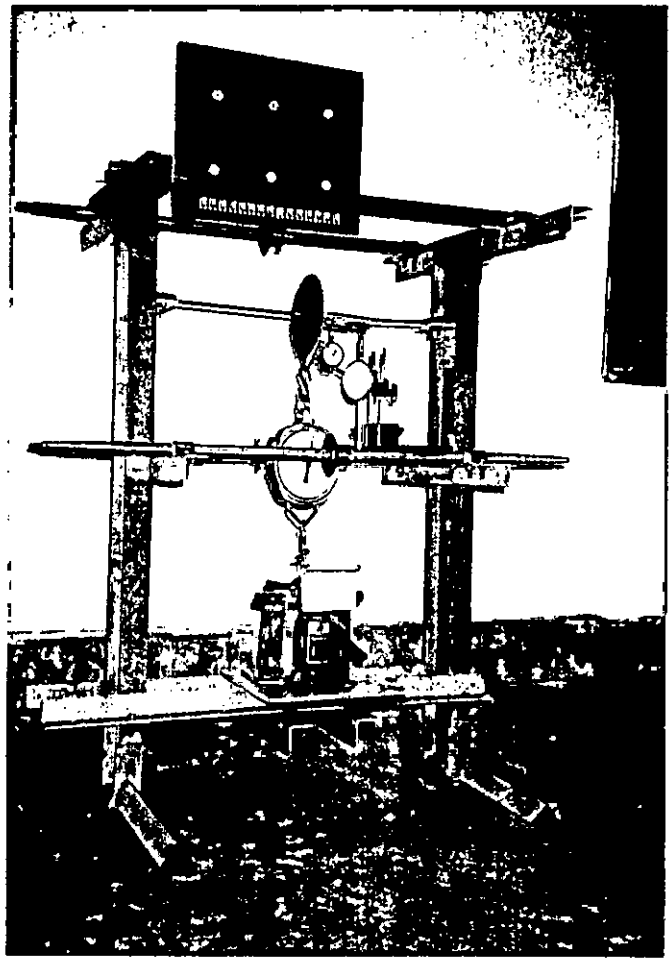

Photograph 3: Loading arrangement for pure bending

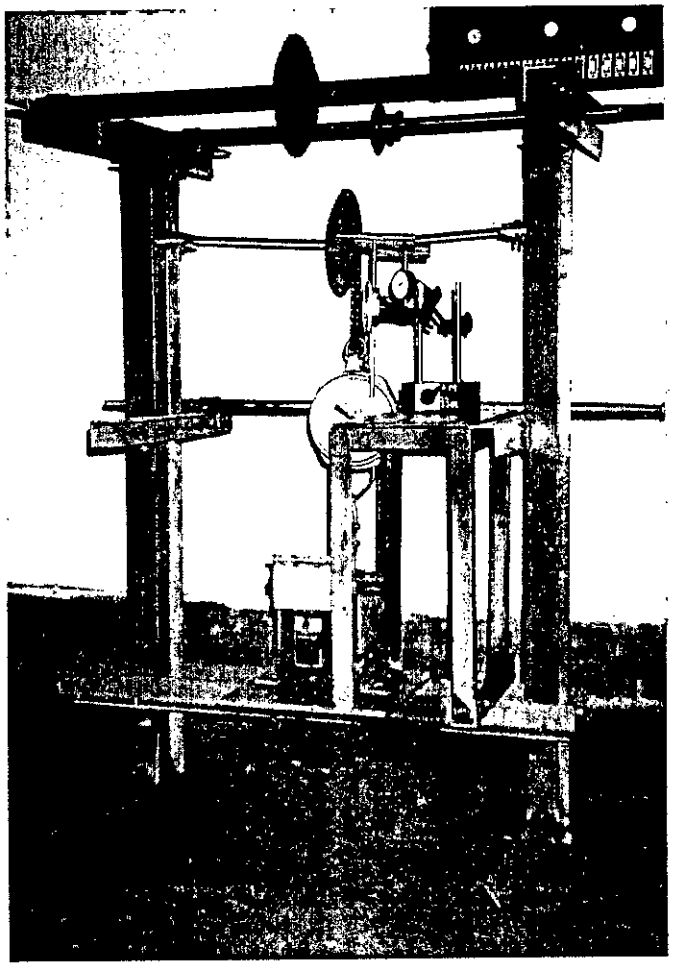

Photograph 4: Loading arrangement for M/T = 1.12

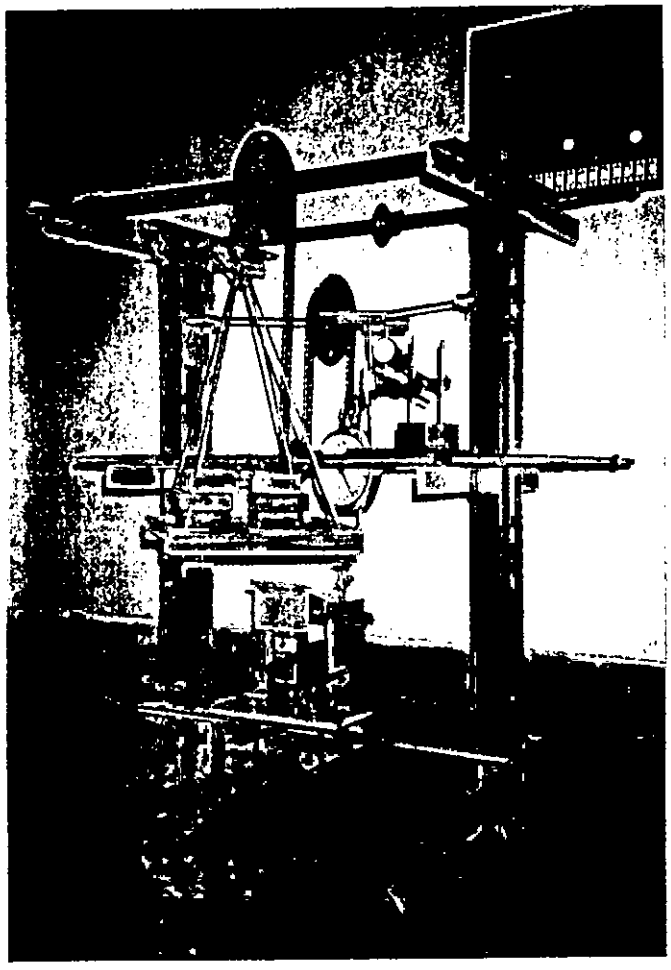

Photograph 5: Loading arrangement for M/T = 2.24 and M/T = 3.36

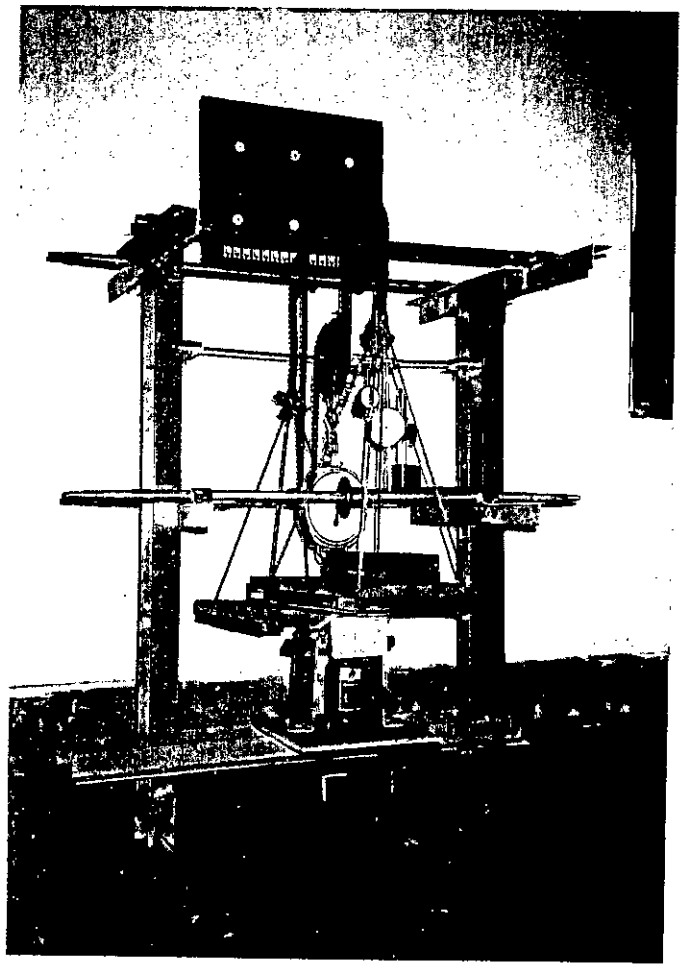

Photograph 6: Loading arrangement for non-proportional tests

APPENDIX – C
PHOTOGRAPHS OF THE TEST RIG

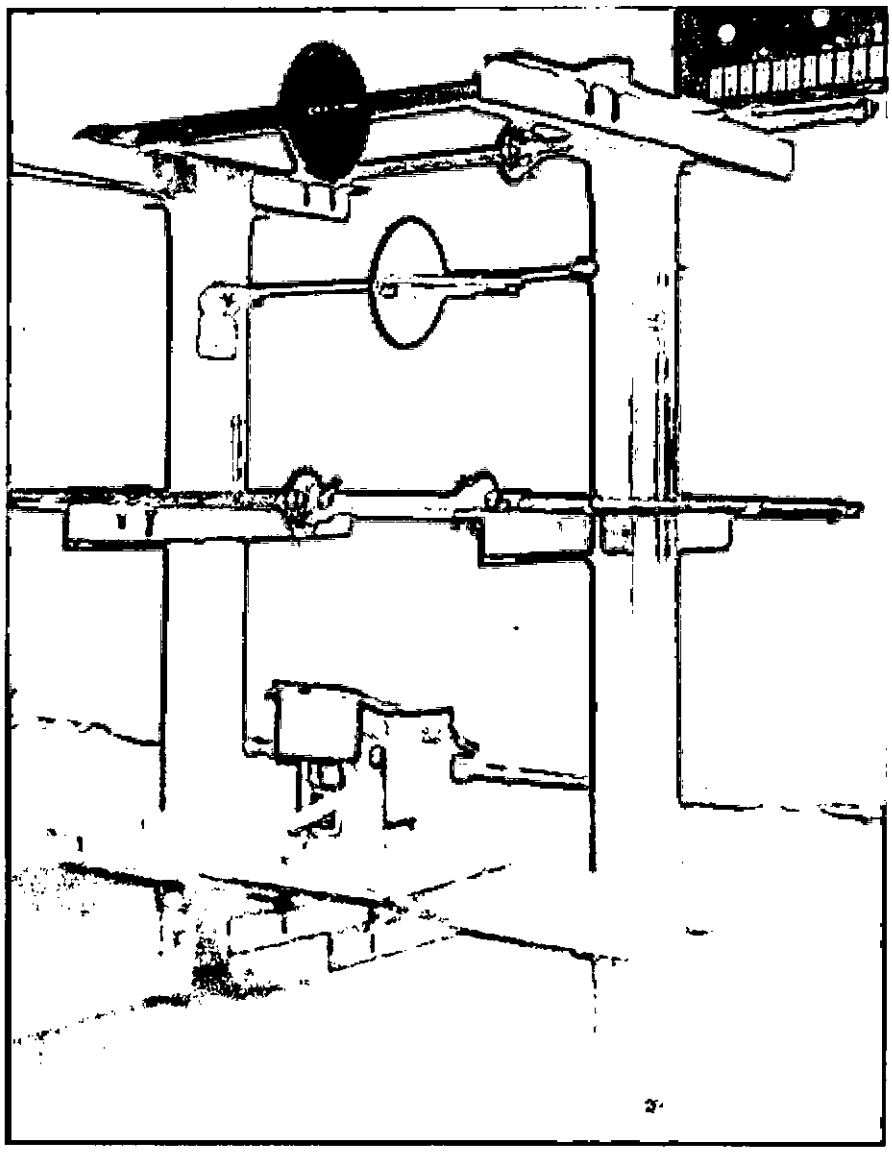

Photograph 1: Main components of the test rig

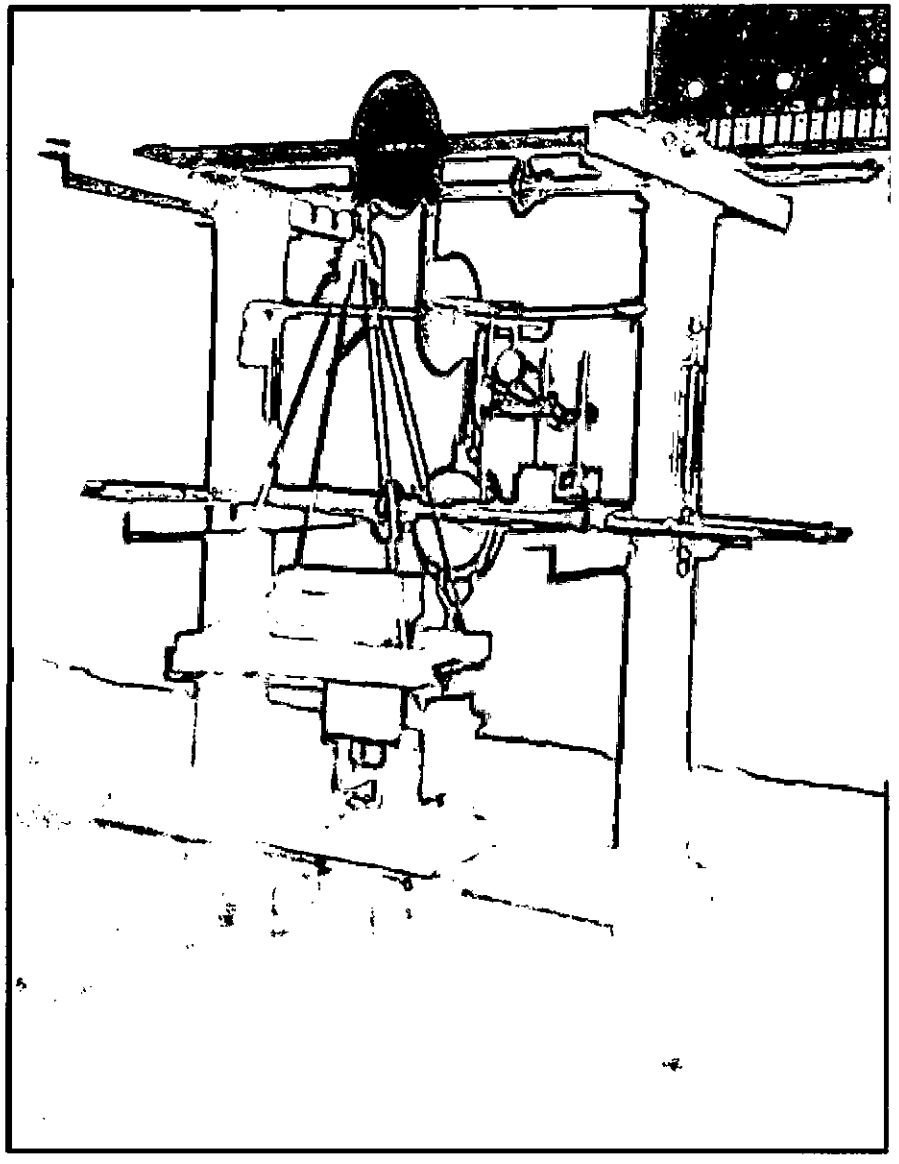

Photograph 2: Loading arrangement for pure torsion and M/T = 0.56

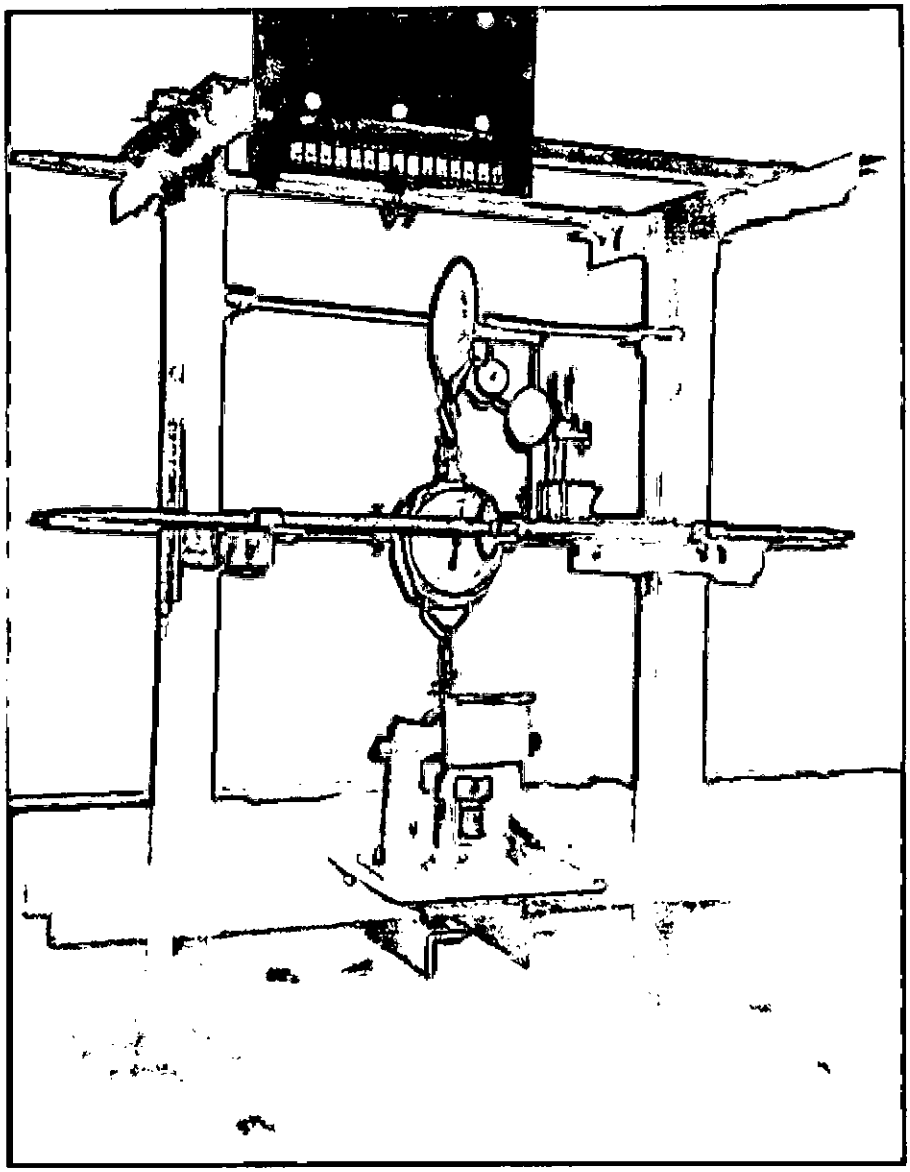

Photograph 3: Loading arrangement for pure bending

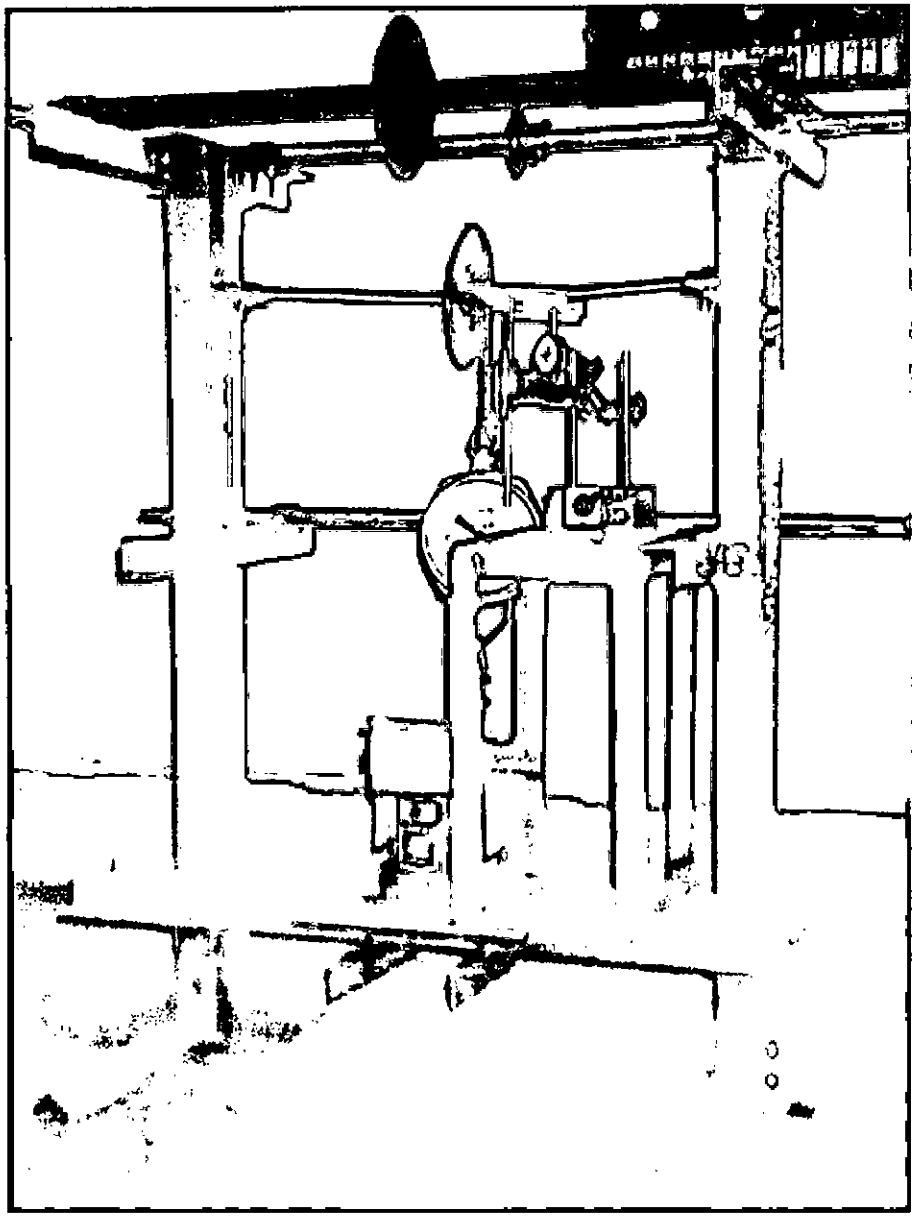

Photograph 4: Loading arrangement for M/T = 1.12

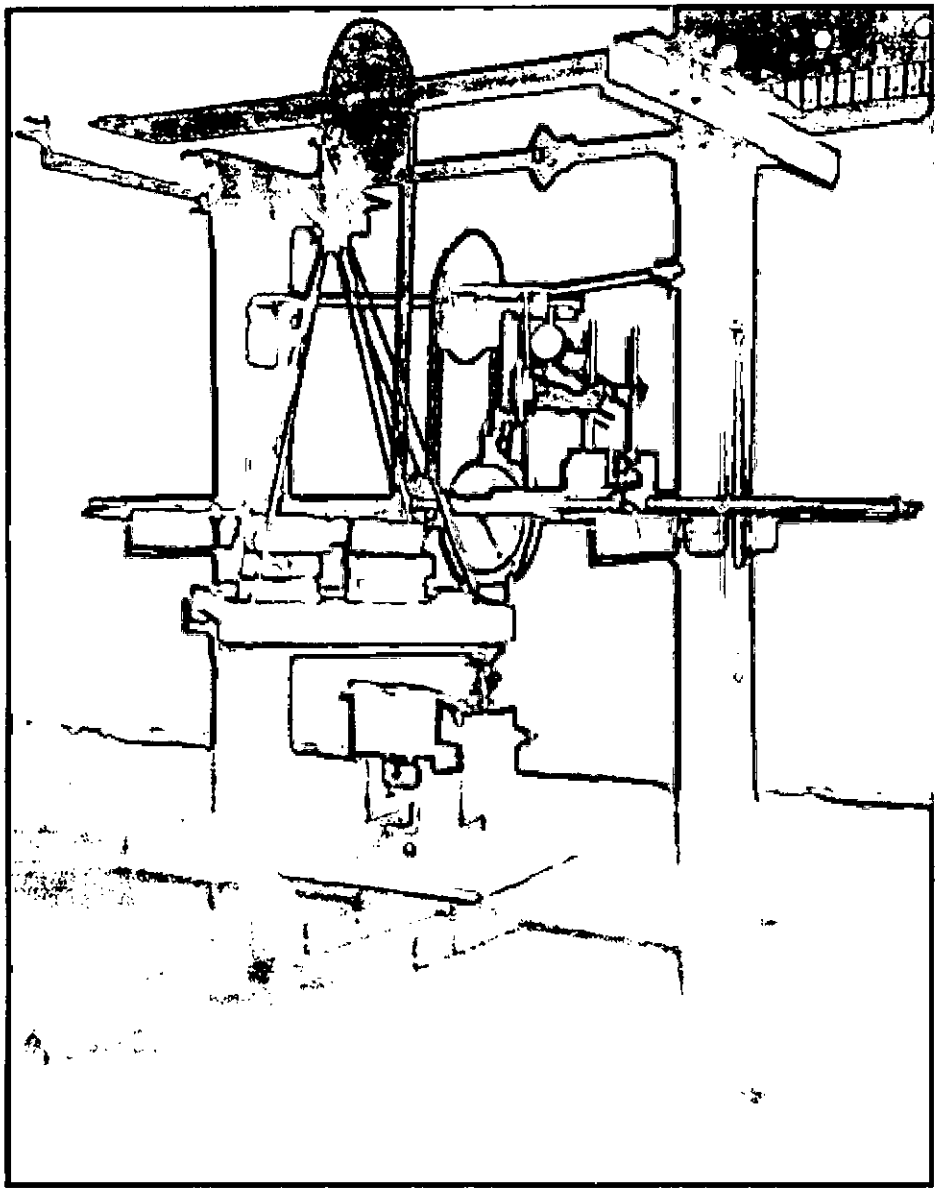

Photograph 5: Loading arrangement for M/T = 2.24 and M/T = 3.36

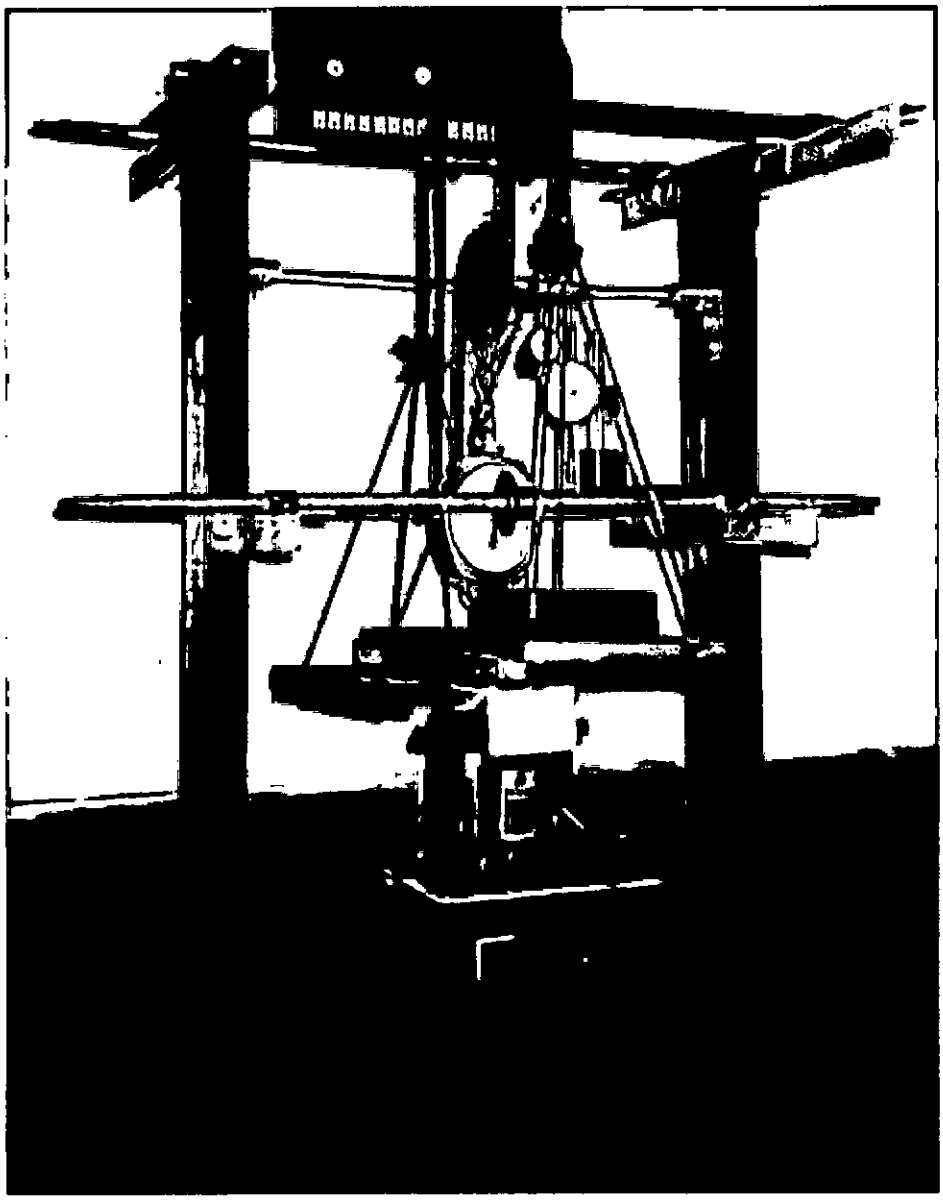

Photograph 6: Loading arrangement for non-proportional tests